Microbial synthesis of 3,4-dihydroxybutyric acid, 3-hydroxybutyrolactone and other 3-hydroxyalkanoic acids

by

Himanshu H. Dhamankar

MS, Chemical Engineering Practice
Massachusetts Institute of Technology, Cambridge, MA, USA, 2009

Bachelor of Chemical Engineering
Institute of Chemical Technology, Mumbai, MH, India, 2007

Submitted to the Department of Chemical Engineering
in Partial Fulfillment of the Requirements for the Degree of

Doctor of Philosophy in Chemical Engineering

at the

Massachusetts Institute of Technology

October, 2013
[FEBRUARY 2014]

Signature of Author.....

Himanshu H. Dhamankar
Department of Chemical Engineering
October 17, 2013

Certified by.....

Kristala L. Jones Prather
Theodore T. Miller Career Development Associate Professor of Chemical Engineering
Thesis Supervisor

Accepted by .....

Patrick S. Doyle
Professor of Chemical Engineering
Chairman, Committee for Graduate Students

Microbial synthesis of 3,4-dihydroxybutyric acid, 3-hydroxybutyrolactone and other 3-hydroxyalkanoic acids

by

Himanshu H. Dhamankar

Submitted to the Department of Chemical Engineering on October 17, 2013
in Partial Fulfillment of the Requirements for the Degree of
Doctor of Philosophy in Chemical Engineering

Abstract

Reducing dependence on petroleum feedstocks motivates engineering novel conversion technologies to convert biomass as a renewable resource into target value-added products. In this thesis we developed a new pathway for the microbial synthesis of 3-hydroxyalkanoic acids as biomass derived value-added products. 3-hydroxyalkanoic acids (3HAs) find applications as monomers for biodegradable polymers and chiral pharmaceutical building blocks.

One part of this thesis focused on investigating the proposed 3-hydroxyalkanoic acid synthesis platform pathway. The platform employs the reactions of the natural polyhydroxyalkanoate synthesis pathway with new substrates, taking advantage of natural enzyme promiscuity for the stereospecific synthesis of a variety of 3HAs of desired carbon chain length and substituents. Using this platform, we have now demonstrated the synthesis of five novel products: 3,4-dihydroxybutyric acid (3,4-DHBA) and 3-hydroxybutyrolactone (3HBL) as pharmaceutical building blocks and 2,3-dihydroxybutyric acid (2,3-DHBA), 3-hydroxy-4-methylvaleric acid (3H4MV) and 3-hydroxyhexanoic acid (3HH) as monomers for novel polymer applications. The synthesis of 2,3-DHBA in particular led to the identification of a novel activity associated with the thiolase enzyme and highlighted the biosynthetic capability of the platform. The experimental study of different pathway enzyme combinations offered insights into their activities and specificities to guide future enzyme selection.

In another part of this thesis, we focused specifically on the hydroxyacid 3,4-DHBA and its lactone 3HBL and their synthesis from glucose as a sole carbon source by integrating the 3HA platform with the endogenous glyoxylate shunt. 3HBL has been identified as a top value-added platform chemical from biomass by the US Department of Energy due to its applications as a chiral synthon for a variety of pharmaceuticals, with an estimated wholesale cost of $450/kg. We were successful in establishing the first biosynthetic pathway for the stereospecific synthesis of 3,4-DHBA and 3HBL from glucose in this thesis, achieving up to 24% of the maximum theoretical yield and titers of the order of 1 g/L at the shake flask scale. Overcoming repression of the glyoxylate shunt and independent control of the glycolate and 3HA pathway enzyme expression using two orthogonal expression systems was critical for product synthesis. Additionally, a study of the 3HBL/DHBA fermentation at the shake flask and bench-top bioreactor scales helped gain an understanding of pH as an important factor affecting the synthesis of these products and informed approaches to improve pathway and process performance.

Thesis Supervisor: Kristala L. Jones Prather
Title: Theodore T. Miller Career Development Associate Professor of Chemical Engineering

Dedication

This thesis is dedicated to my mother, Shubhada (Shubhi) Dhamankar, who was instrumental in getting me excited about microbiology and biochemistry as a kid. Her efforts to offer my brother and me the best of educational and developmental opportunities in the hardest of times and her belief in me and my dreams are a constant source of inspiration. This thesis is as much hers as it is mine.

Acknowledgements

It takes a village to raise a child. This thesis is the product of the guidance, support, encouragement and love of a number of individuals. I would like to thank my thesis committee members, Prof. Bradley Olsen, Prof. Gregory Stephanopoulos and Prof. Graham Walker for their valuable insights, constructive criticism and encouragement over these last four years. Collectively, their combination of engineering and biological perspectives helped me hone a unique perspective of my own and motivated me to pursue both fundamental and application oriented questions in this thesis.

Two individuals have had a profound influence on my journey through graduate school and have helped me find my way through it. The first of these is my thesis advisor, Prof. Kristala Prather, who showed the courage to take on the responsibility of mentoring an inexperienced, and somewhat lost albeit extremely enthusiastic student. Her guidance and undying optimism and encouragement helped me understand and pursue my passion in the field of metabolic and biochemical engineering. I owe this thesis and a good part of my graduate school experience to her. The second is Prof. T. Alan Hatton, who has been a strong source of support and a mentor par excellence. Without his support, I would not be here.

Members of the Prather Lab have been wonderful colleagues and friends. I started off as an apprentice of sorts to Dr. Collin Martin in the Prather Lab and would like to thank him for helping me learn the ropes in those initial few months and initiating me into this exciting project. My collaborators, Micah Sheppard, Hsien-Chung Tseng and Dr. Christopher Reisch on the 3-hydroxyacid project have been fantastic to work with both as researchers and as people. I would particularly like to thank Micah Sheppard and Eric Shiue for many a valuable and intellectually exciting discussions. It has been an equal pleasure working with the 'thiolase group', namely Yekaterina Tarasova, Brian Bonk and Dr. Michael Hicks. Kevin Solomon and Diana Bower have similarly been wonderful mentors, friends, philosophers and guides through these years. Additionally, I would like to thank my undergraduate students Tim Chang, Angel Asante, Michelle Teplensky and Nina Jreige for giving me the opportunity to serve as a mentor. Their enthusiasm kept me going.

Over the years, I have been extremely fortunate to have met and interacted with a number of fantastic people at MIT. Gwen Wilcox is one of them. Her meticulous organizational and management skills and generosity of spirit in going out of her way to help everyone around her are exemplary. Prof. Robert Fischer is yet another individual whose mentorship and friendship I dearly value.

Finally, I would like to acknowledge the support of my family and my extended family of friends here at MIT. My mother Shubhada Dhamankar's belief in my dreams is a constant source of inspiration. Similarly, my brother Adwait Dhamankar and Somani Patnaik have been rock solid supports. Their presence, love and support in my life helped put my efforts and struggles in perspective and truly made this journey enjoyable.

Table of Contents

List of Figures

List of Tables

Chapter 1 Introduction

Parts of this chapter have been published in the manuscript, Dhamankar H. and Prather K.L.J. (2011), Curr. Opin. Struct. Biol., 21 (4) 488 – 494

1.1. Building microbial conversion technologies through *de novo* pathway engineering

Society today relies heavily on the dwindling resource of crude petroleum to supply not only fuels but also an array of valuable chemicals. Globally, roughly 20% of crude petroleum consumed is used for the synthesis of products other than transportation and industrial fuels, a sizeable fraction of which are petrochemicals (BP statistical review, 2010). Petrochemicals are used as raw materials in the manufacturing of a variety of products such as polymers, textiles, paints, solvents, pharmaceuticals, detergents, waxes and lubricants that find applications in our day-to-day lives. The use of biomass as a renewable feedstock and potential replacement for petroleum then requires the identification, design and engineering of conversion technologies to convert biomass, not only into bio-fuels, but also target value-added biochemicals that can serve as effective replacements for petrochemicals. In particular, developing versatile novel platform pathways that allow the synthesis of multiple different molecules or a class of compounds is of particular value in building effective conversion technologies for bio-refineries (Bozell and Petersen, 2010).

Microbes have naturally evolved enzymes to convert biomass into myriad unique chemical structures for sustenance and may be effectively harnessed as efficient microbial chemical factories (MCFs) for synthesis of target molecules from biomass. The evolution of the field of metabolic engineering has led to the development of principles and tools that enable construction and optimization of MCFs by tapping into naturally occurring pathways in specific host organisms, heterologous expression of non-native pathways in well-characterized hosts, or engineering *de novo*

biosynthetic pathways for synthesis of various natural and non-natural products. *De novo* pathway engineering refers to the design and construction of novel pathways (hitherto unknown in nature in any single organism) by assembling multiple existing partial pathways from different organisms and using promiscuous or engineered enzymes as biocatalysts to catalyze a series of biotransformations with non-natural substrates (Prather and Martin, 2008). This capability is of particular importance for truly expanding the repertoire of products that can be synthesized microbially. Biosynthesis also serves as a promising alternative to chemical synthesis processes that often employ expensive, hazardous and non-renewable raw materials and reagents as well as harsh processing conditions and has indeed emerged as a highly promising alternative to traditional organic synthesis for a variety of chemical compounds (Chang and Keasling, 2006; Lee et al., 2011).

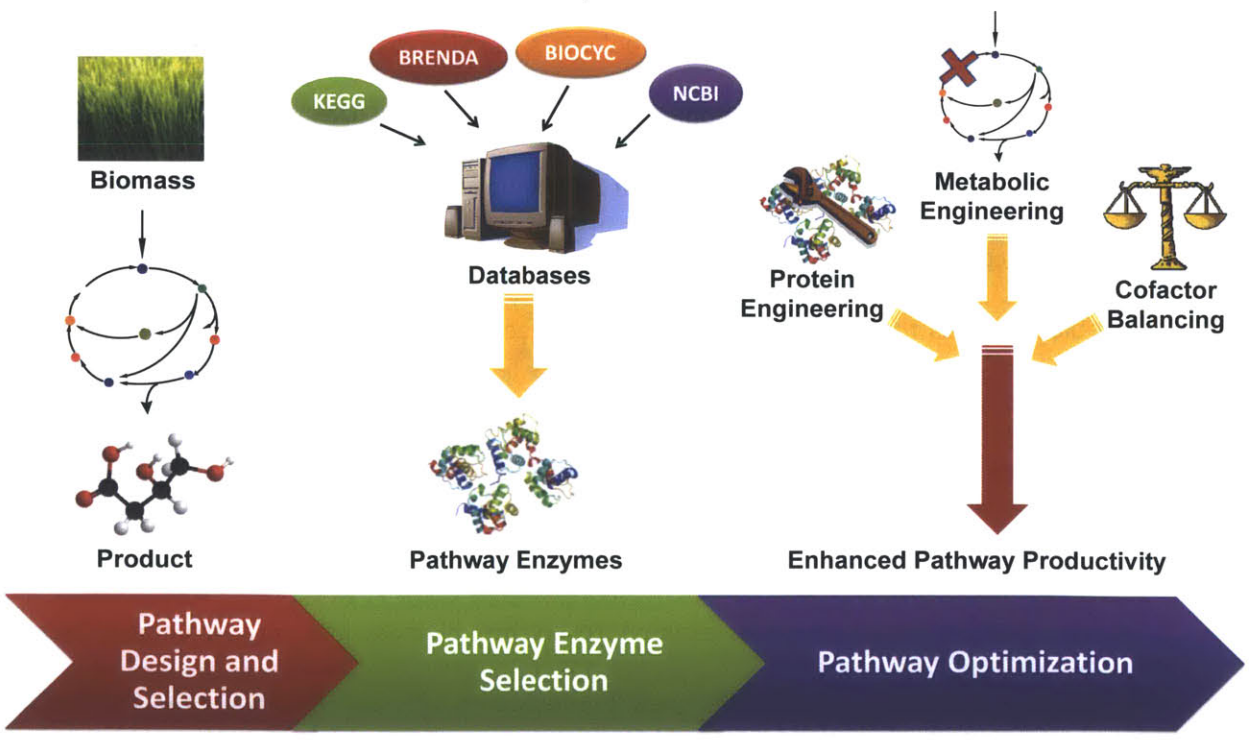

Figure 1-1 | Design and Engineering of Pathways for Microbial Chemical Factories (MCFs)

Figure 1-1 outlines the steps involved in the design of novel pathways for MCFs and various tools and approaches used for their optimization. The first step in engineering novel or natural

pathways is to identify potential natural cell metabolites or biomass derived feedstocks that can serve as starting materials and the series of biochemical reactions required to convert these into the desired product. Martin and co-workers (Martin et al., 2009) have reviewed some of the computational tools available for identifying and selecting from the multiple possible pathways connecting different starting materials to a product of interest. Once a pathway has been selected for experimental exploration, suitable pathway enzymes need to be selected to catalyze individual reaction steps. Pathway enzymes are the tireless machines of the MCFs that govern the pathway rates, selectivity, yield and overall productivity, making enzyme selection a critical step in building new pathways.

Whenever possible, enzymes known to specifically catalyze reactions with the respective pathway intermediates are selected. If no enzyme has been documented to catalyze the required biochemical reaction with the specific pathway intermediate, other enzymes exhibiting the required biocatalytic activity known to act with structurally and chemically similar substrates may be selected to take advantage of natural enzyme promiscuity (Babtie et al., 2010; Khersonsky and Tawfik, 2010). Screening of multiple enzymes from different organisms can be an effective strategy for sampling different naturally evolved enzyme activities and specificities. Computational approaches such as BLAST searches and network maps may be effectively employed to comb through the extensive genomic, metabolic and enzyme databases such as KEGG (Kanehisa et al., 2006), BRENDA (Schomburg et al., 2004), BioCYC (Karp et al., 2005), SwissProt and NCBI (http://www.ncbi.nlm.nih.gov/guide/) that classify well-characterized natural enzymes on the basis of the specific and generalized reactions they catalyze, to identify such enzyme candidates (Baxevanis and Ouellette, 2005; Carbonell and Faulon, 2010). Molecular docking is yet another valuable *in silico* tool to predict promiscuity *a priori* by studying interactions of a given enzyme active site with a range of different substrates of interest when sufficient information about enzyme crystal structures and active sites is available (Babtie et al., 2010; Hermann et al., 2006). The selected enzymes are then expressed in a suitable organism grown in a culture medium

supplemented with the required starting materials for the microbial synthesis of the desired value-added product.

Once a novel or natural pathway has been established and the synthesis of the product of interest has been demonstrated, enhancing pathway performance metrics such as yields, titers and productivity is critical for commercialization. Protein engineering can be used for improving the selectivity and activity of key pathway enzymes and can effectively complement conventional metabolic engineering approaches such as increasing the precursor supply by varying pathway enzyme expression levels or knocking out competing pathways to enhance productivity. Further, pathway enzymes often require cofactors for catalysis. Imbalances and limitations arising out of an inability to effectively recycle cofactors can hamper pathway productivity, warranting specific efforts for cofactor regeneration.

A number of research groups have employed combinations of these strategies towards developing novel pathways and enhancing the performance of already established pathways for the microbial synthesis of a number of value-added biochemicals including the polymer and pharmaceutical building blocks putrescine (Qian et al., 2009), cadaverine (Qian et al., 2011), succinic acid (Blankschien et al., 2010; Raab et al., 2010), native silk protein (Xia et al., 2010), the high value flavoring agent natural vanillin (Hansen et al., 2009; Lee et al., 2009), pharmaceutical drug precursors such as taxadiene (Ajikumar et al., 2010) and amorpha-4,11-diene (Anthony et al., 2009) and plant secondary metabolites such as flavanoids, stilbenoids (Trantas et al., 2009) and isoprenoids (Anthony et al., 2009; Asadollahi et al., 2010). DuPont's 1,3-propanediol (Nakamura and Whited, 2003) and Genomatica's 1,4-butanediol (Yim et al., 2011) are examples of recent industrial successes in developing MCFs for biochemicals. In the Prather Lab as well, we have employed these strategies effectively for developing pathways for the synthesis of various molecules including biofuels such as butanol (Nielsen et al., 2009) and pentanol (Tseng and Prather, 2012) and biochemicals such as D-glucaric acid (Moon et al., 2010), 3-hydroxybutyric

acid (Tseng et al., 2009a) and 3-hydroxyvaleric acid (Tseng et al., 2010a). In this thesis, I discuss the application of this paradigm for developing a novel platform pathway for the synthesis of 3-hydroxyalkanoic acids such as 3,4-dihydroxybutric acid as biomass derived value-added products.

1.2. 3-Hydroxyalkanoic acids (3HAs)

3-Hydroxyalkanoic acids are a versatile class of chiral compounds with hydroxyl and carboxyl groups that can be readily derivatized or modified for the synthesis of various fine chemicals such as antibiotics (Chiba and Nakai, 1985) and drug delivery peptides (Lee et al, 2001 and Chen and Wu, 2005), novel solvents and biodegradable polymers. Hydroxyacids (HA) serve as monomers in the synthesis of polyhydroxyalkanoates (PHAs). PHAs are linear thermoplastic biodegradable polyesters mainly composed of *(R)*-3-hydroxyalkanoic acid monomers (ranging from 3-hydroxypropanoic acid to 3-hydroxyhexadecanoic acid) as well as some other monomers such as 4-, 5- or 6-hydroxyalkanoic acids, with molecular weights of the order of 50,000 to 1,000,000 Daltons that are found to accumulate in bacterial cells in discrete granules as energy and carbon storage units. More than 140 different types of 3-, 4-, 5- and 6-hydroxycarboxylic acids have been found to be incorporated into naturally occurring PHAs (Lee et al., 2001; Steinbuchel and Valentin, 1995). Since PHAs can be produced from renewable resources and are completely biodegradable, they are regarded as potential candidates to replace petroleum derived non-degradable polymers. Their applications include biodegradable packaging materials, films, bottles, coated paper, surgical sutures, controlled release matrices and polymer scaffolds. Mirel™ Bioplastics commercially manufactures PHAs using engineered industrial microbial strains capable of fermenting natural sugars to PHAs.

In addition to serving as monomers for PHAs, 3-hydroxyacids may serve as chiral building blocks for the synthesis of various pharmaceuticals such as antibiotics, synthetic amino acids and peptides for drug delivery and novel solvents. For example, 3-hydroxyacids can be used for the synthesis of

macrolides such as pyrenophorin, colletodiol, grahamimycin A1 and elaiphylidene that serve as antibiotics (Lee et al., 2001). *(R)*-3-hydroxyacids may be used in the synthesis of *(S)*-β-amino acids (Lee et al., 2001). These β-amino acids can be used in the synthesis of β-lactams as antibiotics and β-peptides as peptide drugs.

1.3. Background, Motivation and Thesis Objectives

Thus, chiral 3-hydroxyacids find a number of applications in the synthesis of various valuable chemicals. However, no convenient and economical route has yet been identified for their synthesis. Direct chemical synthesis of enantiomerically pure 3-hydroxyacids is extremely messy, requiring multiple reaction and separation steps (Jaipuri et al, 2004 and Noyori et al, 1987) and expensive reagents and solvents. Enantiomerically pure hydroxyacids may also be synthesized by the chemical degradation of corresponding PHAs isolated from bacteria, however the yields of these reactions are typically low due to the losses in the isolation and purification of PHAs from bacteria as well as incomplete depolymerization. *In vivo* depolymerization may be used to efficiently obtain the main constituents of PHAs accumulated in microbes, namely *(R)*-3-hydroxycarboxylic acids. However, this approach suffers from two drawbacks: 1) one can only obtain the constituent *(R)*-stereoisomer and 2) yields of different hydroxyacids are limited by the composition of the PHAs accumulated by the microbes. While direct biosynthesis of 3-hydroxyacids is an attractive option, the number of 3HA molecules produced directly from simple carbon sources is far smaller. Indeed, only 3-hydroxybutyrate (3HB) and 3-hydroxyvalerate (3HV) have been successfully produced at the gram per litre scale using reactions and enzymes of the PHA biosynthetic pathway (Gao et al., 2002; Tseng et al., 2010b; Tseng et al., 2009b). Thus, there is a need for an economical and simple route towards the stereospecific synthesis of chiral 3-hydrxyalkanoic acids.

Martin (Martin, 2009), explored a new route for the stereospecific synthesis of 3-hydroxyvalerate (3HV) and 3,4-dihydroxybutyrate (3,4-DHBA) by metabolizing small acid molecules such as propionate and glycolate along reactions analogous to the polyhydroxyalkanoate (PHA) synthesis pathway in recombinant *E. coli*, using enzymes from different organisms. While the reactions of the PHA synthesis pathway had been previously used for the synthesis of naturally occurring 3HAs such as 3HB and 3HV (Gao et al., 2002; Tseng et al., 2010b; Tseng et al., 2009b), the synthesis of 3,4-DHBA and its corresponding lactone, 3-hydroxybutyrolactone (3HBL) from glycolic acid using this approach was unique in its biosynthetic capability and led to the first biosynthetic pathway towards these valuable pharmaceutical building blocks. This initial success motivated the exploration of this route as a platform for the synthesis of other 3HAs by analogously metabolizing other small acid molecules.

The overarching goal of this thesis was to follow up on the findings of Martin (2009) with the objective of developing and evaluating the 3HA pathway as a platform for the synthesis of new 3-hydroxyalkanoic acid products. The governing hypothesis was that a condensation reaction between acetyl-CoA and a generic acyl-CoA molecule derived from a supplied small acid molecule via CoA activation (analogous to the condensation between two acetyl-CoAs in poly-3HB (PHB) synthesis) and processing of the resulting condensed product along reactions analogous to the PHB pathway is expected to allow the synthesis of 3-hydroxyacids, the carbon chain length, branching and substituents in which may be controlled by the '**R**' group connected to the carboxyl in the supplied small acid molecule (**Figure 1-2**). Critical to the synthesis of new products is the selection of efficient pathway enzymes. We did not know *a priori* what enzyme substrate combinations would yield products. Both rational and computational approaches were used for enzyme selection. In addition to synthesis of new products, we hoped to gain insights into the activities and specificities of various pathway enzymes explored to guide future enzyme selection and engineering.

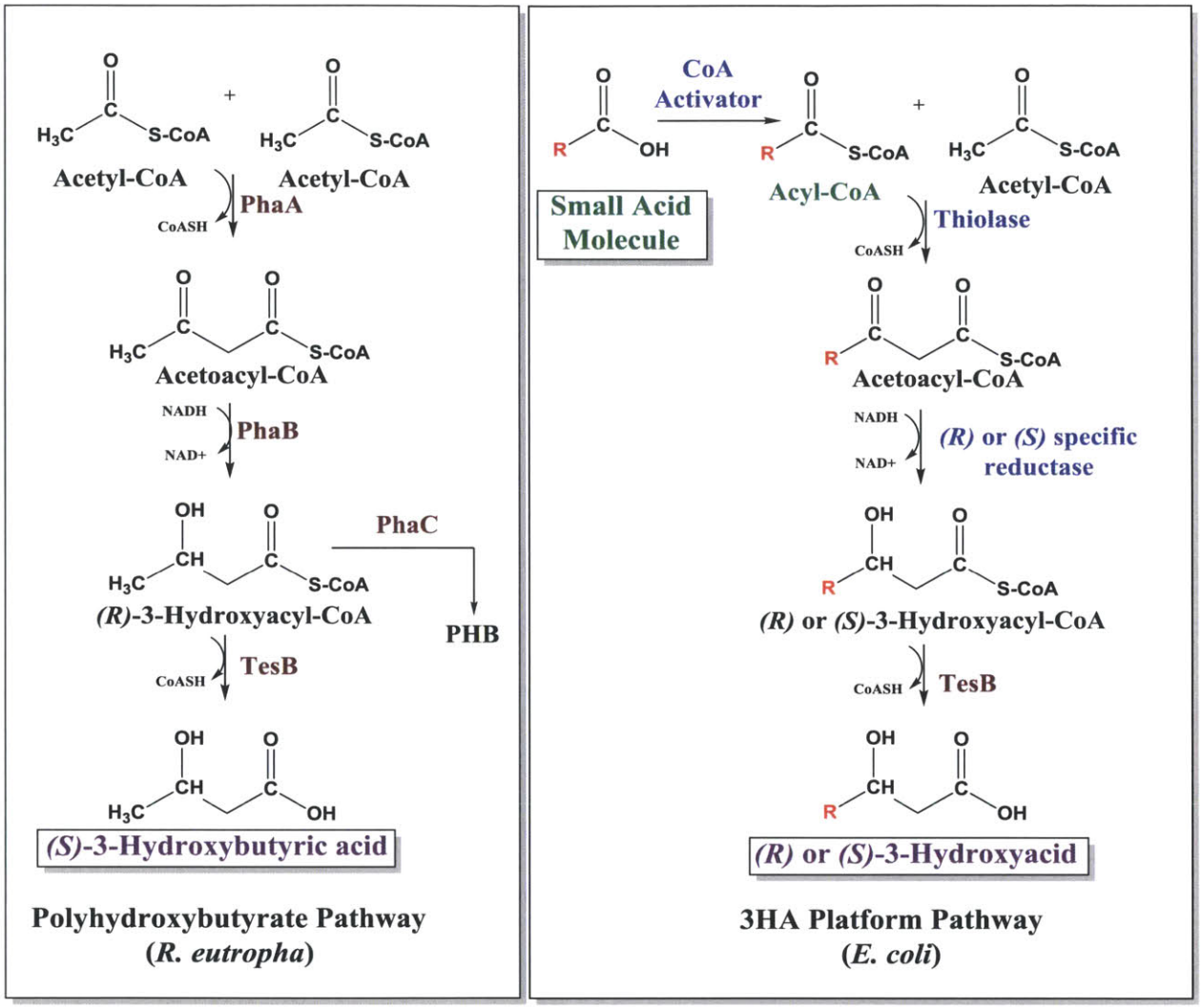

Figure 1-2 | Polyhydroxybutyrate pathway inspired novel 3-hydroxyalkanoic acid synthesis pathway

3,4-DHBA and 3HBL were of particular interest, owing to their applications as valuable chiral pharmaceutical building blocks for statins such as artovastatin (Crestor®) and rosuvastatin (Lipitor®), combined with a lack of an established biosynthetic route towards these chiral synthons. Martin's original demonstration reported DHBA titers up to 3 g/L, amounting to a molar yield of about 62% on the starting substrate glycolate. An important goal of this thesis was to understand and address pathway and bioprocess limitations to improve 3,4-DHBA and 3HBL synthesis along the 3HA pathway beyond these numbers. Glycolate, the starting substrate for 3,4-DHBA and 3HBL can be synthesized from glucose along the endogenous glyoxylate shunt. Endogenous glycolate synthesis is expected to

afford various advantages, including improved yield and selectivity, reduced transport limitations and potential cost savings due to synthesis from a single carbon source. Thus another objective of this thesis was to integrate the endogenous glyoxylate shunt with the 3HA pathway to demonstrate synthesis of 3,4-DHBA and 3HBL from a single carbon source like glucose to establish these as potential biomass derived products.

The specific aims of this thesis project are summarized below:

1. Develop a platform pathway for the synthesis of a variety of chiral 3-hydroxyacids in *E. coli* in the C4 C6 carbon chain length range, using reactions of the PHA synthesis pathway, assembling a repertoire of enzymes selected to catalyze reactions with substrates of interest

2. Study the synthesis of 3,4-dihydroxybutyricacid (3,4-DHBA) and 3-hydroxybutyrolactone (3HBL) as specific target products using the 3HA platform and improve product titers, yield and productivity

3. Establish and evaluate a complete pathway for the synthesis of 3,4-DHBA and 3HBL from glucose or other simple sugars as single carbon sources in *E. coli*

1.4. Thesis overview

Following this overview of the reasons for our interest in the synthesis of 3HAs and specifically 3,4-DHBA and 3HBL, we discuss the challenges encountered and the solutions and successes in meeting the thesis objectives in the subsequent chapters. Chapter 2 focusses on building the proposed 3-hydorxyalkanoic acid platform using enzymes from the PHA and butanol synthesis pathways that eventually allowed the synthesis of five novel products. Chapter 3 discusses the exploration of alternative pathway enzymes in an attempt to improve the synthesis of novel products along the pathway and the lessons learned in the process. In Chapter 4, we discuss the integration of the endogenous glyoxylate shunt with the 3HA platform for the direct synthesis of 3,4-DHBA and 3HBL from glucose as a sole carbon source and an evaluation of the product titers, yield and selectivity. In Chapter

5, we focus on understanding the influence of various process parameters on the DHBA / 3HBL fermentation using bench-top bioreactors to improve the key pathway and process performance metrics, namely yield, titers and productivity. Finally, any good thesis project inevitably gives rise to new questions and directions for exploration. In Chapter 6 we summarize these.

Chapter 2 Building a novel platform for the synthesis of 3-hydroxyalkanoic acids

Parts of this chapter were published in Martin et al (2013), Nat. Commun. 4, 1414 and the data and results presented were obtained in collaboration with Dr. Collin Martin, Dr. Hsien-Chung Tseng, Mr. Micah Sheppard and Dr. Christopher Reisch.

2.1. Introduction

In Chapter 1 we discussed the various applications of 3-hydroxyalkanoic acids as versatile chiral building blocks for pharmaceuticals and biodegradable polymers and the need for an efficient, green and economical route for their synthesis. Of particular interest to us for this project was the synthesis of the hydroxyacid 3,4-dihydroxybutyric acid (3,4-DHBA) and its corresponding lactone, 3-hydroxy-γ-butyrolactone (3HBL). 3HBL is a versatile chiral C4 building block with applications in the synthesis of a variety of pharmaceuticals, polymers and solvents (Werpy and Peterson, 2004). In particular, *(S)*-3-hydroxy-γ-butyrolactone serves as a precursor to various enantiopure intermediates for chiral drugs such as cholesterol-reducing statins like Lipitor® (Pfizer) and Crestor® (AstraZeneca), antibiotics such as carbapenems and linezolid (Zyvox®), and the anti-hyperlipidemic medication Zetia® (Lee and Park, 2009). Artovastatin (the active ingredient in Lipitor®) is synthesized via hydroxynitrile, an intermediate which may be readily synthesized from *(S)*-3HBL. Other pharmaceuticals derived from 3HBL include HIV inhibitors (Kim et al., 1995) and the nutritional supplement L-carnitine (Wang and Hollingsworth, 1999b). Both *(R)*-3HBL and *(S)*-3HBL may be used in the synthesis of the nutritional supplement L-carnitine (Byun et al., 2002; Hwang et al., 2009). 3HBL can also be readily transformed into a variety of three-carbon building blocks (Wang and Hollingsworth, 1999a) and the alcohol and acid functional groups in *(S)*-3HBL can be derivatized to yield various substituted tetrahydrofurans, amides, lactones, nitriles and epoxides that may in turn serve as chiral building blocks (Furrow et al., 1998; Wang and

Hollingsworth, 1999a; Yang et al., 2012) and solvents (Werpy and Peterson, 2004). Owing to these numerous applications, 3HBL has been identified as one of the top value-added chemicals from biomass in a report by the U.S. Department of Energy (Werpy and Peterson, 2004).

There are no identified natural biochemical routes nor have engineered routes been previously reported for the biosynthesis of 3HBL or 3,4-DHBA. 3HBL is currently produced as a specialty chemical and sells at a wholesale cost of approximately $450/Kg. A continuous chemical synthesis process employing high pressure hydrogenation of L-malic acid over a ruthenium-based catalyst in a fixed bed reactor has been developed for the commercial synthesis of *(S)*-3HBL at a capacity of 120 tonnes per year (Kwak, 2003; Rouhi, 2003); however, this process employs hazardous processing conditions and expensive catalyst and purification processes. The various other chemical and chemoenzymatic routes developed for 3HBL synthesis (Lee and Park, 2009) also suffer from similar disadvantages including the use of hazardous materials and processing conditions (Hollingsworth, 1999; Kumar et al., 2005), expensive starting materials, reagents and catalysts (Hollingsworth, 1999; Lee et al., 2008a; Nakagawa et al., 2006; Shin et al., 2005; Suzuki et al., 1999), and poor yield and formation of difficult to separate by-products (Kumar et al., 2005; Nakagawa et al., 2006; Park et al., 2004; Suzuki et al., 1999), driving up the cost of the product. Biosynthesis is expected to alleviate many of these problems and offer an elegant solution towards economical production of this valuable chemical; however, this requires the design of a novel biosynthetic pathway (Dhamankar and Prather, 2011; Martin et al., 2009).

To build a biosynthetic pathway towards 3HBL, Martin (2009) proposed focusing on its free hydroxyacid form (3,4-DHBA) and using the basic reactions of the polyhydroxyalkanoate synthesis pathway for the synthesis of 3,4-DHBA. Reactions of the natural poly-3HB or poly-3HB-co-3HV pathways in organisms such as *C. necator* had been similarly previously used for the synthesis of 3HB and 3HV (Gao et al., 2002; Tseng et al., 2010b; Tseng et al., 2009b). In these reports, 3HB or 3HV synthesis begins

with the condensation of two acetyl-CoA molecules or acetyl-CoA and propionyl-CoA, respectively, through the action of a thiolase enzyme (PhaA or BktB). The β-keto group is subsequently reduced to an alcohol by one of two 3-hydroxybutyryl-CoA dehydrogenases, PhaB or Hbd, yielding the *(R)* or *(S)*-enantiomer, respectively. Finally, CoA cleavage by the enzyme pair phosphotransbutyrylase (Ptb) and butyrate kinase (Buk) (Gao et al., 2002; Liu and Steinbuchel, 2000), or by thioesterase II (TesB) (Liu et al., 2007; Naggert et al., 1991; Tseng et al., 2009b) yields the free acid. TesB is capable of hydrolyzing both enantiomers of 3HB-CoA, while the Ptb-Buk enzyme system is specific to the *(R)*-enantiomer. Unlike acetyl-CoA, propionyl-CoA is not naturally produced in *E. coli* in significant quantities. In Tseng *et al* (Tseng et al., 2010b), exogenously supplied propionate was intracellularly activated to propionyl-CoA using the Ptb-Buk enzymes, known to act reversibly to produce CoA-activated compounds (Liu and Steinbuchel, 2000).

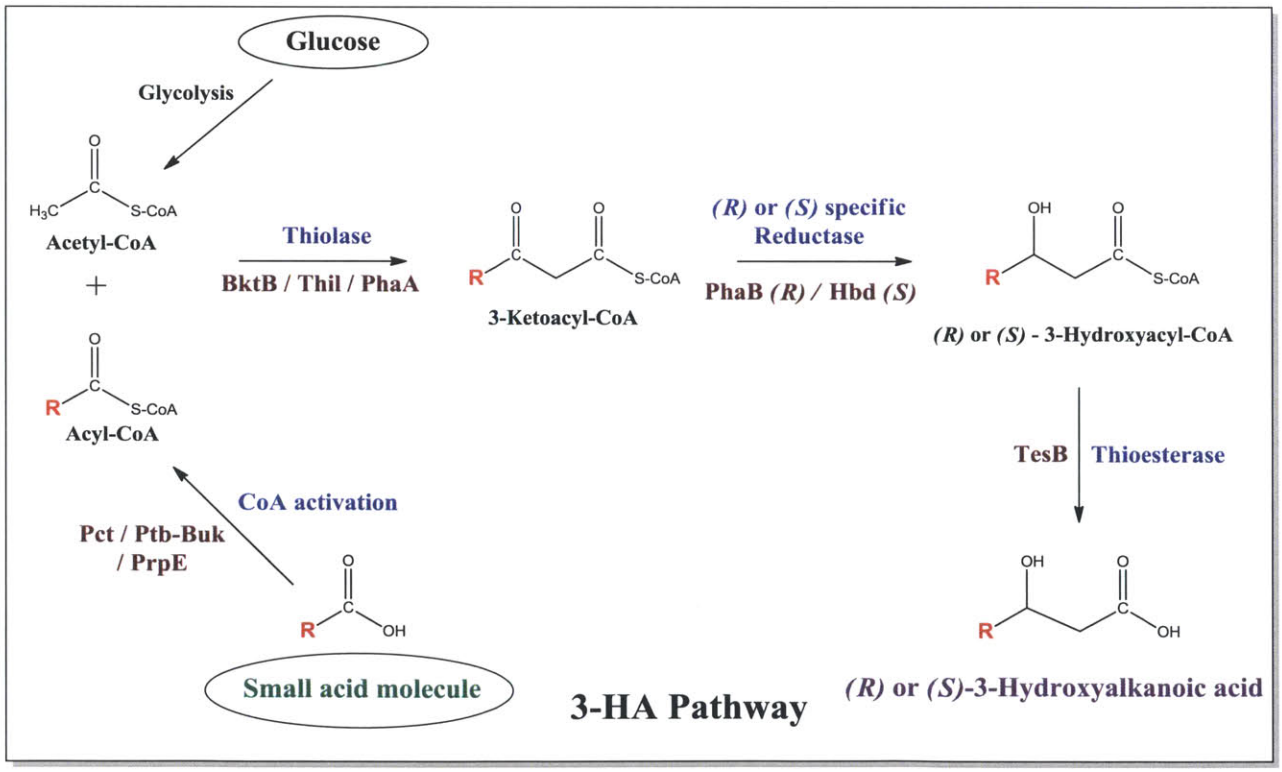

Figure 2-1 | The 3-hydroxyalkanoic acid synthesis platform pathway. The pathway employs 4 enzymes to catalyze the pathway reactions: 1) CoA activator 2) Thiolase 3) Stereospecific reductase and 4) Thioesterase. Highlighted in brown are enzymes from various organisms that have been tested as part of the platform pathway to catalyze the various reactions with various supplied small acid molecules.

The envisaged 3-hydroxyalkanoic acid synthesis pathway then (**Figure 2-1**) employs four key reactions: 1) an intracellular activation of the supplied small acid molecule to form its corresponding acyl-CoA thioester 2) a Claisen condensation reaction between the acyl-CoA and acetyl-CoA catalyzed by the thiolase 3) stereospecific reduction of the keto group in the 3-ketoacyl-CoA intermediate resulting in the corresponding *(R)* or *(S)*-3-hydroxyacyl-CoA intermediate catalyzed by a reductase, and 4) CoA cleavage by a thioesterase to give the *(R)/(S)*-3-hydroxyacid product. The platform is expected to allow the synthesis of 3-hydroxyacids, the carbon chain length, branching and substituents in which may be controlled by the 'R' group connected to the carboxyl in the supplied small acid molecule (**Figure 2-2**).

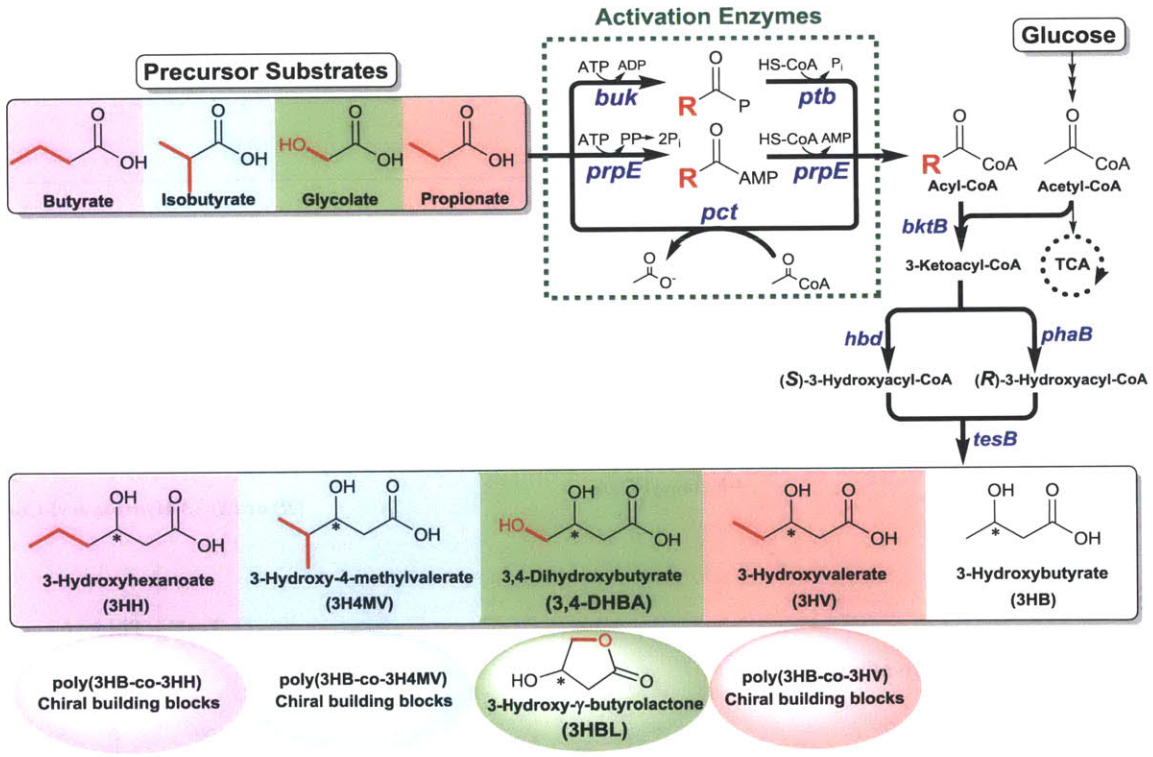

Figure 2-2 | Schematic representation of the 3-hydroxyacid pathway. Genes in blue were overexpressed, including one of the activation enzymes (encoded by *pct*, *prpE*, or *ptb-buk*), one thiolase enzyme (encoded by *bkt*B), one of two 3-hydroxybutyryl-CoA reductases (encoded by *pha*B or *hbd*), and one thioesterase enzyme (encoded by *tes*B). The carbon sources used in the system were glucose and one precursor substrate depicted enclosed by a rectangular box. The precursor substrates and their corresponding products of 3-hydroxyalkonoic acids are colour-coded accordingly.

Martin (2009), demonstrated as proof of concept the biosynthesis of 3,4-DHBA and 3HBL using glycolic acid as the small acid substrate, using a combination of pathway enzymes consisting of Pct (from *M. elsdenii*) as an activator, BktB (from *C. necator*) as a thiolase, PhaB (from *C. necator*) as a reductase and TesB (from *E. coli*) as a thioesterase. Following this initial demonstration of synthesis of 3,4-DHBA, we were interested in further exploring this pathway to evaluate its potential for the synthesis of other 3HAs in the C4 to C6 carbon chain length range from various small acid molecules in addition to improving the synthesis of 3,4-DHBA from glycolate. Pathway enzymes were thus selected based on evidence of activity towards molecules of this carbon chain length. Enzymes involved in PHA biosynthesis and butanol synthesis pathways are known to catalyze the reactions of interest with C4 and C5 intermediates and were a natural first choice in this initial investigation. Glycolate (C2), propionate (C3), butyrate (C4) and isobutyrate (branched C4) were selected as the initial set of test substrates to assay for the synthesis of the corresponding 3HAs.

Pathway enzyme selection

The substrate range of the thiolase enzyme catalyzing the initial carbon-carbon bond-forming reaction is a key element of the pathway. The ability of known thiolases such as BktB or PhaA (from *C. necator*) or ThiI (from *C. acetobutylicum*) to catalyze this reaction with different substrates was unknown. It was however known that the thiolase BktB exhibits a broader substrate range than PhaA (Slater et al., 1998) or ThiI (Martin, 2009) and was hence selected as the primary thiolase enzyme in this study. PhaB and Hbd, previously used in 3HB and 3HV synthesis were employed as *(R)* and *(S)* specific reductases respectively while the broad substrate range thioesterase TesB was employed for CoA cleavage. For the intracellular synthesis of acyl-CoA from the corresponding supplied small acid molecule, three different CoA-activation systems were investigated. These included propionyl-CoA transferase (Pct), a broad substrate-specificity enzyme from *Megasphaera elsdenii* (Schweiger and

Buckel, 1984; Taguchi et al., 2008) that exchanges CoA moieties between short-chain organic acids including acetyl-CoA, and propionyl-CoA synthetase (PrpE) from *Salmonella typhimurium* LT2 (Liu et al., 2009), in addition to the enzyme pair phosphotransbutyrylase (Ptb) and butyrate kinase (Buk) (Gao et al., 2002; Liu and Steinbuchel, 2000). In addition to studying 3,4-DHBA synthesis from glycolate, we further explored extensibility of the pathway by feeding butyrate to determine whether longer chain (C6) hydroxyacids could be produced and isobutyrate to examine the potential for synthesis of branched chain hydroxyacids.

While the different pathway enzyme combinations tested in this preliminary investigation showed considerable differences in *in vivo* activities in synthesizing products from the supplied substrates, the combination consisting of Pct, BktB, PhaB, and TesB was found to be most versatile and allowed synthesis of 5 novel products using the platform, including 3,4-DHBA, 3HBL, 2,3-dihydroxybutyric acid (2,3-DHBA), 3-hydroxyhexanoic acid (3HH) and 3-hydroxy-4-methylvaleric acid (3H4MV). Of particular importance in this investigation was the discovery of the synthesis of 2,3-DHBA from glycolate alongside 3,4-DHBA and 3HBL, which led to the unravelling of a novel activity associated with the thiolase BktB that may be effectively used to further exploit the carbon-carbon bond forming potential of this pathway for the synthesis of additional value-added products as discussed later. This also led to a revision of Martin's initial estimates of 3,4-DHBA and 3HBL titers and yield from the pathway.

2.2. Methods and Materials

2.2.1. Strains and plasmids

E. coli DH10B (Invitrogen, Carlsbad, CA) and ElectroTen-Blue (Stratagene, La Jolla, CA) were used for transformation of cloning reactions and propagation of all plasmids. *E. coli* MG1655 (DE3 Δ*end*A Δ*rec*A) has been described previously (as strain HCT10 (Tseng et al., 2010b)) and was used as the production host for hydroxyacid synthesis.

Genes from *C. acetobutylicum* ATCC 824 (*ptb-buk* and *hbd*), *C. necator* ATCC 17699 (*bkt*B and *pha*B), *E. coli* K-12 (*tes*B, *ycd*W, and *ace*A-*ace*K), *M. elsdenii* (*pct*), *S. typhimurium* LT2 (*prp*E) and *B. subtilis* 3610 (*ptb* and *buk*) were obtained by polymerase chain reaction (PCR) using genomic DNA (gDNA) templates. All gDNAs were prepared using the Wizard Genomic DNA Purification Kit (Promega, Madison, WI). Custom oligonucleotides (primers) were purchased for all PCR amplifications (Sigma-Genosys, St. Louis, MO) as listed in **Table 2-2**. In all cases, Phusion High Fidelity DNA polymerase (Finnzymes, Espoo, Finland) was used for DNA amplification. Restriction enzymes and T4 DNA ligase were purchased from New England Biolabs (Ipswich, MA). Recombinant DNA techniques were performed according to standard procedures.

Two co-replicable vectors, pETDuet-1 and pCDFDuet-1 (Novagen, Darmstadt, Germany), were used for construction of the 3-hydroxyacid pathway plasmids. The sites used for cloning the genes are underlined in **Table 2-2**. PCR products were digested with the appropriate restriction enzymes and ligated directly into similarly digested vectors. The *ptb-buk* fragment was generated by *Eco*RI and *Not*I digestion of pCDF-PB (Tseng et al., 2009b). The *B. subtilis ptb* and *buk* genes were cloned into an artificial operon using Splicing by Overlap Extension (SOE) PCR (Heckman and Pease, 2007; Horton et al., 1989) to mimic the natural *C. acetobutylicum ptb-buk* operon. For the construction of this artificial operon, the *ptb* and *buk* genes from *B. subtilis* were first separately PCR amplified using *ptb(Bs)*-FP-EcoRI

and *ptb(Bs)*-RP and *buk(Bs)*-FP and *buk(Bs)*-RP-NotI respectively (**Table 2-2**). Purified PCR amplified fragments were then added in equimolar concentrations to a third PCR reaction without primers in order to initially splice the two fragments using Splicing by Overlap Extention (SOE) PCR over 3 cycles. The intergenic sequence between *C. acetobutylicum ptb* and *buk* genes in the natural *ptb-buk* operon was used as the intergenic overlapping sequence between the two genes for SOEing in this artificial operon. Finally a second set of forward *ptb* and reverse *buk* primers (*ptb-buk(Bs)*-FP-EcoRI and *ptb-buk(Bs)*-RP-NotI) were added to the same PCR reaction to amplify the complete operon and generate a *B. subtilis ptb-buk* fragment.

Ligation reactions using pETDuet-1 as a vector were used to transform *E. coli* DH10B, while ligations using pCDFDuet-1 were used to transform *E. coli* ElectroTen-Blue. One thiolase (*bkt*B) and one of two 3-hydroxybutyryl-CoA reductases (*pha*B and *hbd*) were cloned into pETDuet-1. The pCDFDuet-based plasmids contained one of four CoA-activation genes (*pct*, *ptb-buk*, *ptb-buk(Bs)* and *prp*E) and one thioesterase (*tes*B). All constructs were confirmed to be correct by restriction enzyme digestion and nucleotide sequencing. Once all plasmids were constructed, one pETDuet-based plasmid and one pCDFDuet-based plasmid were used to co-transform *E. coli* MG1655 (DE3 Δ*endA* Δ*recA)* (MG0) to create hydroxyacid production strains.

Table 2-1 | *E. coli* strains and plasmids used in the 3-hydroxyacid pathway

Name	Relevant Genotype	Reference
Strains		
DH10B	F⁻ *mcr*A Δ(*mrr-hsd*RMS-*mcr*BC) ϕ80*lacZ*ΔM15 Δ*lacX74 recA1 endA1 araD139*Δ(*ara, leu*)7697 *galU galK* λ⁻ *rpsL nupG*	Invitrogen
ElectroTen-Blue	Δ(*mcrA*)*183* Δ(*mcrCB-hsdSMR-mrr*)*173 endA1 supE44 thi-1 recA1 gyrA96 relA1 lac* Kan^r [F′ *proAB lacI*^{q}ZΔM15 Tn*10* (Tet^r)]	Stratagene
MG1655	F⁻ λ⁻ *ilvG- rfb-50 rph-1*	ATCC 700926
MG0	MG1655 (DE3) Δ*end*A Δ*rec*A	Tseng 2010
MG1	MG0 containing pET/bktB/hbd and pCDF/pct/tesB	This study
MG2	MG0 containing pET/bktB/hbd and pCDF/prpE/tesB	This study
MG3	MG0 containing pET/bktB/hbd and pCDF/ptb-buk/tesB	This study
MG3B	MG0 containing pET/bktB/hbd and pCDF/(ptb-buk)$_B$/tesB	This study
MG4	MG0 containing pET/bktB/phaB and pCDF/pct/tesB	This study
MG4A	MG0 containing pET/phaA/phaB and pCDF/pct/tesB	This study
MG4B	MG0 containing pET/thil/phaB and pCDF/pct/tesB	This study
MG5	MG0 containing pET/bktB/phaB and pCDF/prpE/tesB	This study
MG6	MG0 containing pET/bktB/phaB and pCDF/ptb-buk/tesB	This study
MG6B	MG0 containing pET/bktB/phaB and pCDF/(ptb-buk)$_B$/tesB	This study
MG7	MG0 containing pETDuet-1 and pCDFDuet-1	This study
Plasmids		
pETDuet-1	ColE1 (pBR322) *ori*, *lacI*, T7*lac*, Amp^R	Novagen
pCDFDuet-1	CloDF13 *ori*, *lacI*, T7*lac*, Strep^R	Novagen
pET/bktB/hbd	pETDuet-1 harboring *bkt*B from *C. necator* ATCC 17699 and *hbd* from *C. acetobutylicum* ATCC 824	This study
pET/bktB/phaB	pETDuet-1 harboring *bkt*B and *pha*B from *C. necator* ATCC 17699	This study
pET/phaA/phaB	pETDuet-1 harboring *phaA* and *pha*B from *C. necator* ATCC 17699	Martin (2009)
pET/thil/phaB	pETDuet-1 harboring *thil gene from C. acetobutylicum* ATCC 824 and *pha*B from *C. necator*	Martin (2009)
pCDF/pct/tesB	pCDFDuet-1 harboring *pct* from *M. elsdenii*, and *tes*B from *E. coli* MG1655	This study
pCDF/prpE/tesB	pCDFDuet-1 harboring *prp*E from *S. typhimurium* LT2, and *tes*B from *E. coli* MG1655	This study
pCDF/ptb-buk/tesB	pCDFDuet-1 harboring a *ptb-buk* operon from *C. acetobutylicum* ATCC 824, and *tes*B from *E. coli* MG1655	This study
pCDF/(ptb-buk)$_{Bs}$/tesB	pCDFDuet-1 harboring a *ptb-buk* artificial operon from *Bacillus subtilis*, and *tes*B from *E. coli* MG1655	This study

Table 2-2 | List of DNA oligonucleotide primers used in the cloning of genes for the 3-hydroxyacid pathway

Primer names correspond to the name of the gene or vector backbone that the primer amplifies, whether the primer is the forward primer (FP) or reverse primer (RP) of that gene, and the restriction site incorporated into the primer sequence for cloning (restriction sites used for cloning are underlined). For primers used to amplify the *ptb(Bs)* and *buk (Bs)* genes from *B. subtilis* for the construction of the *ptb-buk* operon, sequences indicated in bold correspond to parts of the complementary overlapping regions for SOEing PCR while nucleotides in italics correspond to downstream sequences added to mimic the *C. acetobutylicum ptb-buk* construct.

Primer	Sequence 5'→3'
bktB-FP-NcoI	GACACCATGGGCATGACGCGTGAAGTGGTAG
bktB-RP-EcoRI	GACAGAATTCTCAGATACGCTCGAAGATGG
hbd-FP-NdeI	TATCCATATGAAAAAGGTATGTGTTATAGGTGC
hbd-RP-XhoI	GACACTCGAGTTATTTTGAATAATCGTAGAAACCTTTTC
phaB-FP-NdeI	GACACATATGACTCAGCGCATTGC
phaB-RP-XhoI	GACACTCGAGTCAGCCCATGTGCAGG
pct-FP-EcoRI	GACAGAATTCATGAGAAAAGTAGAAATCATTACAGCTG
pct-RP-PstI	GACACTGCAGTTATTTTTTCAGTCCCATGGG
prpE-FP-EcoRI	ATAGAATTCCGTGATGTCTTTTAGCG
prpE-RP-NotI	TATGCGGCCGCTATTCTTCGATCGCC
tesB-FP-NdeI	GACACATATGAGTCAGGCGCTAAAAAAAT
tesB-RP-XhoI	GACACTCGAGTTAATTGTGAATTACGCATCACC
ptb(Bs)-FP-EcoRI	AAAAGAATTCACCAATGAAGCTGAAAGATTTAATC
ptb(Bs)-RP	**GTTAACATTCCTCCACTTAACTTTAAT**AATGTGTGTATTCTTCA GATG
buk(Bs)-FP	**ATTAAAGTTAAGTGGAGGAATGTTAAC**ATGGGCAGCAGCC
buk(Bs)-RP-NotI	AAAAGCGGCCGC*AAGCTTGTCGACGGTACTGGTTATATTATA TTATTTATGACT*ATTCAATACGATATTGTTTGG
ptb-buk(Bs)-FP-EcoRI	AAAGAATTCACCAATGAAGC
ptb-buk(Bs)-RP-NotI	AAAAGCGGCCGCACT

2.2.2. Culture conditions

Seed cultures of the recombinant *E. coli* strains (**Table 2-1**) were grown in LB medium at 30°C overnight, and were used to inoculate 50 mL LB medium supplemented with 10 g/L glucose at an inoculation volume of 2% in 250 mL flasks. Due to HPLC peak overlapping between 3HH and LB

components, 3HH biosynthesis was conducted in M9 minimal medium supplemented with 10 g/L glucose where seed cultures were washed and re-suspended in M9 minimal medium before inoculation. The shake flask cultures were then incubated at 30°C on a rotary shaker at 250 RPM. Once the cells reached mid-exponential phase (when OD_{600} reached 0.8-1.0), cultures were supplemented (final concentrations in parentheses) with IPTG (1 mM) for induction of gene expression and one of the precursor substrates: neutralized propionate (15 mM), butyrate (15 mM), isobutyrate (15 mM), and glycolate (40 mM). In all cases, culture medium was supplemented with 50 mg/L ampicillin and 25 mg/L streptomycin to provide selective pressure for plasmid maintenance.

1 mL of culture was withdrawn every 24 h for up to 96 h for HPLC and HPLC/MS analysis. Titres of 3-hydroxyacids reached a plateau at 72 h and there was essentially no difference in the titres between 72 h and 96 h; accordingly, only the peak titres observed at 72 h were reported. In general, experiments were performed in triplicates, and data are presented as the averages and standard deviations of the results.

2.2.3. Metabolite analysis

Culture samples were pelleted by centrifugation and aqueous supernatant collected for HPLC analysis using an Agilent 1200 series instrument with a refractive index detector (RID). Analytes were separated using an Aminex HPX-87H anion-exchange column (Bio-Rad Laboratories, Hercules, CA) and a 5 mM H_2SO_4 mobile phase. Glucose, propionate, butyrate, isobutyrate, glycolate, acetate, 3-hydroxybutyrate, 3-hydroxyvalerate, 3-hydroxyhexanoate, and (*S*)-3-hydroxy-γ-butyrolactone were quantified using commercial standards by linear interpolation from calibration of external standards.

Due to the absence of a commercially available standard, the 3,4-DHBA standard used for HPLC analysis was prepared from (*S*)-3-hydroxy-γ-butyrolactone by saponification at 37°C for 3 hours at pH > 10 using 10N sodium hydroxide. Complete conversion of (*S*)-3HBL to (*S*)-3,4-DHBA (as confirmed by

disappearance of the 3HBL peak on the HPLC time trace) was observed during this treatment. Additionally, 3,4-DHBA and 2,3-DHBA synthesis was also confirmed using HPLC/MS analysis on an Agilent 1100 series instrument equipped with 6120 Quadrapole MS with multi-mode source and an Aminex HPX-87H column with 25 mM ammonium formate as the mobile phase. The ammonium adduct of 3,4-DHBA was detected at an m/z ratio of 138.1 to confirm 3,4-DHBA synthesis in the samples. The ammonium adduct of deuterium labelled 3,4-DHBA formed from deuterium labelled 2,2-D2-glycolic acid was detected at an m/z ratio of 140.1 while that of deuterium labelled 2,3-DHBA was detected at an m/z ratio of 139.1. Preparative chromatography (as described below) was used to co-purify 2,3-DHBA and 3,4-DHBA from the culture supernatants. The identity of 3,4-DHBA and 2,3-DHBA was confirmed via ^{1}H, ^{13}C, Heteronuclear Single Quantum Coherence (HSQC), and Heteronuclear Multiple Bond Correlation (HMBC) NMR using a Varian 500 MHz spectrometer. Due to co-elution of 2,3-DHBA with 3,4-DHBA during separation of culture supernatants on the Aminex Column during HPLC analysis, the 3,4-DHBA and 2,3-DHBA titres were estimated indirectly as described below.

3H4MV was analyzed using HPLC/MS since a commercial standard was not available. A Zorbax SB-Aq alkyl bonded phase column (Agilent Technologies, Wilmington, DE) with a 25 mM, pH 3 ammonium formate mobile phase was used to separate 3H4MV for detection with an Agilent 1100 series instrument equipped with either RID or 6120 Quadrapole MS with multi-mode source. The commercial 3HH isomer was used with RID to estimate the concentration of 3H4MV in supernatant samples. The ammonium adducts of 3H4MV and 3HH were detected at an m/z of +150.1 to confirm the presence of the branched isomer.

2.2.4. Purification and NMR analysis of 3,4-DHBA and 2,3-DHBA

Preparative chromatography was used to purify 2,3-DHBA and 3,4-DHBA from the culture supernatants for NMR analysis. Strain MG4 was cultured in minimal medium supplemented with 10 g/L

glucose and 40 mM glycolate. 72 hours post induction with IPTG (1mM), the entire culture was harvested by centrifugation to separate the culture supernatant. The pH of the culture supernatant was adjusted to 7 and 40 mL of this culture supernatant was then concentrated by evaporation of water under a stream of N_2 for 24 hours to reduce the volume down to 1 mL. The resulting concentrated culture supernatant was repeatedly injected onto an Aminex HPX-87H column (50 injections of 20 µL each) and resolved into its various components using 5 mM sulfuric acid as the mobile phase. The fraction containing the two DHBAs was collected from the column outlet and the pH was adjusted back to 7 using 10 N NaOH. The resulting mixture was then dried down completely to obtain a mixture of 2,3-DHBA and 3,4-DHBA in the dry solid form (approximately 5 mg). The mixture of DHBAs was then re-dissolved in D_2O for NMR analysis.

^{1}H, ^{13}C, HSQC, and HMBC NMR spectra were recorded in the MIT Department of Chemistry Instrumentation Facility (DCIF) on a Varian 500 MHz spectrometer, referencing to the residual proton resonance of the deuterated solvent. ^{1}H, HSQC, and HMBC spectra were acquired with an inverse triple resonance probe while ^{13}C spectrum was acquired with a broadband probe (see **Appendix A1** for spectra). All chemical shifts are reported using the standard δ notation in parts per million.

2.2.5. Quantification of 3,4-DHBA and 2,3-DHBA

The co-elution of 2,3-DHBA with 3,4-DHBA during HPLC analysis using an Aminex column and 5 mM sulfuric acid as the mobile phase prevented direct quantification of 3,4-DHBA in the samples by simply integrating the HPLC time trace for peak area. 3HBL on the other hand may be directly quantified by integrating the HPLC time traces. While the HPLC / MS analysis using ammonium formate as a mobile phase allowed resolution of 2,3-DHBA and 3,4-DHBA, the excessively noisy RID signal with this mobile phase impeded direct 3,4-DHBA quantification. Thus, to quantify 3,4-DHBA, the 3HBL titres before and after acid treatment were used in conjunction with the known equilibrium constant (determined as

described in legend to **Figure 2-6**) and following equations to estimate the 3,4-DHBA concentration before and after acid treatment.

$$[\text{DHBA}]_{\substack{\text{post acid}\\ \text{treatment}}} = \frac{[\text{3-HBL}]_{\substack{\text{post acid}\\ \text{treatment}}}}{\text{K}}$$

$$[\text{DHBA}]_{\substack{\text{before acid}\\ \text{treatment}}} = [\text{DHBA}]_{\substack{\text{post acid}\\ \text{treatment}}} + [\text{3-HBL}]_{\substack{\text{post acid}\\ \text{treatment}}} - [\text{3-HBL}]_{\substack{\text{before acid}\\ \text{treatment}}}$$

Since the prescribed acid treatment results in a drop in the pH of the culture supernatants from about 5.5 (before acid treatment) to 0.7 (post acid treatment), a value of K of about 2 (which results in more conservative estimates of $[\text{DHBA}]_{\text{post acid treatment}}$ than that computed using the experimentally observed highest value of 1.9 observed for the 3,4-DHBA standards at a pH of 0.7 (**Figure 2-6**)) was used in the above equations. The calculation doesn't account for any 3,4-DHBA that may be lost due to degradation or polymerization during acid treatment and hence also results in a conservative estimate of 3,4-DHBA concentration. Due to the absence of a standard, 2,3-DHBA was quantified using the 3,4-DHBA standard, assuming similar response behaviour for the two isomers detected with the RID, based on the residual post acid treatment peak area after subtracting the peak area attributable to 3,4-DHBA.

2.3. Results

2.3.1. Validation of pathway enzyme expression through production of 3HV

Propionate is the natural substrate for Pct and PrpE, and the ability of Ptb-Buk to activate propionate had been previously demonstrated (Tseng et al., 2010b). To validate the functional expression of all pathway enzymes and to gain insights into differences in their *in vivo* activities and specificities, propionate and glucose were supplied to cultures of recombinant *E. coli* cells expressing one of the three activators (*pct*, *prp*E, or ptb-*buk*), one of two 3-hydroxybutyryl-CoA reductases (*pha*B or *hbd*), *tes*B, and *bkt*B from their respective plasmids. 3HV was produced in all six recombinant strains, confirming functional expression of all pathway genes (Figure 2-3 and Figure 2-4). Among the three activation enzymes, Pct resulted in the highest *(S)*-3HV titres, up to 18.00 ± 0.23 mM (2130 ± 27 mg/L), when Hbd was utilized as the reductase (strain MG1), followed by Ptb-Buk (strain MG3) and PrpE (strain MG2). In the case of *(R)*-3HV biosynthesis employing PhaB as the reductase, all three activators were generally comparable, with up to 19.65 ± 1.81 mM (2320 ± 213 mg/L) produced by strain MG4. The choice of reductase influenced both final 3HV titres and 3HV production rates as strains utilizing PhaB (strains MG4-6) yielded more 3HV at a faster rate than strains employing Hbd (strains MG1-3) (**Figure 2-3** and **Figure 2-4**).

The differences in 3HV titers for the 3 activators with Hbd as a reductase (strains MG1-3) may be hypothesized to be the combined effect of a limitation in Hbd's activity on the 3-ketovaleryl-CoA intermediate and differences in the intracellular propionyl-CoA levels and resulting reaction driving force due to differences in the activation mechanisms. It is also interesting to note that the two ATP dependent activation systems (PrpE in strain MG2 and Ptb-Buk in strain MG3) result in lower *(S)*-3HV titers in comparison to the ATP independent activator Pct (strain MG1) for which the propionyl-CoA levels are expected to only be a function of the intracellular acetyl-CoA and propionate levels at equilibrium. 3HB is a by-product of the 3-hydroxyacid pathway since BktB retains high activity for the

condensation of two acetyl-CoA molecules (Slater et al., 1998) to produce acetoacetyl-CoA, the natural substrate of both PhaB and Hbd. 3HB production levels were affected by the specific combination of enzymes employed (Figure 2-5). In all of the experiments reported here, much less 3HB was detected in strains utilizing Pct for CoA activation (Figure 2-5, strains MG1 and MG4) compared to strains utilizing Ptb-Buk or PrpE. Pct can transfer the CoA moiety from acetyl-CoA to other short organic acids (Schweiger and Buckel, 1984). This CoA transfer should significantly reduce intracellular acetyl-CoA concentrations, making the second-order condensation of two acetyl-CoA molecules less likely than the condensation of acetyl-CoA with another acyl-CoA (a first-order reaction with respect to acetyl-CoA). Thus, strains utilizing Pct achieved the highest selectivity towards both *(S)*-3HV and *(R)*-3HV (Figure 2-4), but produced the most acetate among the three activators examined (Figure 2-5) as a direct consequence of the transferase reaction.

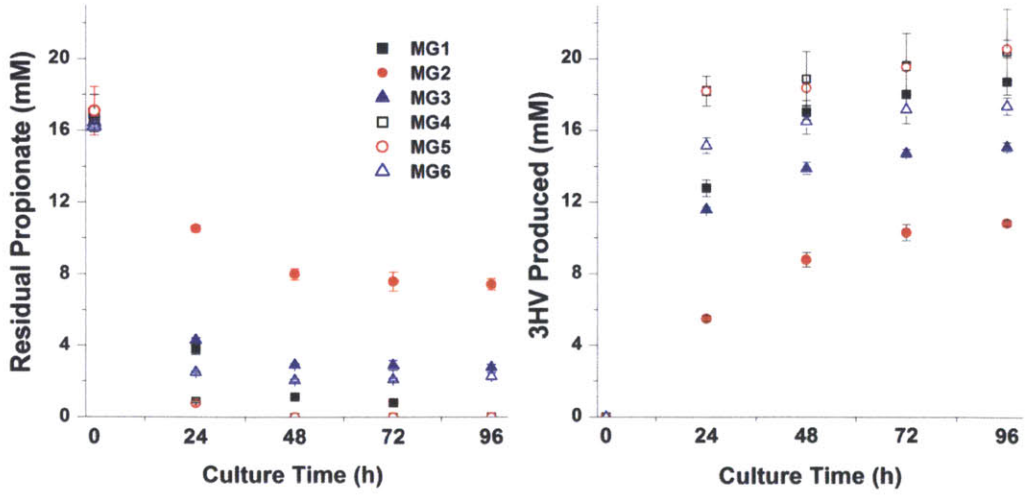

Figure 2-3 | Time course data for residual propionate and 3HV produced. Plots depict changes in titres of the precursor substrate propionate and the desired 3-hydroxyacid 3HV for the different strains up to 96h.

2.3.2. Production of 3,4-DHBA and 3HBL from glucose and glycolate

The platform pathway was designed to produce 3,4-DHBA from glycolate as a precursor (**Figure 2-2**). In cultures supplemented with glycolate and glucose, only the *pct*-expressing strains, MG1 and MG4, produced 3,4-DHBA, while strains expressing the activators *prpE* and *ptb-buk* only synthesized 3HB and acetate (**Figure 2-4** and **Figure 2-5**).

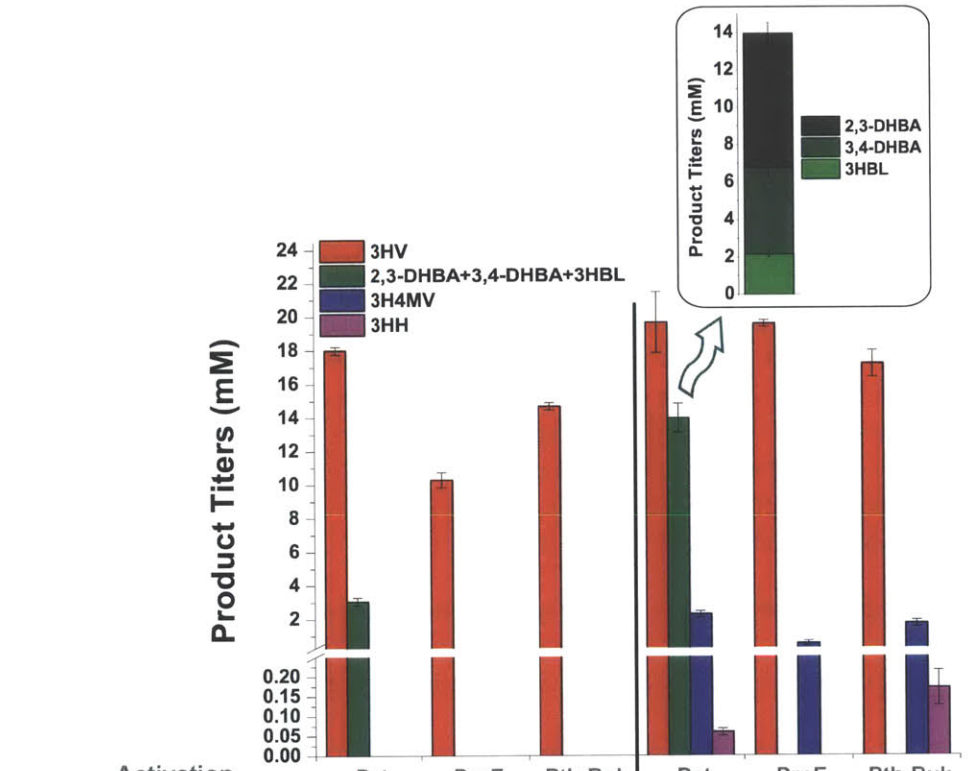

Activation	Pct	PrpE	Ptb-Buk	Pct	PrpE	Ptb-Buk
Reduction		Hbd			PhaB	
***E. coli* Strain**	**MG1**	**MG2**	**MG3**	**MG4**	**MG5**	**MG6**
3HV/3HB	3.60	0.37	0.85	1.46	0.76	0.68
(2,3-DHBA+3,4-DHBA+3HBL)/3HB	1.05	0.00	0.00	2.58	0.00	0.00
3H4MV/3HB	0.00	0.00	0.00	0.21	0.02	0.15
3HH/3HB	0.00	0.00	0.00	0.04	0.00	0.03

Figure 2-4 | Biosynthesis of 3-hydroxyacids through pathways with different genes and feeding of various precursor substrates. Shake-flask production of chiral 3-hydroxyacids at 72h. The various recombinant strains are described in **Table 2-1**. Production of 3HV (red bars), 2,3-DHBA+3,4-DHBA+3HBL (green bars), 3H4MV (blue bars) and 3HH (pink bars) was achieved with supplementation of propionate, glycolate, isobutyrate and butyrate, respectively, in addition to glucose. Data are presented as the mean ± s.d. (n=3). The specific activation enzymes and reductases used in each pathway are shown on the x-axis. Product selectivity, defined as the molar ratio of the quantity of desired 3-hydroxyacid to the quantity of concomitant product of 3HB, is shown below the x-axis. Inset shows breakdown of 2,3-DHBA, 3,4-DHBA and 3-HBL synthesized by strain MG4. 2,3-DHBA was below the limit of quantitation for strain MG1. **Table 2-3** shows the product yields on the supplied substrates.

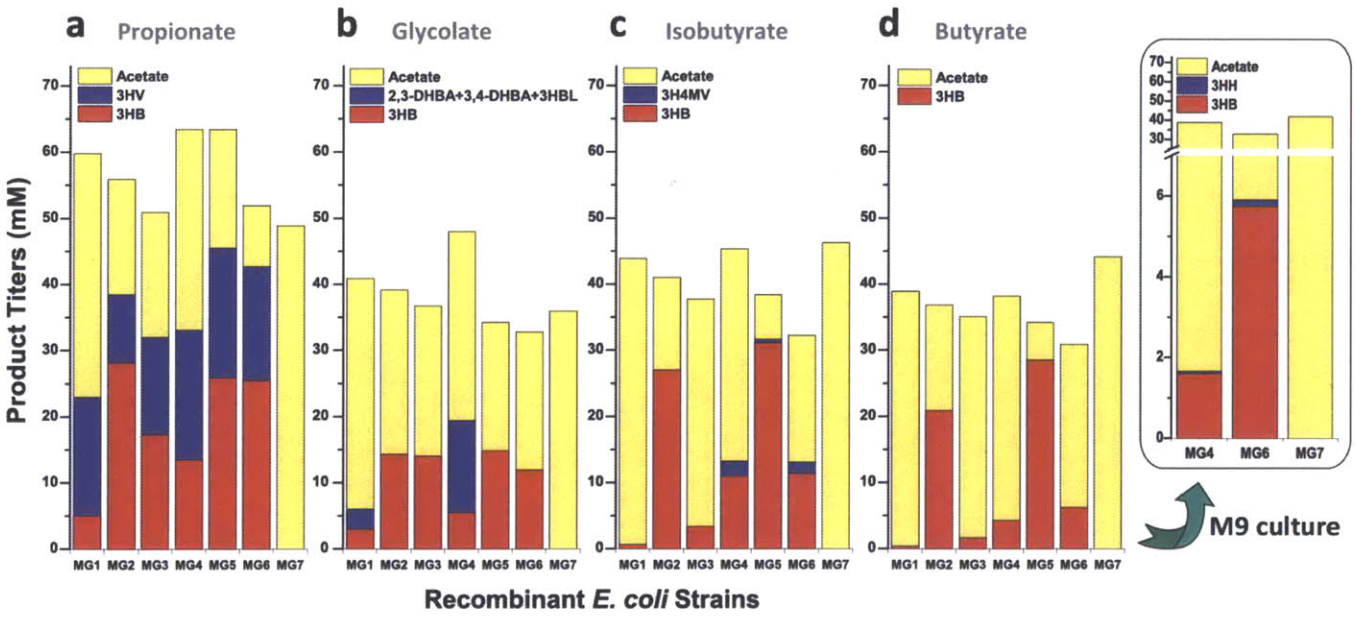

Figure 2-5 | Metabolite profile of the various recombinant E. coli cultures supplemented with various precursor substrates Metabolite profile of major products, including the desired 3-hydroxyacid, 3HB, and acetate, from various combinations of pathway enzymes supplemented with various precursor substrates ((a) propionate; (b) glycolate; (c) isobutyrate; and (d) butyrate). The specific recombinant strains used are shown on the x-axis (**Table 2-1**). As mentioned in the **Section 2.2.2.**, 3HH cannot be resolved during HPLC separation from one of the LB peaks; hence 3HH titers were not plotted for LB cultures in (d). The inset in (d) shows titers for M9 cultures of the two 3HH producing strains MG4 and MG6 and the control strain MG7.

Unexpectedly, these cultures also directly produced small quantities of 3HBL. The lactone could be formed either due to direct spontaneous lactonization of the 3,4-dihydroxybutyryl-CoA intermediate or from free 3,4-DHBA upon equilibration under the culture conditions. If the former were true, then elimination of TesB from the pathway should result in increased 3HBL synthesis. However, Martin (2009) had observed that in strains not expressing the *tes*B gene, 52% more 3HBL and 96% less 3,4-DHBA was produced. Moreover, in the present study, equilibration of 3,4-DHBA standards under final culture conditions (pH≈5.5, 30˚C) did not result in detectable lactonization of 3,4-DHBA to 3HBL. These results support the hypothesis that 3HBL was produced by the direct cyclization of the 3,4-dihydroxybutyryl-CoA intermediate, occurring either spontaneously or catalysed by the action of an endogenous enzyme. A similar spontaneous lactonization is hypothesized to result in the synthesis of γ-butyrolactone from 4-hydroxybutyryl-CoA (Yim et al., 2011). The identity of 3,4-DHBA and 3HBL was

confirmed through HPLC and HPLC/MS analysis (see **Section 2.2.3.** and **Figure 2-8**). Strain MG4, expressing *pct* and *phaB* in addition to *bktB* and *tesB*, synthesized up to 4.62 ± 0.33 mM (555 ± 52 mg/L) of 3,4-DHBA and 2.17 ± 0.15 mM (221 ± 15 mg/L) of 3HBL. The total 3,4-DHBA and 3HBL titres estimated on a molar basis were about two fold higher with PhaB as a reductase than with Hbd (**Figure 2-4**), indicating limitations associated with the activity of Hbd towards the non-natural substrate 4-hydroxy-3-ketobutyryl-CoA.

2.3.3. 3,4-DHBA to 3HBL conversion by acid treatment

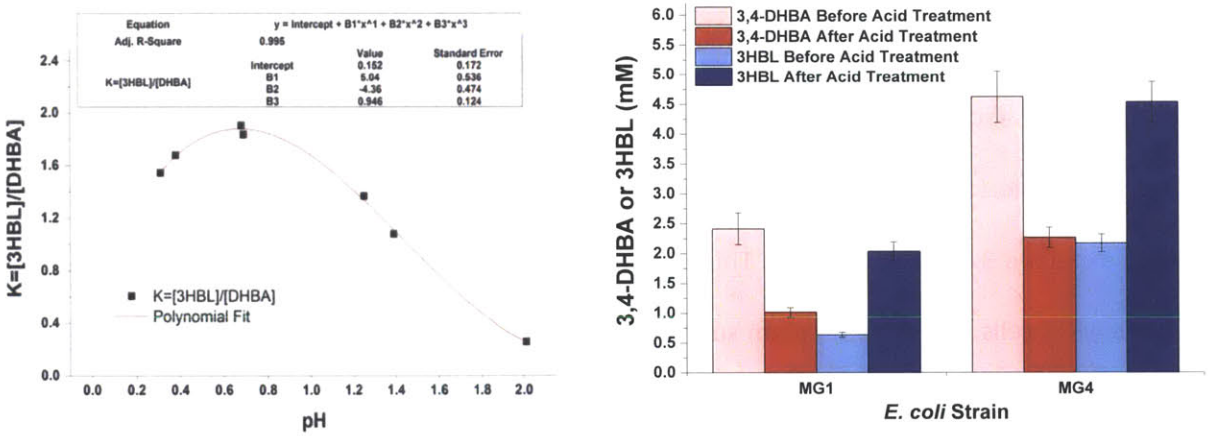

Figure 2-6 | Effect of pH on equilibrium between 3,4-DHBA and 3HBL. a) Subjecting 3,4-DHBA standards in LB to an overnight acid treatment at 37°C with increasing amounts of 6 N hydrochloric acid results in lactonization under decreasing pH conditions, with the equilibrium progressively shifting in favour of the lactone, as observed from the plot above. **b)** Culture supernatants from strains MG1 and MG4 were subjected to overnight treatment with 50 mM hydrochloric acid at 37˚C, allowing for effective conversion of 3,4-DHBA to 3HBL. Bars in light colours represent samples before acid treatment while bars in dark colours represent samples after acid treatment.

Lactonization is an acid-catalyzed reaction (Carey, 2000); hence, the equilibrium between 3,4-DHBA and 3HBL was expected to be governed by pH, amongst other factors. Overnight acid treatment of 3,4-DHBA standards in LB with 6 N hydrochloric acid at 37˚C resulted in a progressive shift in the equilibrium towards 3HBL with decreasing pH, with a maximum K of 1.9 (K=[3HBL]/[DHBA]) at a pH close to 0.7 (**Figure 2-6a**). Acid treatment of culture supernatants from strains MG1 and MG4 allowed effective conversion of 3,4-DHBA to 3HBL. Strain MG4 expressing the *pct-phaB* activator-reductase

combination showed the highest post-acid treatment 3HBL titres of 4.53 ± 0.33 mM (462 ± 35 mg/L) and corresponding 3,4-DHBA titres of 2.27 ± 0.17 mM (272 ± 20 mg/L) (**Figure 2-6b**).

2.3.4. Investigating a pathway side product: synthesis of 2,3-DHBA

In addition to 3,4-DHBA, strains MG1 and MG4 synthesized a second species that co-eluted with 3,4-DHBA during HPLC analysis (**Figure 2-7**). We first suspected the co-elution of this second species along with 3,4-DHBA due to a discrepancy in the elution times between the 3,4-DHBA standard and the suspected 3,4-DHBA peaks in the culture supernatants from MG1 and MG4 cultures, during HPLC separation on an Aminex HPX-87H column. As observed from the LC time trace in **Figure 2-7**, the 3,4-DHBA sample peaks from MG4 culture supernatants do not align exactly with the standard (there being a discrepancy of about 0.07 minutes between the two peak means). Also, the 3,4-DHBA peak is not a perfect symmetrical Gaussian curve. This caused us to suspect the co-elution of a second species along with the expected 3,4-DHBA product. This unidentified product was only observed to be synthesized by MG1 and MG4 cells in culture medium supplemented with glycolate. Moreover, just as with 3,4-DHBA synthesis, expression of the pathway enzymes Pct, BktB, PhaB or Hbd and TesB was essential for the synthesis of this product from glycolate and MG7 cell cultures fed with glycolate were unable to synthesize it.

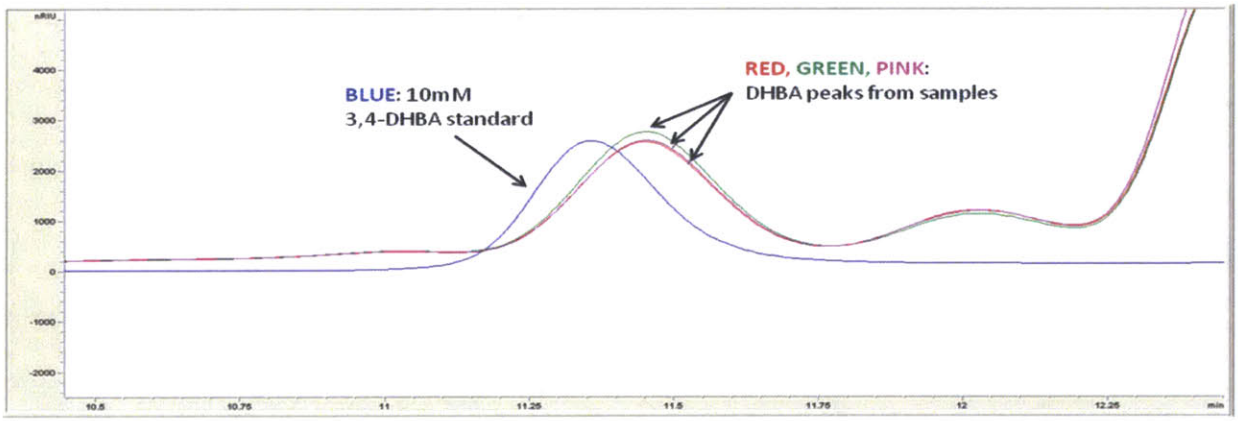

Figure 2-7 | Co-elution of a side product with 3,4-DHBA 3,4-DHBA peaks observed during HPLC separation of culture supernatant from MG4 cultures grown in LB supplemented with 1% glucose and fed with 40 mM glycolate (red, green, pink represent peaks from 3 replicates). 10 mM 3,4-DHBA standard is shown in blue. All samples were collected 72 hrs post induction (induction with 1 mM IPTG).

Our initial suspicion about co-elution was further confirmed by a discrepancy in the equilibrium molar ratio of 3HBL to 3,4-DHBA post acid treatment between the samples and standards. The overnight acid treatment of 3,4-DHBA standards in LB with 6 N hydrochloric acid at 37˚C results in a K value of 1.9 (K=[3HBL]/[DHBA]) at a pH close to 0.7 (**Figure 2-6a**). Similar acid treatment of culture supernatants from Strains MG1 and MG4 also allowed effective conversion of 3,4-DHBA to 3HBL. However, quantification of 3,4-DHBA and 3HBL using the HPLC time traces for the samples showed a much lower K of 0.6 post acid treatment with much of the suspected 3,4-DHBA HPLC peak remaining undiminished. Two possible causes for this discrepancy were hypothesized: a) altered equilibrium between 3,4-DHBA and 3HBL in the samples in the presence of other culture components and b) co-elution of a second species at the same position as 3,4-DHBA on the HPLC time trace resulting in erroneous 3,4-DHBA quantification.

To determine if culture medium components affected the equilibrium between 3,4-DHBA and 3HBL, a control experiment involving acid treatment of spent culture medium spiked with 3,4-DHBA standard was performed. The spent culture medium in this case was derived from a no glycolate control experiment involving strain MG4 cells grown in LB supplemented only with glucose and induced with IPTG (1 mM). In the absence of glycolate, induced MG4 cells were expected to synthesize metabolites similar to those observed for glycolate fed cultures (such as 3HB and acetate), but devoid of 3,4-DHBA, 3HBL and glycolate. Acid treatment of such spent culture broth spiked with 3,4-DHBA standard showed an equilibrium 3HBL to 3,4-DHBA molar ratio close to 1.9 allowing us to rule out culture components as a cause of the altered equilibrium. We thus concluded that the observed discrepancy was a result of erroneous over-estimation of 3,4-DHBA using the HPLC time traces due to co-elution of a second species.

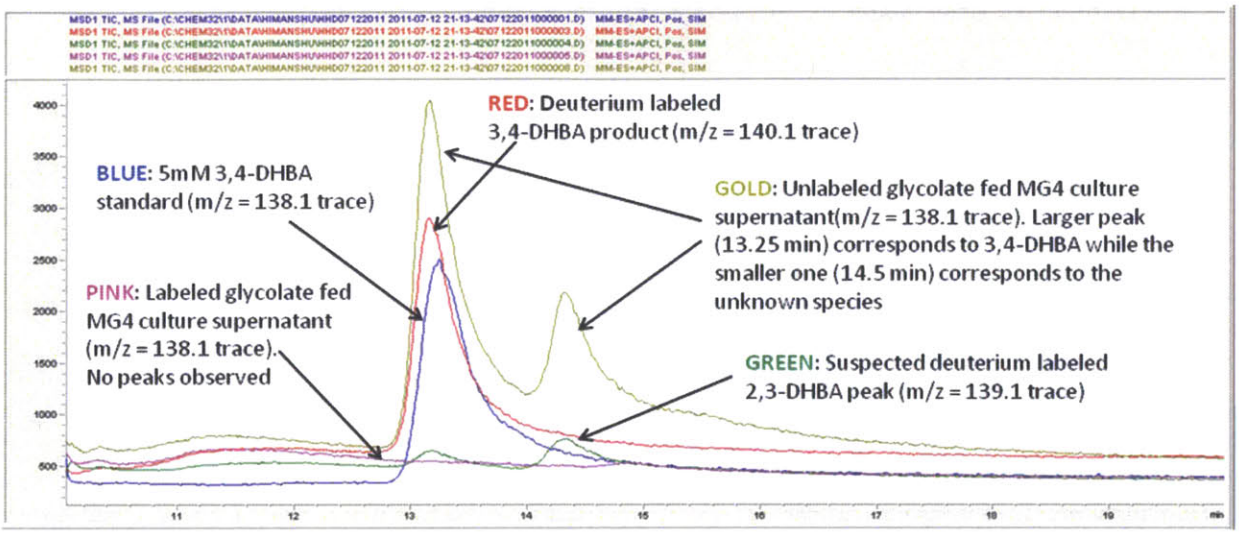

Figure 2-8 | HPLC – MS analysis time traces for detection of various deuterium labelled and unlabelled products synthesized by MG4 cell cultures (72 hrs post induction). All cultures grown in LB supplemented with 1% glucose and 40 mM glycolate (labelled or unlabelled).

Finally, HPLC separation using ammonium formate as the mobile phase on the Aminex HPX-87H column followed by MS analysis of glycolate fed MG1 and MG4 strain culture supernatants at a m/z ratio of 138.1 allowed not only the detection of the 3,4-DHBA ammonium adduct but also an additional peak immediately adjacent to the 3,4-DHBA ammonium adduct peak (**Figure 2-8**, trace in gold). Based on these results, we hypothesized that separation using ammonium formate had allowed resolution between 3,4-DHBA and the co-eluting species. The fact that the co-eluting species is detected at the same m/z ratio as 3,4-DHBA and was only synthesized by strains expressing pathway enzymes in the presence of glycolate, suggested that the species was an isomer of 3,4-DHBA.

2,3-DHBA was one possible isomeric product, identical in mass to 3,4-DHBA, that we hypothesized could be formed through an alternative Claisen condensation reaction (Wade Jr, 2006) catalyzed by BktB (Masamune et al., 1989). The condensation reaction between glycolyl-CoA and acetyl-CoA that results in the synthesis of 3,4-DHBA involves formation of a covalent complex between glycolyl-CoA and BktB followed by the abstraction of an α-proton from acetyl-CoA to generate a carbanion that initiates the formation of the carbon-carbon bond in the 4-hydroxy-3-ketobutyryl-CoA intermediate

(**Figure 2-9**). Alternatively, the formation of a covalent complex between acetyl-CoA and BktB, followed by the abstraction of an α-proton from glycolyl-CoA (**Figure 2-10**) is expected to result in the synthesis of 2,3-DHBA via the 2-hydroxy-3-ketobutyryl-CoA intermediate.

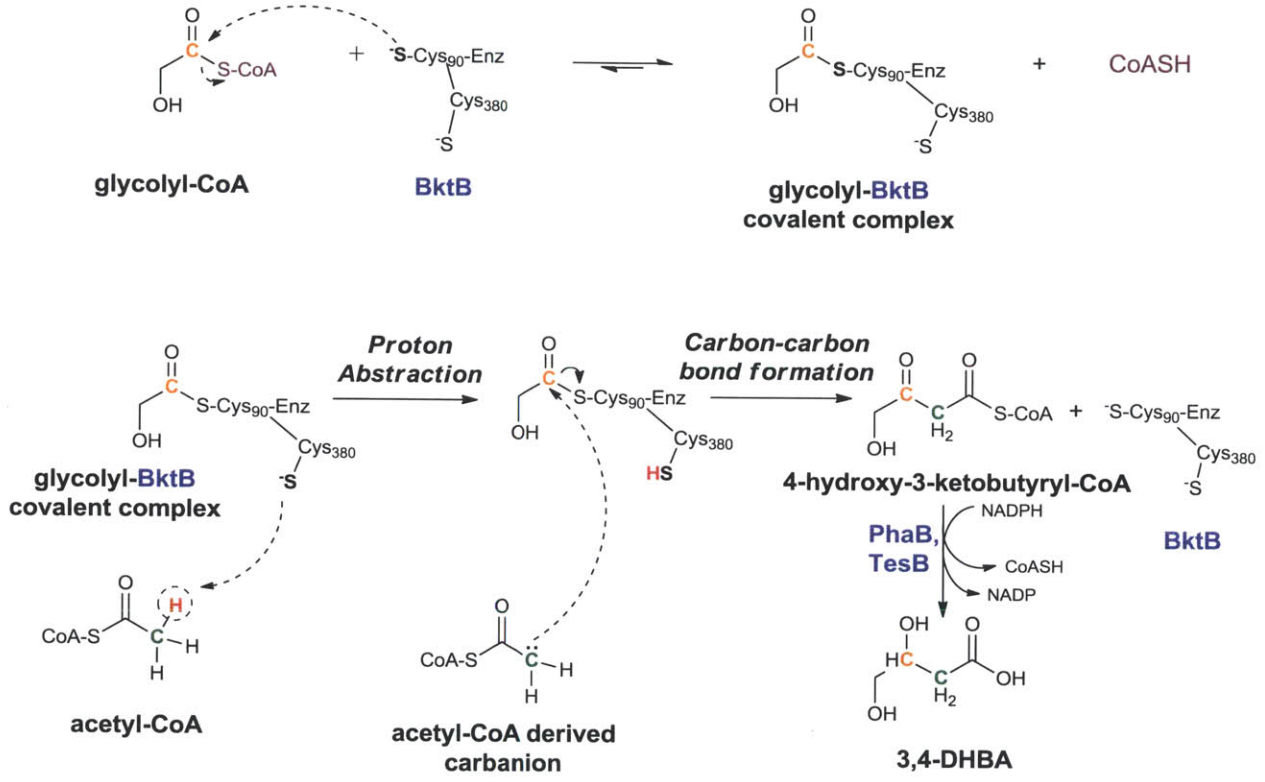

Figure 2-9 | Mechanism for formation of the 3,4-DHBA precursor (4-hydroxy-3-ketobutyryl-CoA) via a Claisen condensation reaction between glycolyl-CoA and acetyl-CoA, catalyzed by BktB. The reaction involves formation of a glycolyl-CoA-enzyme complex followed by a nucleophilic substitution by the carbanion formed due to the abstraction of an α-proton from acetyl-CoA resulting in the condensation product 4-hydroxy-3-ketobutyryl-CoA which upon further reduction and CoA cleavage gives 3,4-DHBA. Formation of 3-hydroxyvaleryl-CoA and 3-hydroxybutyryl-CoA is expected to involve a similar nucleophilic attack by an acetyl-CoA derived carbanion on propionyl-CoA-enzyme and acetyl-CoA-enzyme complexes respectively.

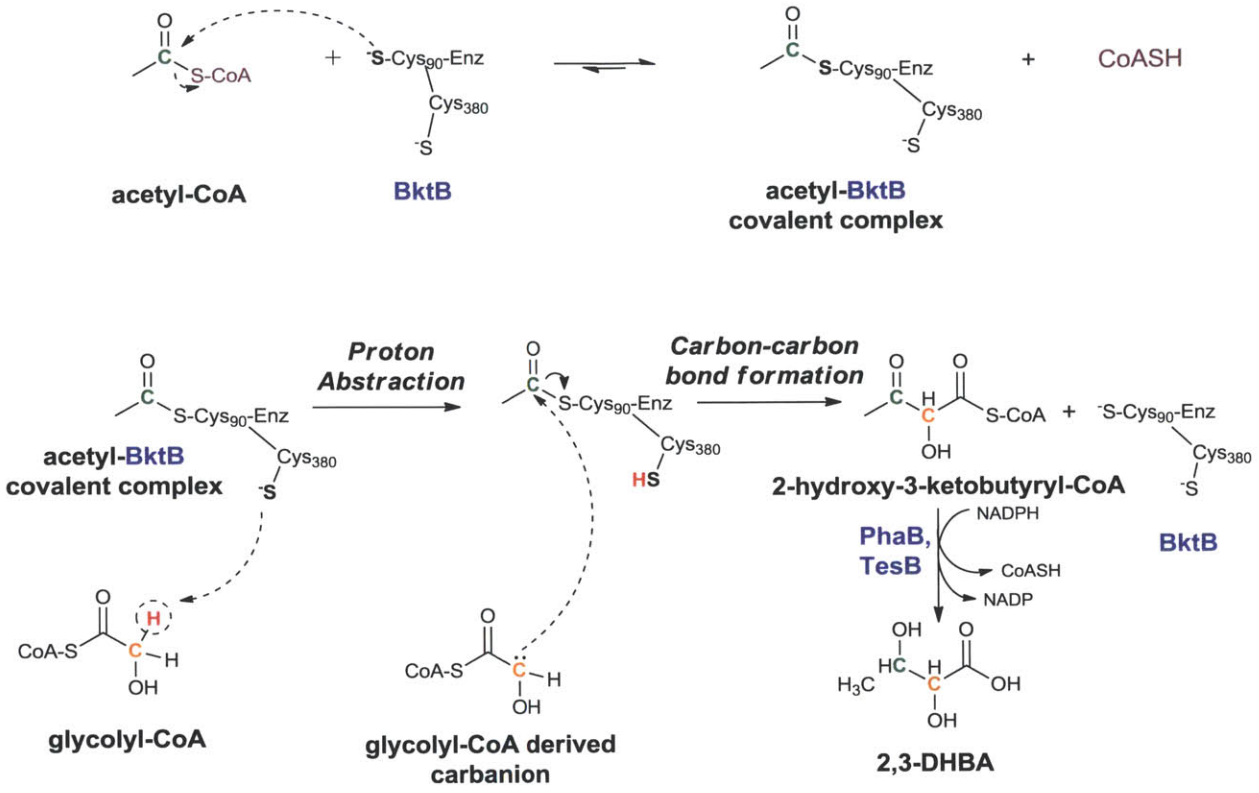

Figure 2-10 | Hypothesized mechanism for formation of the 2,3-DHBA precursor (2-hydroxy-3-ketobutyryl-CoA) via an alternative Claisen condensation reaction between glycolyl-CoA and acetyl-CoA, catalyzed by BktB. The mechanism involves a nucleophilic attack by a glycolyl-CoA derived carbanion, formed due to abstraction of an α-proton from glycolyl-CoA instead of acetyl-CoA on the acetyl-CoA-enzyme complex.

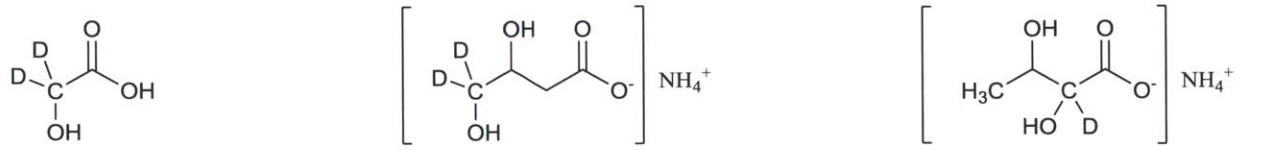

3,4-DHBA (labelled) ammonium adduct
m/z = 140.1

2,3-DHBA (labelled) ammonium adduct
m/z = 139.1

Figure 2-11 | Structures of the deuterium labelled glycolate, 3,4-DHBA and 2,3-DHBA ammonium adducts detected via HPLC / MS.

The absence of a commercially available standard for 2,3-DHBA prevented the direct confirmation of this hypothesis using HPLC/MS analysis. Instead, we used labelled glycolate (2,2-(D2)-glycolic acid) in which both of the hydrogen atoms on the α-carbon were replaced with deuterium to investigate further (**Figure 2-11**). MG4 cells were grown in LB supplemented with 40 mM of this

deuterium labelled glycolate and 10 g/L glucose. Culture supernatants after t=72 hrs were analyzed on the HPLC/MS. As expected, a peak corresponding to the doubly deuterated 3,4-DHBA ammonium adduct (**Figure 2-11**) was observed at an m/z ratio of 140.1 (**Figure 2-8**, trace in red) that coincided with the peak for the unlabelled 3,4-DHBA standard detected at an m/z of 138.1 (**Figure 2-8**, trace in blue), confirming 3,4-DHBA synthesis in strain MG4. Further, two additional smaller peaks were observed at an m/z =139.1 (**Figure 2-8**, trace in green) in these samples, the second of which (after 14 mins) coincided with the suspected 2,3-DHBA peak observed for supernatants from MG4 cultures fed with unlabelled glycolate (**Figure 2-8**, trace in gold, 2nd peak). The loss of 1 mass unit relative to the labelled 3,4-DHBA ammonium adduct was consistent with the mechanism for formation of 2,3-DHBA by the alternative Claisen condensation reaction (**Figure 2-10**). The 2,3-DHBA isomer was subsequently confirmed via NMR analysis (see **Section 2.2.4.** and **Appendix A1**).

MG4 supplied with unlabelled glycolate was estimated to have synthesized 7.17± 0.54 mM (860 ± 65 mg/L) of 2,3-DHBA (**Figure 2-4**). These titres were comparable to the total of 3,4-DHBA and 3HBL (about 6.8 mM) produced in the same cultures and suggest a roughly equal selectivity of BktB towards both isomers. These results also suggest that the titers and yield specifically for 3,4-DHBA + 3HBL (about 3 g/L of 3,4-DHBA amounting to 62% molar yield) reported in Martin's original work (Martin, 2009) were overestimated by almost a factor of 2, with roughly half of the reported DHBA being composed of the 2,3-DHBA isomer. The revised estimates for 3,4-DHBA, 2,3-DHBA and 3HBL titers and yields for the strain employed in Martin's work are discussed in Chapter 4, section 4.3.1. While MG1 cultures also synthesized small quantities of 2,3-DHBA, these were too small to be quantified accurately using HPLC.

2.3.5. Investigating 2,3-DHBA synthesis with other thiolases

We were also interested in investigating if and to what extent 2,3-DHBA synthesis is catalysed by thiolases other than BktB. We thus compared DHBA synthesis in strains MG4, MG4A and MG4B expressing BktB, PhaA and Thil respectively as thiolases for the 3HA pathway in addition to Pct, PhaB and TesB.

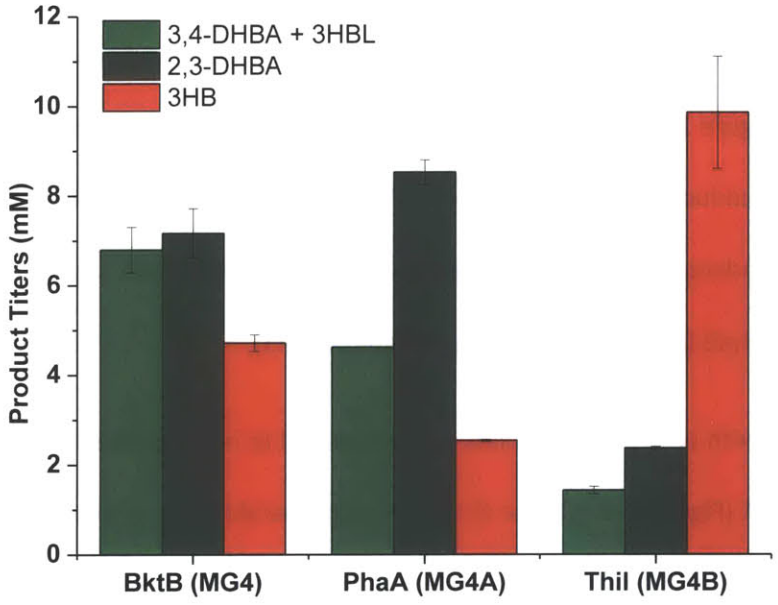

Thiolase	[3,4-DHBA + 3HBL] / [2,3DHBA]	[Total DHBA + 3HBL] / [3HB]
BktB	0.95 ± 0.09	2.58 ± 0.04
PhaA	0.53 ± 0.01	5.14 ± 0.13
Thil	0.61 ± 0.08	0.39 ± 0.06

Figure 2-12 | 2,3-DHBA vs. 3,4-DHBA synthesis comparison by different thiolases. The plot shows the t=72 h time point product titers for strains expressing different thiolases. Also calculated in the table under the plot are the selectivity ratios for the different products. Total DHBA accounts for the combined titers of the 2,3 and 3,4-isomers.

Both PhaA and Thil were observed to synthesize both the DHBA isomers. As observed previously (Martin, 2009), Thil showed selective synthesis of its natural product (3HB), with limited synthesis of the two DHBA isomers. While the total 2,3-DHBA + 3,4-DHBA + 3HBL titers with PhaA were comparable to those obtained with BktB, it was observed that PhaA resulted in lower 3,4-DHBA + 3HBL titers and more 2,3-DHBA synthesis (**Figure 2-12**). Interestingly, while the selectivity with respect to

synthesis of 3,4-DHBA for PhaA was lower than that of BktB, that with respect to 3HB was observed to be two fold higher, with PhaA resulting in 3HB titers roughly half of those observed with BktB. This suggests that the active site residues for the acetylated-PhaA enzyme complex offer better stabilization of the carbanion generated from the abstraction of an α-proton from glycolyl-CoA in comparison to acetyl-CoA, resulting in preferred synthesis of 2,3-DHBA over both 3,4-DHBA and 3HB. Similarly, it is also possible that the formation of the glycolyl-PhaA enzyme complex is more difficult for PhaA, resulting in reduced 3,4-DHBA synthesis. Modelling of the interactions of glycolyl-CoA versus acetyl-CoA for the acetylated PhaA enzyme through docking simulations can help shed light over this hypothesis. These findings also indicate that the synthesis of the 2,3-DHBA isomer is not unique to BktB and that the choice of the thiolase employed can be used to influence the selectivity between the different 3HA products synthesized.

2.3.6. Synthesis of C6 hydroxyacids

To explore the potential of the pathway to incorporate longer chain, aliphatic substrates, isobutyrate and butyrate were supplied to the culture medium to investigate the production of the six carbon isomers 3-hydroxy-4-methylvalerate (3H4MV) and 3-hydroxyhexanoate (3HH), respectively. While DHBA synthesis was only observed with Pct, all three CoA-activation systems resulted in the production of 3H4MV, and all except PrpE could produce 3HH (**Figure 2-4** and **Figure 2-5**, strains MG4-6). However, both 3H4MV and 3HH were detected only with the PhaB reductase (**Figure 2-4** and **Figure 2-13**, strains MG4-6). For 3H4MV, a fourth CoA-activation system was tested, namely, *B. subtilis* Ptb-Buk. This system was chosen because of its association with genes involved in branched-chain fatty acid synthesis, suggesting a preference for branched acids such as isobutyrate (Debarbouille et al., 1999). The *B. subtilis* Ptb-Buk enzyme system resulted in 3H4MV titres comparable to those obtained with the *C. acetobutylicum* homologs, but produced more 3HB and less acetate (**Figure 2-13**). This suggests that the two Ptb-Buk homologs may be equally efficient in activating isobutyrate, but the *B. subtilis* pair has

lower activity with acetyl-CoA resulting in lower acetate and higher 3HB, as the increased acetyl-CoA pool would favour 3HB synthesis. Overall, 3H4MV titres were observed up to 2.27 ± 0.18 mM (300 ± 25 mg/L) in strain MG4 and 3HH titres up to 0.170 ± 0.04 mM (22.5 ± 5.9 mg/L) were achieved in strain MG6.

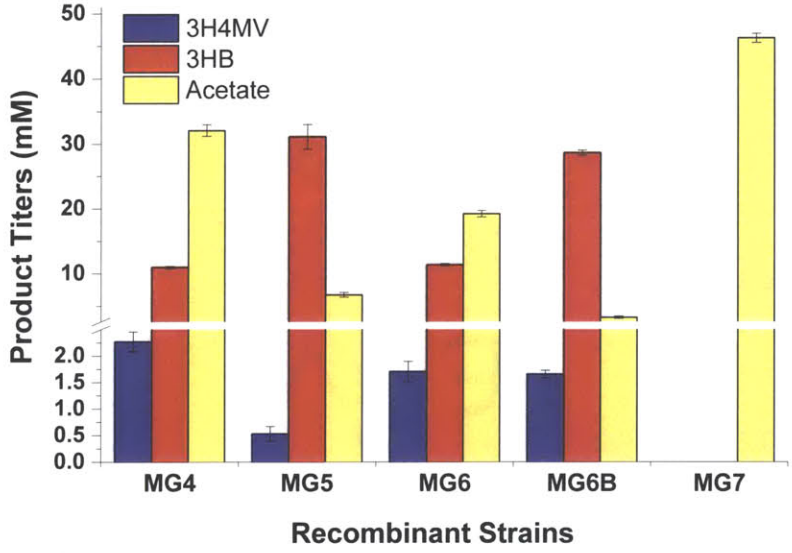

Figure 2-13 | 3H4MV biosynthesis from glucose and isobutyrate. Four activation systems, including Pct transferase, PrpE synthetase, and two Ptb-Buk transferase-kinase systems from C. acetobutylicum and B. subtilis, were examined for 3H4MV production using BktB and PhaB.

2.3.7. Comparison of 3HA synthesis with different substrates

Comparing the synthesis of the different products using the different enzyme combinations, it is observed that while the 3HA pathway allows the synthesis of 5 different products, the extent of conversion of the supplied substrates and final product titers vary vastly from substrate to substrate (**Figure 2-4** and **Table 2-3**). The pathway intermediates in 3HV (C5) synthesis are the native substrates for the enzymes Pct, BktB and PhaB, resulting in 100% conversion of propionate to 3HV. In comparison, synthesis of the other products such as DHBA, 3H4MV and 3HH relies on the promiscuous activity of enzymes towards non-native substrates. As a result only about 37% of the supplied glycolate was converted to DHBA (C4), only 15% of isobutyrate was converted to 3H4MV (branched-C6) and as little as

1% of butyrate was converted to 3HH (C6), suggesting pathway enzyme limitations. In particular, the pathway enzymes show much lower activity towards synthesis of the longer chain C6 3HAs, suggesting the need to explore or engineer alternative enzymes.

Table 2-3 | Molar Yields of 3HA products on respective substrates for different strains

		3HV	DHBA + 3HBL	3H4MV	3HH
Strain	**Enzymes**	**% molar yield on 15 mM supplied propionate**	**% molar yield on 40 mM supplied glycolate**	**% molar yield on 15 mM supplied isobutyrate**	**% molar yield on 15 mM supplied butyrate**
MG1	*pct – hbd*	~100 %	9 %	ND	ND
MG2	*prpE- hbd*	62 %	ND	ND	ND
MG3	*ptb-buk- hbd*	89.2 %	ND	ND	ND
MG4	*pct – phaB*	~100 %	37 %	15 %	0.4 %
MG5	*prpE- phaB*	~100 %	ND	4 %	ND
MG6	*ptb-buk – phaB*	~100 %	ND	11 %	1 %
MG7	*ptb(Bs)-buk(Bs) - phaB*	NT	NT	11 %	NT

* % Molar yield is calculated as ratio of moles of product synthesized to moles of substrate supplied. For DHBA & 3HBL, the yield is calculated as total sum of the two DHBA isomers and 3HBL to the glycolate supplied. ND = not detected. NT = Not Tested.

2.4. Discussion

Biological synthesis of chemical compounds is an attractive option that is in part limited by the availability of synthetic pathways for molecules of interest. Expanding this capacity requires the *de novo* design of biosynthetic routes and relies on natural enzyme promiscuity. It was our objective in this investigation to construct such a *de novo* pathway for the synthesis of 3HAs as a proof of concept, using the reactions of the PHA synthesis pathways and expanding on the substrate range of the natural enzymes in these pathways. Using the 3HA platform, we have so far demonstrated the synthesis of five new products (3,4-DHBA, 2,3-DHBA, 3HBL, 3HH and 3H4MV).

A key enzyme in the 3HA platform is the thiolase, BktB, which catalyzes the carbon-carbon bond forming Claisen condensation reaction. Carbon-carbon bond forming chemistry provides a unique way to extend beyond naturally-occurring backbones to generate a wider array of compounds. In most other examples of pathway design for targeted molecule production, carbon-carbon bonds are either broken through decarboxylation (e.g., production of 1,2,4-butanetriol from pentose sugars (Niu et al., 2003) ; fusel alcohols from amino acid precursors (Atsumi et al., 2008)) or the carbon chain length is already set through a naturally-occurring metabolic intermediate (e.g., 3-hydroxypropionic acid from pyruvate or alanine (Gokarn et al., 2011); 1,4-butanediol from succinate or succinyl semialdehyde through decarboxylation of alpha-ketoglutarate (Yim et al., 2011)). The 3HA platform has the flexibility to produce various molecules based on the precursors supplied and to generate different stereoisomers based on the choice of reductase employed. An ability to set carbon skeletons with unnatural substrates in this manner represents an entirely new opportunity to envision and achieve targeted microbial synthesis of value-added compounds.

A notable finding in the context of this carbon-carbon bond formation was the observation of the alternative Claisen condensation reaction that results in the 2,3-DHBA isomer. Since the reaction

mechanism requires the abstraction of an α-proton to initiate nucleophilic attack, we do not expect all molecular pairs to be equally likely to form both isomers. Indeed, our inability to observe any alternative products in the synthesis of 3HV is consistent with a previous report that found no activity with a BktB homolog from *Zoogloea ramigera* (51% identity/68% similarity) in the thiolytic direction with the branched 2-methylacetoacetyl-CoA isomer of β-ketovaleryl-CoA (Masamune et al., 1989). The unexpected production of 2,3-DHBA is an exciting development because of the implication for other molecular structures that could be formed using substrates with sufficiently electronegative α-protons. This activity is not limited to BktB and is exhibited by other thiolases as well, albeit to different extents. Specifically in the context of 3,4-DHBA and 3HBL synthesis, the discovery of 2,3-DHBA helped us identify a major source of loss of carbon and yield that can guide future efforts for improving pathway performance. The finding also highlights the importance of the sequential order of interaction of the two reacting thioesters with the active site in this condensation reaction; a fact that may be used to guide protein engineering of the thiolase enzyme to preference certain products as discussed in the next chapter. Additionally, the compound 2,3-DHBA itself is of specific commercial interest as a monomer in the synthesis of hyperbranched polymers (Voit, 2005).

The reductase enzyme employed affords stereospecificity to the pathway with PhaB resulting exclusively in *(R)*-3-hydroxyacids while Hbd yielding the *(S)* stereoisomers (Lee et al., 2008b; Liu et al., 2007). In the case of 3,4-DHBA, due to a change in the stereochemical priority of the different atoms of the molecule about its stereocenter, PhaB is expected to result in *(S)*-3,4-DHBA while Hbd should yield *(R)*-3,4-DHBA. PhaB results in significantly higher titres, and fortunately, the *(S)* stereoisomer is predominately used in the production of pharmaceuticals and high-value compounds (Lee and Park, 2009). Hbd is observed to be similarly limiting in the synthesis of the *(S)* isomers for 3HH, 3H4MV and 3HV (with PrpE and Ptb-Buk). This necessitates the identification and screening of *hbd* homologs to

identify a reductase with identical stereochemical preference but with an increased substrate tolerance for the production of *(R)*-3,4-DHBA and *(R)*-3HBL as well as *(S)*-3HH and *(S)*-3H4MV using this pathway.

Taken together, the initial findings of novel molecules produced here point to three main avenues for greatly enhancing the potential of this pathway to launch new commercial bio-products. First, the full potential of the wild-type enzymes tested here remains unknown from the small subset of four substrates that were screened. The broad substrate range exhibited by the combination of Pct, BktB, PhaB and TesB that allowed the synthesis of five new products, enables one to envision a wide array of novel compounds that could be produced from different substrates and subsequently transformed into products ranging from medicines to materials. Second, while we have been successful in the synthesis of five new products, not all of them are synthesized equally well. As observed from **Table 2-3**, the set of enzymes tested so far works well for the synthesis of C4 and C5 3HAs such as 3HV and the two DHBA isomers, while the yields for the longer or branched chain C6 3HAs are much lower. Improving upon the activities of the pathway enzymes, either through screening for more active homologs or through protein engineering as discussed in Chapter 3, should result in both broader substrate range and higher production titers and yields. Of particular interest is protein engineering of the thiolase enzyme that catalyzes the key carbon-carbon bond forming reaction to influence product formation (Leonard et al., 2010), for example, to preference 3,4- over 2,3-DHBA synthesis or to accelerate the alternative Claisen condensation, producing novel branched or α-substituted molecules. Finally, production strains for hydroxyacid synthesis can be further engineered to produce the starting small acid substrates endogenously to allow 3HA synthesis from simple sugars, as described previously in the case of production of 3HV from glucose or glycerol as the sole carbon source (Tseng et al., 2010b). In Chapter 4, we discuss using this approach for engineering endogenous glycolate synthesis for the production of DHBA and 3HBL from glucose as a sole carbon source. Intracellular production of pathway

substrates would mitigate the cost and/or toxicity associated with the secondary carbon sources as well as eliminate the need for substrate transport across the cellular envelope, potentially accelerating production. Each of these approaches has the potential to further enhance the platform pathway developed here as an efficient and sustainable avenue for the production of value-added biochemicals.

Chapter 3 Exploring the 3HA platform

3.1. Introduction

The initial exploration of the 3HA pathway in Chapter 2 and the synthesis of five new products from four different substrates revealed the versatility of the established platform and validated our approach with respect to using the biosynthetic capacity of the Claisen condensation reaction to synthesize desired 3HAs. The molar yields for the novel products were however substantially lower than those for 3HV or 3HB, the natural products synthesized by the selected enzymes. In particular, the pathway enzymes explored thus far showed much lower activity towards synthesis of the longer chain C6 3HAs (with yields as low as 11% for 3H4MV and 1% for 3HH), indicating limitations with the accommodation and interactions of bulkier non-native substrates within the active site. Even in the synthesis of the two DHBA isomers (C4), the yield was limited to about 37% with the *E. coli* K-12 strain MG1655 (DE3 *ΔendA ΔrecA*) and could be improved to a maximum of 53% with the strain MG1655 (DE3) (see **Section 4.3.1.**). Enhancing titers and yields for these novel 3HAs is critical for any foreseeable scale up or commercial applications of this platform.

Improving pathway performance by overcoming enzyme limitations requires a two pronged approach: 1) screening alternative pathway enzymes and 2) engineering rate limiting pathway enzymes for improved activity / selectivity to increase productivity and reduce the formation of pathway side-products such as 3HB and acetate. We discuss the application of both these approaches in this chapter. In addition to improving pathway performance, we were also interested in gaining insights into the activities and specificities of the individual enzymes to guide future enzyme selection. In the absence of *in vitro* assays to systematically study the limiting enzymes, the synthesis of known products using the

3HA platform itself served as a functional *in vivo* assay for this purpose. Finally, we were also interested in exploring the synthesis of alternative products using the pathway by feeding new substrates.

3.1.1. Screening pathway enzyme homologs

The pathway enzymes selected in our initial exploration of the 3HA platform were well characterized enzymes selected either from the PHA synthesis or butanol synthesis pathways, known to function with C4 and C5 substrates. In an attempt to improve the synthesis of C6 hydroxyacids, we explored additional enzymes from the PHA synthesis, fatty acid degradation and small acid catabolism pathways from various organisms. Protein BLAST searches (Baxevanis and Ouellette, 2005) using sequences of already tested enzymes were initially employed to identify pathway enzyme homologs, from amongst which, enzymes were specifically picked for experimental testing for which there was evidence of activity toward C6 or longer substrates in the literature. The various additional enzymes explored and the rationale for their selection is discussed below.

Activators

In *E. coli*, growth on short chain fatty acids such as butyrate or acetoacetate depends on activation of these molecules to CoA thioesters by acetyl-CoA: acetoacetate transferase coded by the *atoA-atoD* genes of the *atoDAE* operon. The enzyme catalyzes the transfer of CoA from acetyl-CoA to the corresponding short chain fatty acid, similar to the Pct enzyme. Though the purified enzyme exhibits higher specificity towards β-ketoacids like acetoacetate, it has been reported to also use a variety of short chain carboxylic acids as substrates (Black and DiRusso, 1993). Thus, the enzyme product of *atoA-atoD* was a promising candidate for activating small acid molecules to CoA thioesters. The *atoE* gene of the operon has been identified as a short chain fatty acid transporter and its expression in conjunction with *atoD-atoA* was also tested.

Thiolases

Thiolase enzymes may be classified into two classes on the basis of the preferred length of the 3-ketoacyl-CoA substrate. The first class of enzymes, referred to as acetyl-CoA acyltransferase or thiolase I (EC 2.3.1.16) demonstrate a greater specificity towards longer chain substrates ($C_{10} - C_{16}$) and bring about thiolytic cleavage of 3-ketoacyl-CoAs in fatty acid degradation via β-oxidation and are often termed as degradative thiolases. The second class of enzymes, referred to as acetyl-CoA acetyltransferases or thiolase II (EC 2.3.1.9) are specific to short chain substrates (typically C_4 & C_5) and in most cases bring about condensation of two acetyl-CoA molecules to acetoacetyl-CoA and are operative in mixed acid fermentation and PHA synthesis pathways as well as growth on short chain fatty acids. In *E. coli*, the gene *atoB* of the *ato* operon codes for a thiolase II enzyme while the fatty acid degradation enzyme complex, coded by the genes *fadA* and *fadB*, shows thiolase I activity. We had thus far only explored thiolase II enzymes for the 3HA platform and were hence particularly interested in evaluating the FadAB complex as a thiolase I enzyme, both because of its physiological preference for long chain fattyacyl-CoAs and due to evidence suggesting activity towards synthesis of shorter C5 3-ketoacyl-CoA species (Feigenbaum and Schulz, 1975; Rhie and Dennis, 1995).

Brandl and co-workers (Brandl et al., 1989) studied PHA synthesis in *Rhodospirillum rubrum* during growth on a variety of n-alkanoic acids. Their studies revealed incorporation of high percentages of 3-hydroxyvalerate (C_5) and small fractions of 3-hydrohexanoate (C_6) units in addition to 3-hydroxybutyrate units in the PHAs accumulated by strains grown on propionic and butyric acid respectively. These results suggest the presence of genes that code for thiolases capable of bringing about condensation of acetyl-CoA with propionyl-CoA and butyryl-CoA (C_3 and C_4) to form 3-ketoacyl-CoAs with 4 to 6 carbon atoms, and reductases capable of reducing these. While genes specific to PHA synthesis have not been identified in *R. rubrum*, genes coding a number of thiolases and reductases

have been annotated, some of which may exhibit broad substrate specificity towards a number of different metabolites. *Rru_A0274, Rru_A1380, Rru_A1469, Rru_A1946* and *Rru_A3387* are genes in the *R. rubrum* genome annotated to code for thiolase II enzymes and were also investigated in this study.

Reductases

Given the limitations arising out of the strict substrate specificity of Hbd, we were interested in identifying a more versatile *(S)* specific reductase. Haywood *et al* purified and characterized two distinct acetoacetyl-CoA reductases from *C. necator* that use NADH and NADPH respectively as co-factors (Haywood et al., 1988). The NADH related reductase (EC 1.1.1.35) brings about stereo-specific reduction of 3-ketoacyl-CoAs to *(S)*-hydroxyacyl-CoA and is accompanied by concomitant oxidation of the cofactor NADH to NAD^+. It was observed to exhibit broad substrate specificity with respect to oxidation of *(S)* and *(R)*-3-hydroxyacyl-CoAs with 4 to 10 carbon atoms. Three genes (*paaH1*, *paaH2* and h16_*B1652*) have been annotated in the *C. necator* genome to code for such NADH related reductases and each reductase is suspected to be active in glucaryl-CoA, butanoate and fatty acid metabolism. Of these, the enzyme product of *paaH1* has a molecular weight of 30 kD, the same as the reductase studied by Haywood and co-workers and is hence of particular interest.

3.1.2. Engineering the thiolase enzyme for specific products

A key reaction in the 3HA pathway is the thiolase catalyzed carbon-carbon bond formation via the Claisen condensation reaction (Masamune et al., 1989) between the small acid derived acyl-CoA (**R**-(C=O)-SCoA) and acetyl-CoA (CH_3-(C=O)-SCoA). As described in Chapter 2, the reaction can occur in two ways (Type I and Type II) as observed in the synthesis of 2,3 vs. 3,4-DHBA. The Type I reaction involves acylation of the enzyme in step 1, followed by abstraction of an α-proton from acetyl-CoA during the formation of the carbon-carbon bond in step 2. Type 2 reactions on the other hand involve the

formation of an acetylated enzyme complex and abstraction of an α-proton from the acyl-CoA during the carbon-carbon bond formation in step 2 (**Figure 3-1**).

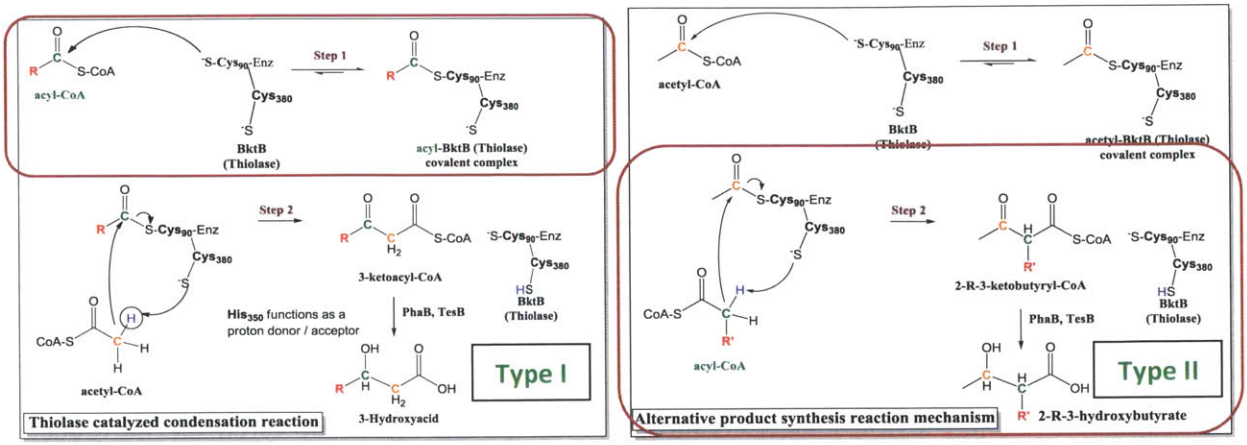

Figure 3-1 |Targeting different steps in the Claisen condensation reaction to preference product outcome via protein engineering

We envisage preferencing each of these activities (Type I and Type II) by targeting different sets of residues via protein engineering for specific products. In the absence of a high-throughput screen, we are essentially limited to a small number of rational site directed mutants. To enhance the synthesis of C6 or longer 3HAs such as 3HH over 3HB, we need to target Step 1 in the reaction mechanism and facilitate the formation of the acylated enzyme complex (as opposed to the acetylated complex) by expanding the binding pocket for the acyl-CoA and increasing its hydrophobicity. Using docking simulations (in collaboration with Prof. Bruce Tidor's group at MIT) as well as rational approaches, several mutations have been identified to facilitate 3HH synthesis. One such mutation was tested in the thiolases BktB and PhbA (from *Z. ramigera*) and is discussed in this chapter. On the other hand, preferencing (or suppressing) the Type II reaction involves stabilizing (or destabilizing) the abstraction of an α-proton and the resulting carbanion in Step 2. Mutations in residues to alter the ratios of 2,3- vs 3,4-DHBA using this approach are the subject of future investigations.

3.2. Methods and Materials

3.2.1. Strains and plasmids

E. coli MG1655 (DE3 Δ*end*A Δ*rec*A) was used as the production host for hydroxyacid synthesis, as in Chapter 2. *E. coli* DH10B (Invitrogen, Carlsbad, CA) and ElectroTen-Blue (Stratagene, La Jolla, CA) were used for transformation of cloning reactions and propagation of all plasmids.

Genes from *R. rubrum* ATCC 11170 (*Rru_A0274, Rru_A1308, Rru_A1469, Rru_A1946* and *Rru_A3387*), *C. necator* ATCC 17699 (*phaB* or *paaH1*), *E. coli* K-12 (*atoD, atoA ,atoE* and *fadA, fadB*) and *Z. ramigera* (*phbA*) were obtained by polymerase chain reaction (PCR) using genomic DNA (gDNA) templates. All gDNAs were either prepared using the Wizard Genomic DNA Purification Kit (Promega, Madison, WI) or purchased as such from ATCC (Manassas, VA). A strain of *Z. ramigera* was obtained from the Sinskey Lab (PI: Prof. Anthony Sinskey) in the Department of Biology at MIT and was used to isolate gDNA. Cloning of various genes into the respective vectors was done using methods described in Chapter 2. Custom oligonucleotides (primers) were purchased for all PCR amplifications (Sigma-Genosys, St. Louis, MO) as listed in **Table 3-2**. In all cases, Phusion High Fidelity DNA polymerase (Finnzymes, Espoo, Finland) was used for DNA amplification. Restriction enzymes and T4 DNA ligase were purchased from New England Biolabs (Ipswich, MA). Recombinant DNA techniques were performed according to standard procedures.

pETDuet-1 and pCDFDuet-1 (Novagen, Darmstadt, Germany), were again used for construction of the 3-hydroxyacid pathway plasmids. The sites used for cloning the genes are underlined in **Table 3-2**. PCR products were digested with the appropriate restriction enzymes and ligated directly into similarly digested vectors. The *R. rubrum* thiolases (*Rru_A0274, Rru_A1380, Rru_A1469* and Rru_A3387) were initially cloned into pETDuet-1 using the NcoI an NotI sites, while *Rru_A1946* was cloned using the BamHI and NotI sites to construct the pETDuet-Rru_Axxxx vectors, into which one of the two reductases

(*phaB* or *hbd* flanked by NdeI and AatII sites) was subsequently cloned. For the construction of pETDuet/fadAB and pETDuet/fadAB/phaB, *fadA-fadB* flanked by BamHI and NotI sites were initially cloned into MCSI of pETDuet-1, following which *phaB* or *paaH1* flanked by MfeI and AatII sites was cloned into MCSII. For pETDuet/fadAB/hbd on the other hand, *fadA-fadB* flanked by NcoI and EcoRI sites were used to replace *bktB* from pETDuet/bktB/hbd digested with NcoI and EcoRI. For the construction of pETDuet/phbA$_{ZR}$/phaB, pETDuet-phaB backbone with flanking SpeI and EcoRI sites was generated using pETDuet/bktB/phaB as a template for PCR and *phbA$_{ZR}$* flanked by these sites was cloned into the resulting backbone. This plasmid was then used as a template to generate the PhbA$_{ZR}$(L88G) variant.

Ligation reactions using pETDuet-1 as a vector were used to transform *E. coli* DH10B, while ligations using pCDFDuet-1 were used to transform *E. coli* ElectroTen-Blue. One thiolase (*bkt*B, one of the five *R. rubrum* thiolases or FadAB) and one of three 3-hydroxybutyryl-CoA reductases (*pha*B ,*hbd or paaH1*) were cloned into pETDuet-1. The pCDFDuet-based plasmids contained one of four CoA-activation genes (*pct*, *ptb-buk*, *atoDA or atoDAE*) and one thioesterase (*tes*B). All constructs were confirmed to be correct by restriction enzyme digestion and nucleotide sequencing. Once all plasmids were constructed, one pETDuet-based plasmid and one pCDFDuet-based plasmid were used to co-transform *E. coli* MG1655 (DE3 Δ*endA* Δ*recA*) (strain MG0) to create hydroxyacid production strains.

Table 3-1 | *E. coli* strains and plasmids used in the 3-hydroxyacid pathway

Name	Relevant Genotype	Reference
Strains		
DH10B	F⁻ *mcr*A Δ(*mrr-hsd*RMS-*mcr*BC) ϕ80*lac*ZΔM15 Δ*lacX74 recA1 endA1 araD139*Δ(*ara, leu*)7697 *galU galK* λ⁻ *rpsL nupG*	Invitrogen
ElectroTen-Blue	Δ(*mcrA*)*183* Δ*(mcrCB-hsdSMR-mrr)173 endA1 supE44 thi-1 recA1 gyrA96 relA1 lac* Kan^r [F′ *proAB lacI*^{q}ZΔM15 Tn*10* (Tet^r)]	Stratagene
MG1655	F⁻ λ⁻ *ilvG- rfb-50 rph-1*	ATCC 700926
MG0	MG1655 (DE3) Δ*end*A Δ*rec*A	Tseng 2010
MG1	MG0 containing pET/bktB/hbd and pCDF/pct/tesB	
MG3	MG0 containing pET/bktB/hbd and pCDF/ptb-buk/tesB	
MG4	MG0 containing pET/bktB/phaB and pCDF/pct/tesB	This study
MG6	MG0 containing pET/bktB/phaB and pCDF/ptb-buk/tesB	
MG7	MG0 containing pETDuet-1 and pCDFDuet-1	This study
MG8	MG0 containing pET/fadAB and pCDF/pct/tesB	This study
MG9	MG0 containing pET/fadAB/hbd and pCDF/pct/tesB	This study
MG10	MG0 containing pET/fadA/phaB and pCDF/pct/tesB	This study
MG11	MG0 containing pET/Rru_A0274/phaB and pCDF/pct/tesB	This study
MG12	MG0 containing pET/Rru_A1380/phaB and pCDF/pct/tesB	This study
MG13	MG0 containing pET/Rru_A1469/phaB and pCDF/pct/tesB	This study
MG14	MG0 containing pET/Rru_A1946/phaB and pCDF/pct/tesB	This study
MG15	MG0 containing pET/Rru_A3387/phaB and pCDF/pct/tesB	This study
MG16	MG0 containing pET/fadAB and pCDF/(ptb-buk)/tesB	This study
MG17	MG0 containing pET/fadAB/hbd and pCDF/(ptb-buk)/tesB	This study
MG18	MG0 containing pET/fadAB/phaB and pCDF/(ptb-buk)/tesB	This study
MG19	MG0 containing pET/Rru_A0274/phaB and pCDF/(ptb-buk)/tesB	This study
MG20	MG0 containing pET/bktB/phaB and pCDF/(atoD-atoA)/tesB	This study
MG21	MG0 containing pET/bktB/phaB and pCDF/(atoD-atoA-atoE)/tesB	This study
MG22	MG0 containing pET/bktB(L89G)/phaB and pCDF/pct/tesB	This study
MG23	MG0 containing pET/phbA$_{ZR}$/phaB and pCDF/pct/tesB	This study
MG24	MG0 containing pET/ phbA$_{ZR}$ (L88G)/phaB and pCDF/pct/ tesB	This study
MG25	MG0 containing pET/bktB/paaH1 and pCDF/pct/tesB	This study
MG26	MG0 containing pET/bktB/paaH1 and pCDF/(ptb-buk)/tesB	This study
MG27	MG0 containing pET/fadAB/paaH1 and pCDF/(ptb-buk)/tesB	This study
Plasmids		
pETDuet-1	ColE1(pBR322) *ori*, *lacI*, T7*lac*, Amp^R	Novagen
pCDFDuet-1	CloDF13 *ori*, *lacI*, T7*lac*, Strep^R	Novagen
pET/bktB/hbd	pETDuet-1 harboring *bkt*B from *R. eutropha* H16, and *hbd* from *C. acetobutylicum* ATCC 824	This study

pET/bktB/paaH1	pETDuet-1 harboring *bkt*B and *paaH1* from *C. necator* ATCC 17699	This study
pET/bktB/phaB	pETDuet-1 harboring *bkt*B and *pha*B from *C. necator* ATCC 17699	This study
pET/fadAB	pETDuet-1 harboring *fadAB* from *E. coli*	This study
pET/fadAB/hbd	pETDuet-1 harboring *fadAB* from *E. coli*, and *hbd* from *C. acetobutylicum* ATCC 824	This study
pET/fadAB/paaH1	pETDuet-1 harboring *fadAB from E. coli* and *paaH1* from *C. necator* ATCC 17699	This study
pET/fadAB/phaB	pETDuet-1 harboring *fadAB* from *E. coli*, and *phaB* from *C. necator* ATCC 17699	This study
pET/Rru_A0274/phaB	pETDuet-1 harboring *Rru_A0274* from *R. rubrum* ATCC 11170 and *phaB* from *C. necator* ATCC 17699	This study
pET/Rru_A1380/phaB	pETDuet-1 harboring *Rru_A1380* from *R. rubrum* ATCC 11170 and *phaB* from *C. necator* ATCC 17699	This study
pET/Rru_A1469/phaB	pETDuet-1 harboring *Rru_A1469* from *R. rubrum* ATCC 11170 and *phaB* from *C. necator* ATCC 17699	This study
pET/Rru_A1946/phaB	pETDuet-1 harboring *Rru_A1946* from *R. rubrum* ATCC 11170 and *phaB* from *C. necator* ATCC 17699	This study
pET/Rru_A3387/phaB	pETDuet-1 harboring *Rru_A3387* from *R. rubrum* ATCC 11170 and *phaB* from *C. necator* ATCC 17699	This study
pET/ $phbA_{ZR}$ /phaB	pETDuet-1 harboring *$phbA_{ZR}$ rom Z. ramigera* and *phaB* from *C. necator* ATCC 17699	
pCDF/pct/tesB	pCDFDuet-1 harboring *pct* from *M. elsdenii*, and *tes*B from *E. coli* MG1655	This study
pCDF/ptb-buk/tesB	pCDFDuet-1 harboring a *ptb-buk* operon from *C. acetobutylicum* ATCC 824, and *tes*B from *E. coli* MG1655	This study
pCDF/(atoD-atoA)/tesB	pCDFDuet-1 harboring the *atoD-atoA* genes from the *atoDAE* operon and *tes*B from *E. coli* MG1655	This study
pCDF/(atoD-atoA-atoE)/tesB	pCDFDuet-1 harboring harboring the *atoD-atoA-atoE* operon and *tes*B from *E. coli* MG1655	This study

Table 3-2 | List of DNA oligonucleotide primers used in the cloning of genes for the 3-hydroxyacid pathway

Primer names correspond to the name of the gene or vector backbone that the primer amplifies, whether the primer is the forward primer (FP) or reverse primer (RP) of that gene, and the restriction site incorporated into the primer sequence for cloning (restriction sites used for cloning are underlined). For primers used to amplify the *ptb(Bs)* and *buk (Bs)* genes from *B. subtilis* for the construction of the *ptb-buk* operon, sequences indicated in bold correspond to parts of the complementary overlapping regions for SOEing PCR while nucleotides in italics correspond to downstream sequences added to mimic the *C. acetobutylicum ptb-buk* construct.

Primer	Sequence 5'→3'
atoD-atoA-FP-EcoRI	TAAAAAGAATTCATGAAAACAAAATTGATGACATTACAAG
atoD-atoA-RP-PstI	TAAAAACTGCAGTCATAAATCACCCCGTTGC
atoD-atoA-atoE-FP-SacI	TAAAAAGAGCTCTATGAAAACAAAATTGATGACATTACAAG
atoD-atoA-atoE-RP-NotI	TAAAAAGCGGCCGCTCAGAACAGCGTTAAACCAATG
Rru_A0274-FP-NcoI	TAAAAACCATGGGCATGACCGATATCGTCATTG
Rru_A0274-RP-NotI	TAAAAAGCGGCCGCTTAGCGCTCGACGCAGAG
Rru_A1380-FP-NcoI	TAAAAACCATGGGCATGAATGACGTTGTGATCGC
Rru_A1380-RP-NotI	TAAAAAGCGGCCGCTTAGCCGCGCTCAACG
Rru_A1469-FP-NcoI	TAAAAACCATGGGCATGAACGACATCGTCATCG
Rru_A1469-RP-NotI	TAAAAAGCGGCCGCTTAGGGCCGTTCGACG
Rru_A1946-FP-BamHI	TAAAAAGGATCCATGTCGTCTGCCGCC
Rru_A1946-RP-NotI	TAAAAAGCGGCCGCCTATGACGCAAGTTCCACG
Rru_A3387-FP-NcoI	TAAAAACCATGGGCATGACCGATGCGGTG
Rru_A3387-RP-NotI	TAAAAAGCGGCCGCTCATCGCGGGAAGGTC
fadAB-FP-NcoI	TAAAAACCATGGGCATGCTTTACAAAGGCGACACC
fadAB-RP-EcoRI	TAAAAAGAATTCTTAAACCCGCTCAAACACC
fadAB-FP-BamHI	TAAAAAGGATCCATGCTTTACAAAGGCGACACC
fadAB-RP-NotI	TAAAAAGCGGCCGCTTAAACCCGCTCAAACACC
phaB-FP-NdeI	TAAAAACATATGACTCAGCGCATTGC
phaB-RP-AatII	TAAAAAGACGTCTCAGCCCATGTGCAGG
phaB-FP-MfeI	TAAAAACAATTGAACTAGTGAAAGAGGAGAAATACTAGATG ACTCAGCGCATTGC
paaH1-FP-NdeI	TAAAAACATATGAGCATCAGGACAGTGG
paaH1-RP-AatII	TAAAAAGACGTCTTACTTGCTATAGACGTACACGCC
paaH1-FP-MefI	TAAAAACAATTGAACTAGTGAAAGAGGAGAAATACTAGATG AGCATCAGGACAGTGG
hbd-FP-NdeI	TAAAAACATATGAAAAAGGTATGTGTTATAGGTGCAG
hbd-RP-AatII	TAAAAAGACGTCTTATTTTGAATAATCGTAGAAACCTTTTCC
pETDuet-FP-EcoRI	TAAAAAGAATTCGAGCTCGGCG
pETDuet-RP-SpeI	TAAAAAACTAGTATGAGCACCCCGTCCATC

$phbA_{ZR}$ -FP-SpeI	TAAAAAACTAGTATGAGCACCCCGTCCATCG
$phbA_{ZR}$ -RP-EcoRI	TAAAAAGAATTCCTAAAGGCTCTCGATGCACATC
bktB(L89G)-FP	GACCGTGAACCGC**GGG**YGCGGCYCGGGC
bktB(L89G)-RP	GCCCGAGCCGCA**CCC**GCGGTTCACGGTC
$phbA_{ZR}$ *(L88G)-FP*	GGGCATGAACCA**GGG**TTGCGGCTCGGGC
$phbA_{ZR}$ (L88G)-RP	GCCCGAGCCGCAA**CCC**TGGTTCATGCCC

3.2.2. Culture conditions

Seed cultures of the recombinant *E. coli* strains (**Table 3-1**) were grown in LB medium at 30°C overnight, and were used to inoculate 50 mL LB medium supplemented with 10 g/L glucose at an inoculation volume of 2% in 250 mL flasks. Due to HPLC peak overlapping between 3HH and LB components, 3HH biosynthesis was conducted in M9 minimal medium supplemented with 10 g/L glucose where seed cultures were washed and re-suspended in M9 minimal medium before inoculation. The shake flask cultures were then incubated at 30°C on a rotary shaker at 250 RPM. Once the cells reached mid-exponential phase (when OD_{600} reached 0.8-1.0), cultures were supplemented (final concentrations in parentheses) with IPTG (1 mM) for induction of gene expression and one of the precursor substrates: neutralized propionate (15 mM), butyrate (15 mM or 20 mM), *(R)* or *(S)*-lactate (15 mM), valerate (15 mM), formate (15 mM) or 3-hydroxypropionate (15 mM). In all cases, the culture medium was supplemented with 50 mg/L ampicillin and 50 mg/L streptomycin to provide selective pressure for plasmid maintenance.

1 mL of culture was withdrawn every 24 h for up to 96 h for HPLC and HPLC/MS analysis. Titres of 3-hydroxyacids reached a plateau at 72 h and there was essentially no difference in the titres between 72 h and 96 h; accordingly, only the peak titres observed at 72 h were reported. In general, experiments were performed in triplicates, and data are presented as the averages and standard deviations of the results.

3.2.3. Metabolite analysis

Culture samples were pelleted by centrifugation and aqueous supernatant was collected for HPLC analysis. Formate, lactate, 3-hydroxypropionate, valerate and 3-hydroxyhexanoate were detected with a refractive index detector after HPLC separation on an Aminex column (5 mM sulphuric acid as mobile phase) using the method described in Chapter 2. While standards were not available for 3,4-dihydroxyvalerate and 3,5-dihydroxyvalearte (expected 3HA products of lactate and 3-hydroxypropionate respectively), their synthesis would be expected to result in new peaks detectable on the RID as compared to the empty vector controls. The lack of product synthesis was thus confirmed by the absence of such new peaks in the LC time traces.

3.2.4. Site-directed mutagenesis

To introduce the L88G and L89G mutations respectively into the $phbA_{ZR}$ and BktB thiolases, primers (listed in **Table 3-2**) were designed using the online Agilent 'QuickChange Primer Design' program. These were used to PCR amplify the respective pETDuet/ $phbA_{ZR}$ /phaB or pETDuet/bktB/phaB templates to generate the corresponding pETDuet/ $phbA_{ZR}$(L88G)/phaB and pETDuet/bktB(L89G)/phaB vectors. Phusion High Fidelity DNA polymerase (Finnzymes, Espoo, Finland) was used for these reactions.

3.3. Results

3.3.1. Comparing 3HV synthesis with different thiolases

Strain MG4 expressing the combination of enzymes Pct, BktB, PhaB and TesB was earlier observed to effectively convert propionate completely to 3HV. Thus, 3HV synthesis was used to validate the expression and activity of new thiolases expressed in conjunction with Pct, PhaB and TesB. None of the five annotated thiolases from the *R. rubrum* genome had been previously characterized. As a preliminary characterization of these thiolases, 3HV synthesis with these was studied in strains MG11-MG15 fed with propionate (**Figure 3-2**). This led to the identification of two thiolases that showed 3HA synthesis activity (Rru_A0274 and Rru_A1469), with only Rru_A0274 (strain MG11) showing 3HV synthesis. Rru_A0274 was observed to show titers and selectivity comparable to those obtained with the thiolase BktB (strain MG4). Rru_A1469 on the other hand only catalyzed 3HB synthesis. While the other thiolases were expressed recombinantly (as confirmed by protein gels) in the respective strains, they did not show any activity towards 3HV or 3HB synthesis. Of these, domain analysis of Rru_A3387 using the Pfam database (Punta et al., 2012) indicated missing residues resulting in the lack of a proper catalytic triad characteristic of thiolases. The reasons for the inactivity of the other two thiolses remain to be investigated.

3HV synthesis was also studied with strains MG8-MG10 expressing the *E. coli* FadAB complex with or without reductases. Surprisingly, only strain MG9 expressing FadAB in combination with the *(S)*-specific reductase Hbd showed synthesis of *(S)*-3HV (9.43 ± 0.89 mM), representing a molar yield of about 66% and a selectivity ratio of 3HV / 3HB of about 6.91. FadAB is known to code 4 different activities including a thiolase and reductase activity. To ascertain the role (if any) played by the reductase activity, 3HV synthesis was studied in MG8 expressing only FadAB without any additional

reductase. The lack of 3HV synthesis by MG8 suggests that the reductase does not show activity towards C5 substrates.

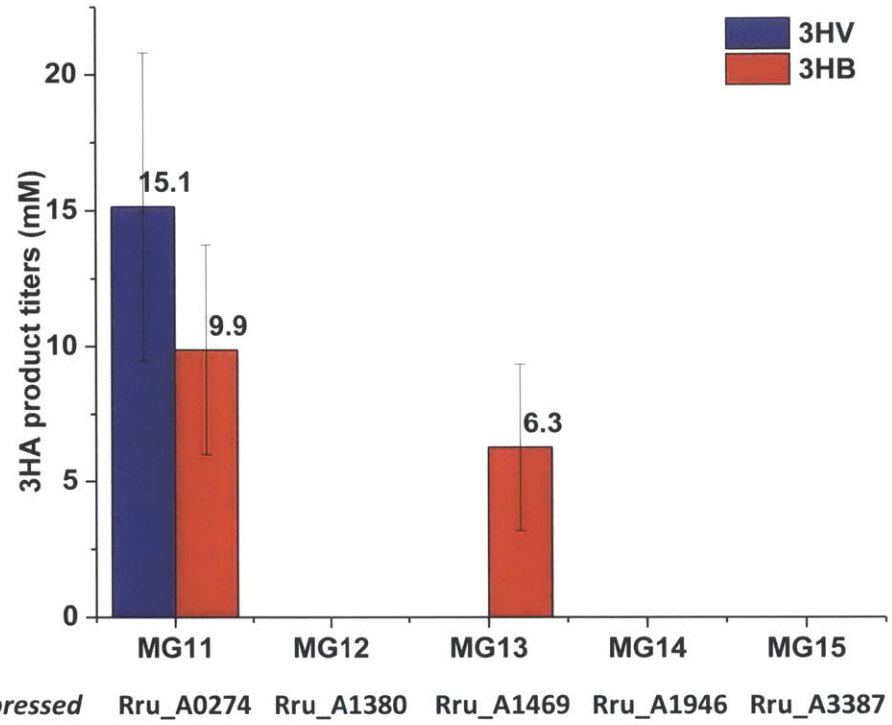

Figure 3-2 | 3HV synthesis by strains expressing *R. rubrum* thiolases. All strains were supplied with 15 mM propionate. All strains express Pct, PhaB and TesB in addition to one of the five *R. rubrum* thiolases. Product titers are reported for samples collected 72 hours post induction. 3HV / 3HB selectivity ratio for strain MG8 expressing the thiolase Rru_A0274 is 1.52.

The activator AtoD-AtoA proved unsuccessful in the activation of propionate, as indicated by the lack of synthesis of 3HV by the strain MG20 and MG21. On the other hand, the reductase PaaH1 showed activity comparable to Hbd, with MG25 (expressing Pct, BktB, PaaH1, TesB) resulting in almost complete conversion of the supplied propionate to 3HV.

3.3.2. 3HH synthesis with different thiolases

Following the confirmation of 3HV synthesis activity by the thiolases Rru_A0274 and FadAB, we investigated the ability of these thiolases to synthesisze the C6 hydroxyacid 3HH (**Figure 3-3**). Interestingly, both Rru_A0274 and the FadAB complex showed 3HH synthesis. Rru_A0274 was again

observed to result in product titers and selectivity comparable BktB, highlighting the similarity in activity and specificity exhibited by the two thiolases.

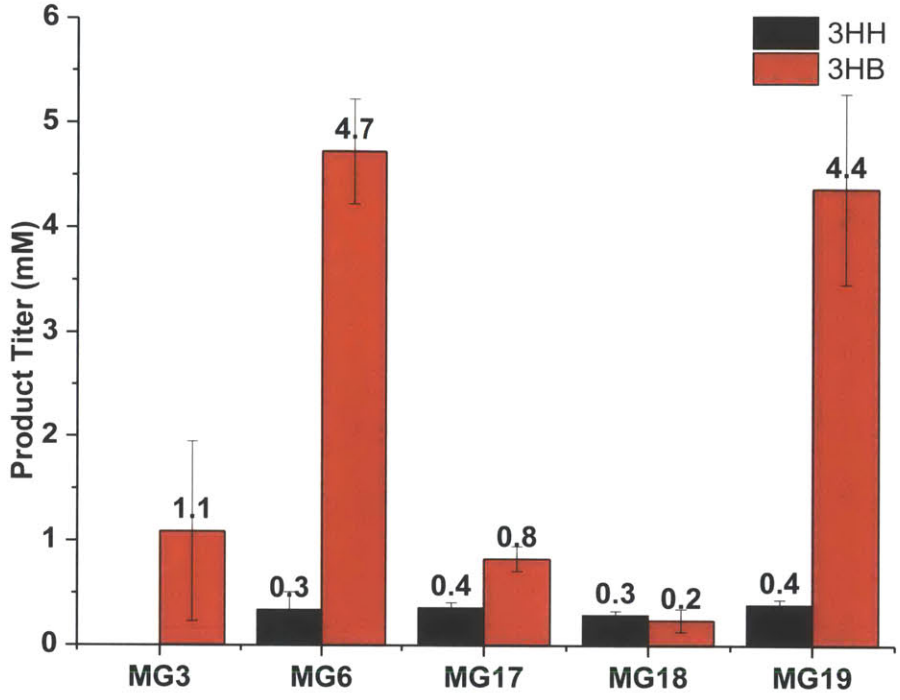

Thiolase	BktB	BktB	FadAB	FadAB	Rru_A0274
Reductase	Hbd	PhaB	Hbd	PhaB	PhaB
3HH / 3HB	-	0.06	0.5	1.5	0.1
Molar Yield	-	1.5%	2%	1.5%	2%

Figure 3-3 | 3HH synthesis by strains expressing *R. rubrum* thiolases. All strains were supplied with 20 mM butyrate. All strains express Ptb-Buk, one of three thiolases (BktB, FadAB or Rru_A0274), one of two reductases (Hbd or PhaB) and TesB. Product titers are reported for samples collected 72 hours post induction.

Interestingly, FadAB for the first time also allowed the synthesis of *(S)*-3HH with Hbd as a reductase, in addition to the synthesis of *(R)*-3HH with PhaB. The synthesis of *(S)*-3HH may not be attributed to the endogenous reductase activity of the FadAB, as confirmed by the lack of 3HH synthesis by strain MG16 solely expressing FadAB, Ptb-Buk and TesB, without any reductase. Thus the synthesis of *(S)*-3HH by MG17 is suggestive of FadAB's superior activity in condensing butyryl-CoA with acetyl-CoA in comparison to BktB. In a separate experiment, 3HH synthesis was also studied in strain MG27

expressing Ptb-Buk, FadAB, PaaH1 and TesB. 3HH titers obtained were comparable to those with MG17, indicating the similarity between PaaH1 and Hbd.

3.3.3. Investigating synthesis of new products with the 3HA platform

BktB as a thiolase and Pct as an activator in combination with PhaB and TesB had been observed to be most versatile with respect to novel product synthesis. Additionally, the thiolase FadAB was of interest due to its expected activity with longer chain substrates. We thus tested the synthesis of new products by feeding different substrates to strains MG1, MG4, MG8, MG9 and MG10 expressing Pct as an activator, BktB or FadAB as a thiolase and one of the reductases (Hbd or PhaB) and TesB. Cultures in LB were supplemented individually with 15 mM of formate, *(R)* or *(S)*–lactate, valerate or 3-hydroxypropionate as small acid substrates to investigate the synthesis of the corresponding 3HAs listed in **Table 3-3** below.

Table 3-3 | Substrates and expected 3HA products

Small Acid Molecule Fed to Cells	Expected Hydroxyacid Product
Formate (C_1)	**3-Hydroxypropionate** (C_3)
Glycolate (C_2)	**3,4-DHBA , 2,3-DHBA and 3HBL (C_4)**
Isobutyrate (C_3)	**3-hydroxy-4-methylvalerate (C_5)**
Propionate (C_3)	**3-hydroxyvalerate (C_5)**
Lactate (C_3)	**3,4-Dihydroxyvalerate (C_5)**
3-Hydroxypropionate (C_3)	**3,5-Dihydroxyvalerate (C_5)**
Butyrate (C_4)	**3-Hydroxyhexanoate** (C_6)
Valerate (C_4)	**3-Hydroxy-4-methylhexanoate (C_6)**

None of the substrates however yielded products. While lactate and formate were consumed as carbon sources by the end of the culture, valerate and 3-hydroxypropionate remained unconsumed. The lack of product synthesis was not unexpected. Indeed, it is known that the pathway shows limited

activity toward synthesis of C6 3HAs and barring formate, all of the substrates were either comparable or bulkier than butyrate.

3.3.4. Investigating protein engineering of BktB for C6 hydroxyacid synthesis

A rational approach to improve the activity of BktB towards the synthesis of 3HH through protein engineering involves increasing the size and hydrophobicity of the binding pocket by replacing bulkier and hydrophilic residues with smaller hydrophobic ones. The idea is to essentially promote the binding of butyryl-CoA in the first step of the reaction mechanism. Using the *Z. ramigera* thiolase crystal structure as a representative analogous crystal structure for BktB, the Tidor group predicted various potential mutations designed to minimize the binding energy of butyryl-CoA, while incurring minimum penalty with respect to any destabilization of the protein due to the introduced mutation (see **Appendix A2**).

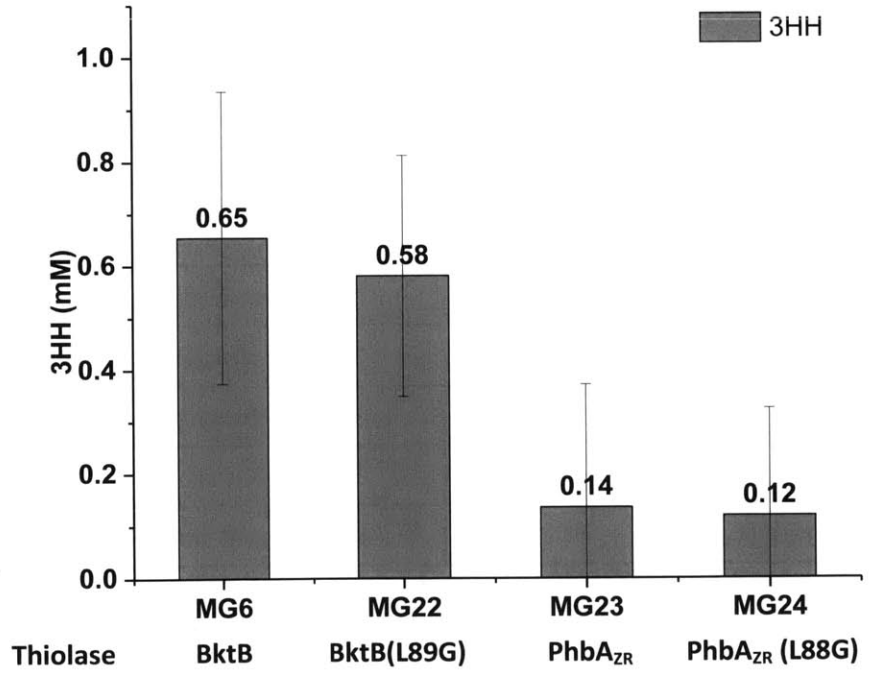

Figure 3-4 | Comparing 3HH synthesis with wild type and mutatant thiolases. All strains were supplied with 20 mM butyrate. All strains express Ptb-Buk, one of thiolases (BktB, BktB(L89G), PhbA$_{ZR}$ or PhbA$_{ZR}$ (L88G), the reductase PhaB and TesB. Product titers are reported for samples collected 72 hours post induction.

We experimentally tested one of the recommended mutations that involved mutating the leucine 88 residue in the *Z. ramigera* thiolase to a glycine (and the analogous BktB L89 residue to a G). While this mutation did not result in improved 3HH titers (**Figure 3-4**), it was not detrimental to the thiolase acitivity and may be used in conjunction with other mutations designed to similarly expand the thiolase binding pocket. The *Z. ramigera* thiolase ordinarily shows a strict substrate specificity towards the synthesis of C4 3HAs and shows negligible 3HH synthesis, as confirmed by the five fold lower titers for the wild type $PhbA_{ZR}$ in comparison to BktB.

3.4. Discussion

Our exploration of alternative pathway enzymes led to the identification of a new hitherto uncharacterized thiolase (Rru_A0274) from the organism *R. rubrum* that is capable of both C5 and C6 3HA synthesis. Similarly, the investigation of FadAB as a thiolase I enzyme in the pathway revealed its biosynthetic potential and also allowed for the first time the synthesis of the *(S)*-3HH isomer. At this point, we can only hypothesize that this *(S)*-isomer synthesis is a result of a higher activity exhibited by FadAB for the condensation reaction between butyryl-CoA and acetyl-CoA in comparison to BktB. Thiolase I enzymes are sometimes somewhat misleadingly referred to as degradative due to their role in catalyzing the thiolytic reaction in fatty acid degradation pathways. It must however be remembered that both biosynthetic and degradative thiolases are capable of catalyzing both the forward and reverse reactions. FadAB's ability to synthesize 3HV and 3HH in this study highlighted this potential.

At the outset of this project, there was very little information available about the potential of many of the enzymes selected to work with the various substrates of interest. While the testing of different pathway enzymes did not result in drastic improvements with respect to the synthesis of products and in particular improving 3HH synthesis (over our best combination of Pct, BktB, PhaB and TesB), this study helped garner valuable activity / specificity information about the various tested enzymes that may help better elucidate the sequence function relationships for these enzymes. It is interesting to note, for example, that while Rru_A0274 shares a higher overall sequence identity with the *C. necator* thiolase PhaA as compared to BktB (61% identity with PhaA as compared to 52% with BktB), it closely resembles BktB in its activity and substrate preference. Identification of other thiolases similar to BktB and Rru_A0274 and comparison of their sequences may allow identification of specific consensus residues attributing the observed activity / specificity common to these enzymes. This structure function relationship information can in turn inform homology search based identification of

desired activities, specifically using information about the active site and specificity loops. This approach is now being explored in the Prather Lab for further bio-prospecting to identify thiolase enzyme candidates through network maps designed to represent sequence similarity relationships between proteins of interest.

It is also important to note that the various enzymes have so far been assayed using the 3HA platform as an *in vivo* end point assay that uses the 3HA product titer as a measure of the collective ability of the four pathway enzymes to catalyze reactions with the supplied small acid substrates and the resulting intermediates. Such an assay is inherently incapable of identifying the exact limiting step (in the absence of standards and detection methods for accumulation of CoA-intermediates). In other words, while such an assay may allow us to identify a particular enzyme that works better when used in place of another in a functional system with known substrates, it will not allow us to identify the exact limiting step or enzyme with unknown substrates. Thus, while we now know that the pathway is incapable of metabolizing substrates like formate, lactate or valerate, it is difficult to identify which if not all enzymes are limiting. Similarly, if a given enzyme results in titers just as good as another, it does not allow us to determine if the similar product titers are a result of similar activities or a limitation due to another pathway step. *In vitro* assays thus need to be developed for each of the pathway enzymes. The challenge in developing such *in vitro* assays has been the availability of the respective CoA intermediates. Chemical and enzymatic synthesis processes are currently being investigated in the Prather Lab for this. Alternatively, in the absence of reliable *in vitro* assays, if enzyme crystal structure information is available, molecular docking simulations may be used to study and identify limiting substrate interactions. Both these approaches are currently being actively investigated in the Prather and Tidor groups.

Chapter 4 Direct synthesis of DHBA and 3HBL from glucose as a sole carbon source

Parts of this chapter are in preparation for a manuscript to be submitted for publication to Metabolic Engineering

4.1. Introduction

The 3HA platform allows synthesis of 3,4-DHBA and 3HBL using glycolate and glucose as starting materials with 2,3-dihydroxybutyric acid (2,3-DHBA) and 3-hydroxybutyric acid (3HB) as major competing side products and acetate as an inevitable pathway byproduct (**Figure 4-1**). Glycolate itself may be synthesized in *E. coli* from glyoxylate by the enzyme glyoxylate reductase, encoded by the endogenous *ycdW* gene. Endogenous synthesis of glycolate from glucose in cells expressing the 3,4-DHBA / 3HBL pathway enzymes can allow direct synthesis of these molecules from glucose as a single carbon source, eliminating the need to supply glycolic acid as a separate feedstock. In addition to mitigating cost, such intracellular glycolate synthesis is also expected to overcome any limitations in pathway yield and productivity associated with the transport of exogenously supplied glycolate across the cell membrane and boost intracellular glycolate and glycolyl-CoA levels, improving selectivity and productivity. Further, direct synthesis of 3,4-DHBA and 3HBL from substrates such as glucose opens avenues towards the synthesis of these valuable chemicals from other simple sugars derived from biomass.

Such direct synthesis of 3,4-DHBA and 3HBL is expected to afford a maximum theoretical pathway yield Y^P (Dugar and Stephanopoulos, 2011) of 0.66 mole / mole of glucose which may be increased to 1 mole / mole by recycling acetate that is formed as a by-product of the activation reaction (see yield calculations in Appendix A3). While this is lower than the absolute pathway independent maximum yield, Y^E of 1.33 moles / mole on glucose as a substrate, to the best of our knowledge, to date, there aren't known processes or catalysts that allow such an efficient conversion of an inexpensive sugar

like glucose to 3HBL or 3,4-DHBA in a stereospecific manner. Thus, the direct synthesis of 3,4-DHBA and 3HBL from glucose as a sole carbon source represents a promising opportunity for the stereospecific biosynthesis of these valuable chemicals.

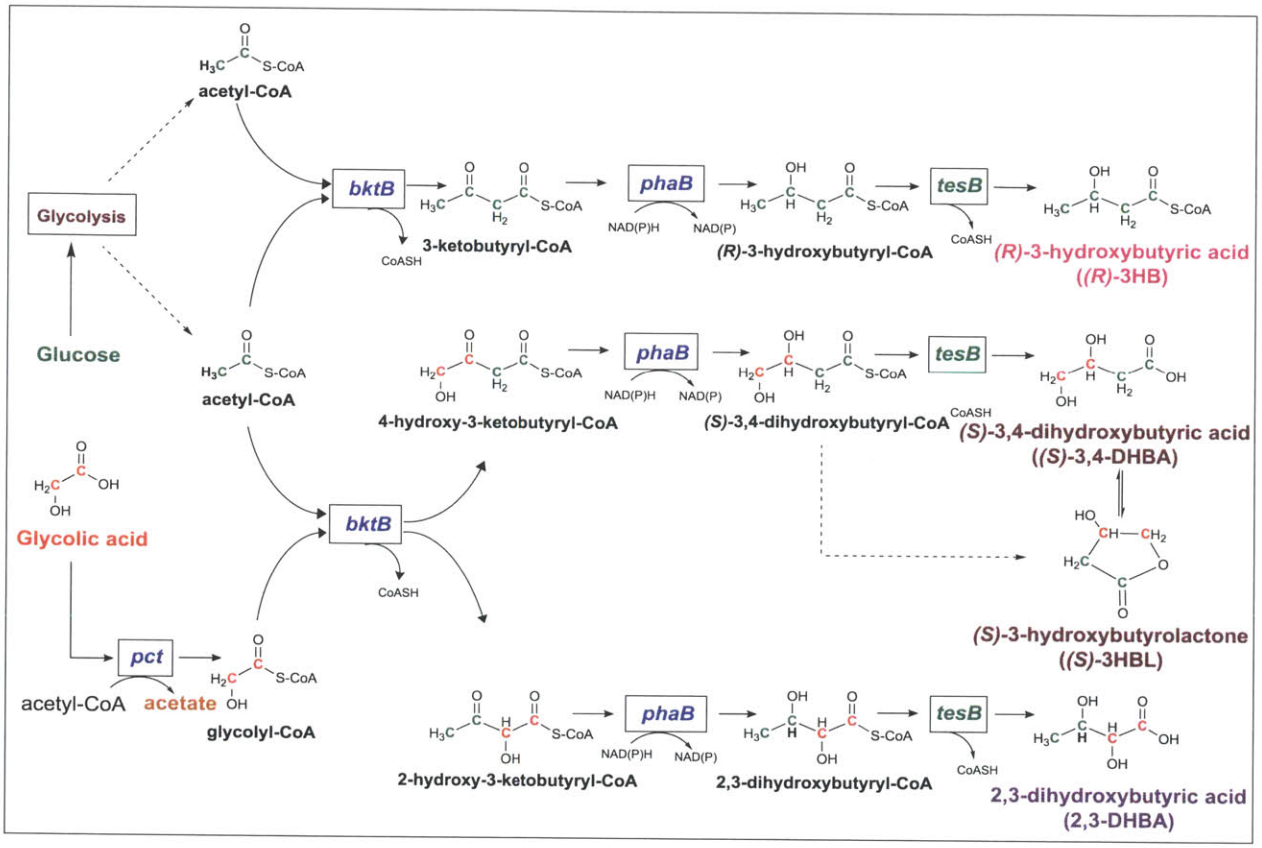

Figure 4-1 | DHBA and 3-HBL synthesis pathway Expression of *pct*, *bktB*, *phaB / hbd* and *tesB* in *E. coli* allows DHBA and 3-HBL synthesis from glucose and glycolic acid. Pct activates glycolic acid to glycoly-CoA. BktB brings about condensation with acetyl-CoA (from glycolysis) to form 4-hydroxy-3-ketobutyryl-CoA, which is reduced by PhaB to *(S)*-3,4-dihydroxybutyryl-CoA. TesB cleaves CoA form *(S)*-3,4-dihydroxybutyryl-CoA to form *(S)*-3,4-DHBA while a part of the *(S)*-3,4-dihydroxybutyryl-CoA spontaneously lactonizes to *(S)*-3HBL. An alternative condensation reaction between glycolyl-CoA and acetyl-CoA results in the 2,3-DHBA isomer, while a condensation between two acetyl-CoAs results in 3-hydroxybutyrate (3HB).

In wild type *E. coli* the glyoxylate shunt is heavily regulated and only active during growth on acetate or fatty acids where it is required for carbon assimilation for synthesis of cell building blocks (Cozzone, 1998). It is repressed during growth on glucose or in rich medium (such as LB). Such a binary response to changes in available fermentable sugars and metabolites is achieved by controlling the expression of the enzymes of the glyoxylate shunt (AceA, AceB and AceK) and by re-directing part of the

flux of isocitrate from the TCA cycle to the glyoxylate shunt by reducing the activity of isocitrate dehydrogenase (Idh, coded by the gene *icd*) through reversible phosphorylation by the enzyme Idh kinase/phosphatase (AceK) (Laporte and Koshland, 1982). Expression of the *aceBAK* operon is regulated at the transcriptional level by the repressor protein IclR. During growth on acetate or fatty acids, this repression by IclR is relieved, and phosphorylation of Idh by AceK results in a drastic drop in its activity. Simultaneously, expression of isocitrate lyase (AceA) which catalyzes the cleavage of isocitrate into glyoxylate and succinate, results in re-directing the isocitrate flux towards the glyoxylate shunt. On the other hand, changes in the levels of metabolites in the presence of glucose or other readily fermentable sugars result in AceK dephosphorylating Idh (Nimmo and Nimmo, 1984), thereby activating Idh and diverting the isocitrate flux back through the TCA cycle.

To achieve glycolate synthesis from glucose via the glyoxylate shunt, we investigated different approaches to overcome this endogenous repression, such as the use of two different culture media (LB vs. M9), varying the glucose supplementation, over-expression of the enzymes of the glyoxylate shunt and enhancing endogenous expression of the *aceBAK* operon by knocking out the transcriptional regulator *iclR*. Further, glyoxylate and glycolate synthesized endogenously, are readily metabolized into a number of cell building blocks such as malate, 3-phosphoglycerate and 2-keto-4-hydroxyglutarate via a number of competing pathways (**Figure 4-2**). As part of this study, we also investigated the effect of knocking out some of these competing pathways on glycolate and DHBA / 3HBL synthesis.

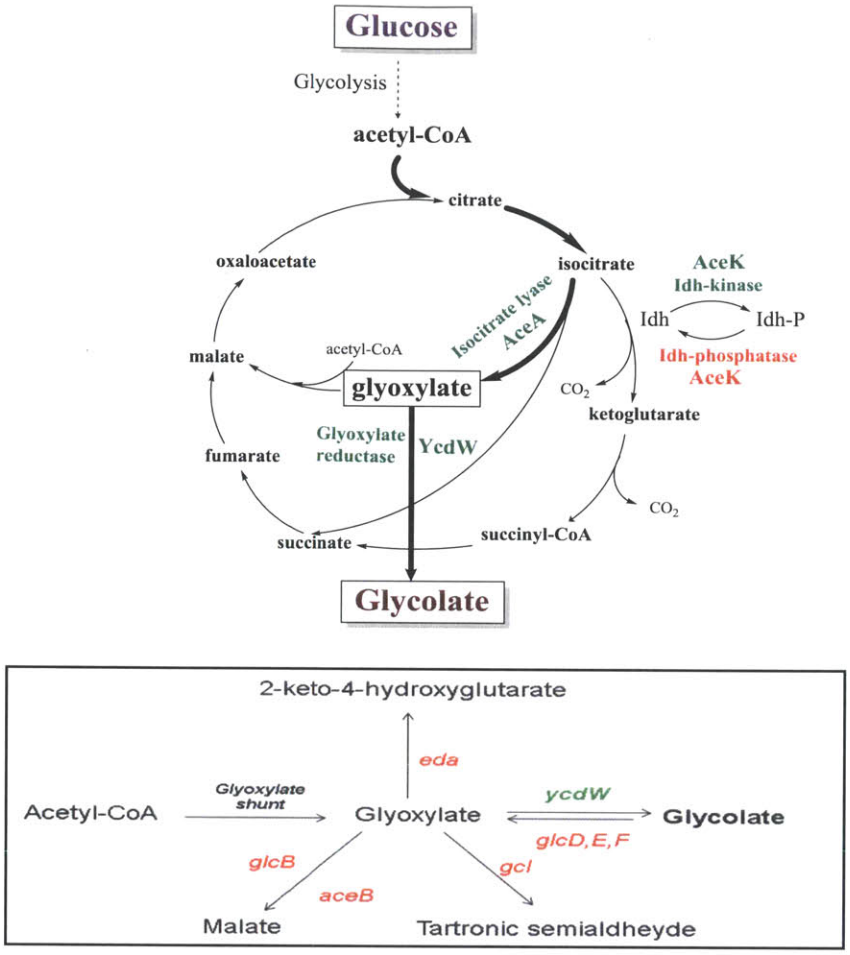

Figure 4-2 | Pathway for glycolate synthesis in *E. coli*. During growth on limited amount of glucose or acetate, Idh-kinase / phosphatase phosphorylates Idh, causing a drop in its activity, thereby reducing isocitrate flux through the TCA cycle. Simultaneous expression of isocitrate lyase (AceA) diverts isocitrate flux through the glyoxylate shunt, synthesizing glyoxylate which is reduced to glycolate by glyoxylate reductase (YcdW). The enzymes marked in green promote glycolate synthesis while those in red are detrimental to its synthesis.

Integration of the glycolate and 3,4-DHBA / 3HBL pathways requires the simultaneous over-expression of seven different pathway enzymes, imposing considerable metabolic stress. In addition to overcoming the endogenous repression of the glyoxylate shunt, achieving expression of all pathway enzymes and controlling the distribution of carbon between the two pathways is critical for effective product synthesis and improving pathway yield. It is our objective in this chapter to discuss the different challenges encountered and strategies employed to engineer the integration of these pathways and construct an *E. coli* strain capable of endogenous glycolate, 3,4-DHBA and 3HBL synthesis from glucose as a sole carbon source. Finally, one mole of acetate is produced per mole of 3,4-DHBA synthesized as a

by-product of the activation reaction of glycolate to glycolyl-CoA by Pct. Recycling this acetate back to acetyl-CoA using acetyl-CoA synthetase is expected to increase the acetyl-CoA availability for product synthesis and improve the overall pathway yield. The effect of over-expression of acetyl-CoA synthetase on the product titers and overall pathway yield was also assessed.

4.2. Materials and Methods

4.2.1. Microbial strains and plasmids

Table 4-1 lists the various strains and plasmids used in this study. *E. coli* MG1655 (DE3) strain (Tseng et al., 2009a), allows expression of various pathway genes cloned into Duet vectors (Novagen, Darmstadt, Germany) upon induction with isopropyl β-D-1-thiogalactopyranoside (IPTG) and was selected in place of M1655 (DE3 *ΔendA ΔrecA*) (used in our initial exploration of the 3HA pathway in the earlier chapters) for this study as it is capable of expressing RecA and is amenable to chromosomal modifications via homologous recombination. This strain served as the host strain for subsequent chromosomal modifications for construction of various glycolate producing strains. *E. coli* DH10B (Invitrogen, Carlsbad, CA) and ElectroTen-Blue (Stratagene, La Jolla, CA) electrocompetent cells were used for transformation with ligation reactions and propagation of all plasmids.

The construction of the two co-replicable plasmids, pDHP-1 (pET/bktB/phaB) and pDHP-2 (pCDF/pct/tesB) has been previously described in Chapter 2. Both of these plasmids contain the respective pathway genes cloned in front of T7*lac* promoters and ribosome binding sites in the respective Duet vectors and are capable of expressing *bktB*, *phaB*, *pct* and *tesB* for the 3,4-DHBA and 3HBL synthesis. These have been renamed here for ease of reference in the text. The *ycdW* gene was cloned between the NdeI and XhoI sites in MCSII of pCOLADuet-1 to first construct pCOLADuet/ycdW. The *aceA-aceK* genes from the *aceBAK* operon were amplified with flanking NcoI and EcoRI restriction sites via polymerase chain reaction (PCR) using MG1655 (DE3) genomic DNA (gDNA) as template and cloned into MCSI between the NcoI and EcoRI sites of pCOLADuet/ycdW to construct pGLY-1. pDHP-2a (pCDFDuet/pct/(acs-tesB)) was constructed by cloning an artificial operon consisting of the *acs* and *tesB* genes from *E. coli* into the NdeI and PacI sites of pCDFDuet/pct (construction described in Chapter 2). For the construction of this operon, the genes *acs* and *tesB* were PCR amplified from MG1655 (DE3) gDNA template using the primer pairs NdeI-*acs*-FP + *acs*-RP and tesB-FP + PacI-*tesB*-RP (**Table 4-2**) and

were subsequently spliced together using SOEing PCR (Heckman and Pease, 2007; Horton et al., 1989). The primers used to amplify different fragments for cloning reactions are listed in **Table 4-2.**

pKVS45 had been constructed by Kevin Solomon in the Prather Lab by separately PCR amplifying the pBAD30 backbone (Guzman et al., 1995) (using pBAD30-FP-XhoI and pBAD30-RP-AvrII, **Table 4-2**) and TetR cassette of pWW308 (Moon et al., 2009) (using *tetR*-FP-XhoI and *tetR*-RP-AvrII, **Table 4-2**) and ligating together the two gel purified PCR products at the introduced AvrII and XhoI sites. pHHD01K was constructed in turn from pKVS45 by replacing the AmpR cassette with KanR (to ensure co-replication with other hydroxyacid pathway plasmids) and eliminating the f1 origin (to limit the overall construct size). The pKVS45 backbone (with its tetracycline inducible promoter system and multi-cloning site, but without the AmpR cassette and f1 origin) and KanR cassette from pKD13 were separately PCR amplified using primers shown in **Table 4-2** and the resulting gel purified products were spliced together using SOEing PCR. The purified linear spliced product was finally ligated with the introduced flanking AatII terminal sites to obtain the pHHD01K plasmid which was then used to construct pGLY-2.

For the construction of the plasmid pGLY-2 (plasmid pHHD01K/ycdW-aceA-aceK), an artificial operon consisting of the genes *ycdW, aceA* and *aceK* was constructed and cloned into the multi-cloning site of pHHD01K, downstream of the Ptet promoter and ribosome binding site between the EcoRI and BamHI sites. For the construction of the *ycdW-aceA-aceK* artificial operon, the *ycdW* and *aceA-aceK* genes (from the *aceB-aceA-aceK* operon) from *E. coli* were first separately PCR amplified using *ycdW*-FP-EcoRI and *ycdW*-RP and *aceA-aceK*-FP and *aceA-aceK*-RP-BamHI respectively (**Table 4-2**). Purified PCR amplified fragments were then added in equimolar concentrations to a third PCR reaction without primers in order to initially splice the two fragments using SOEing PCR over 3 cycles. The intergenic sequence between the *E. coli aceB* and *aceA-aceK* genes in the natural *aceB-aceA-aceK* operon was used

as the intergenic overlapping sequence between *ycdW* and the *aceA-aceK* genes for SOEing in this artificial operon. Finally the *ycdW*-FP-EcoRI and *aceA-aceK*-RP-BamHI primers were added to the same PCR reaction to amplify the complete *ycdW-aceA-aceK* operon. The vector allows polycistronic expression of the *ycdW-aceA-aceK* genes upon induction with anhydrotetracycline (aTc).

Plasmids pETDuet-ΔT7 and pCDFDuet-ΔT7 were constructed by deleting the two regions containing the T7*lac* promoters, RBSs and multi-cloning sites from the parent plasmids pETDuet-1 and pCDFDuet-1, using primers listed in **Table 4-2**. High fidelity Phusion Polymerase (Finnzymes, Espoo, Finland) was used for all PCR reactions to construct various fragments for cloning. MG1655 (DE3) gDNA template used for these reactions was isolated using the Wizard Genomic Purification Kit (Promega, Madison, WI).

The glycolate producing strains GP1, GP2, GP3, GP3*ΔsucA* and GP4 (**Table 4-1**) were constructed via successively knocking out genes *iclR*, *aceB*, *gcl* and *glcB* from the parent strain MG1655 (DE3) (GP0) using P1 transduction to transfer knockout mutations from the corresponding Keio collection single knockout donor strains (Baba et al., 2006). Strain GP0-1 was constructed by transforming strain GP0 with the plasmid pGLY-1 to allow expression of *ycdW*, *aceA* and *aceK* on induction with IPTG. Similarly, strains GP0-2, GP1-2 GP2-2, GP3-2, GP3*ΔsucA*-2 and GP4-2 were constructed by transforming GP0 to GP4 with the plasmid pGLY-2 which expresses the same enzymes upon induction with aTc. Positive transformants were isolated on LB agar plates supplemented with 50 μg/ml of kanamycin. Strains GP0-1-DHP and GP0-2-DHP were created by co-transforming strains GP0-1 and GP0-2 with the 3,4-DHBA / 3-HBL pathway plasmids pDHP-1 and pDHP-2, respectively, for integration of the glycolate and 3,4-DHBA / 3HBL pathways and positive transformants were selected on LB agar plates supplemented with 50 μg/ml of ampicillin, 50 μg/ml of streptomycin and 30 μg/ml of kanamycin. Similarly, strains GP1-2-DHP to GP4-2-DHP were constructed by co-transforming pDHP-1 and pDHP-2 into strains GP1-2 to GP1-4. Strain GP0-1-EC was derived from GP0-1 by co-transforming with the empty Duet vectors pETDuet-1 and

pCDFDuet-1, while the GP0-1-ΔT7C strain was obtained by co-transforming with the control vectors pETDuet-ΔT7 and pCDFDuet-ΔT7 lacking the T7*lac* promoter sites.

Table 4-1 | *E. coli* strains and plasmids

Name	Relevant Genotype	Reference
Strains		
DH10B	F⁻ *mcr*A Δ(*mrr-hsd*RMS-*mcr*BC) ϕ80*lacZ*ΔM15 Δ*lacX74 recA1 endA1 araD139*Δ(*ara, leu*)7697 *galU galK* λ⁻ *rpsL nupG*	Invitrogen
ElectroTen-Blue	Δ(*mcrA*)*183* Δ*(mcrCB-hsdSMR-mrr)173 endA1 supE44 thi-1 recA1 gyrA96 relA1 lac* Kan^r [F′ *proAB lacI*^{q}ZΔM15 Tn*10* (Tet^r)]	Stratagene
MG1655 (DE3)	F⁻ λ⁻ *ilvG- rfb-50 rph-1 with the DE3 prophage integrated*	Tseng 2010
DHP0	MG1655 (DE3) carrying pDHP-1 and pDHP-2	This study
DHP0+*acs*	MG1655 (DE3) carrying pDHP-1 and pDHP-2a	This study
GP0-1	MG1655 (DE3) carrying pGLY-1	This study
GP0-1-DHP	GP0-1 containing pDHP-1 and pDHP-2	This study
GP0-2	MG1655 (DE3) carrying pGLY2	This study
GP0-1-EC	GP0-1 containing pETDuet-1 and pCDFDuet-1	This study
GP0-1-ΔT7	GP0-1 containing pETDuet-ΔT7 and pCDFDuet-ΔT7	This study
GP0-2-DHP	GP0-2 carrying pDHP-1 and pDHP-2	This study
GP1	MG1655 (DE3) Δ*iclR*	This study
GP2	MG1655 (DE3) Δ*iclR,* Δ*aceB*	This study
GP3	MG1655 (DE3) Δ*iclR,* Δ*aceB,* Δ*gcl*	This study
GP3 Δ*sucA*	MG1655 (DE3) Δ*iclR,* Δ*aceB,* Δ*gcl,* Δ*sucA*	This study
GP4	MG1655 (DE3) Δ*iclR,* Δ*aceB,* Δ*gcl,* Δ*glcB*	This study
GP1-2	GP1 carrying pGLY-2	This study
GP2-2	GP2 carrying pGLY-2	This study
GP3-2	GP3 carrying pGLY-2	This study
GP3 Δ*sucA*-2	GP3 Δ*sucA* carrying pGLY-2	This study
GP4-2	GP4 carrying pGLY-2	This study
GP1-2-DHP	GP1-2 carrying pDHP-1 and pDHP-2	This study
GP2-2-DHP	GP2-2 carrying pDHP-1 and pDHP-2	This study
GP3-2-DHP	GP3-2 carrying pDHP-1 and pDHP-2	This study
GP3 Δ*sucA*-2-DHP	GP3 Δ*sucA*-2 carrying pDHP-1 and pDHP-2	This study
GP4-2-DHP	GP4-2 carrying pDHP-1 and pDHP-2	This study
GP3-J23108-*Y*	GP3 with the promoter and RBS preceding the gene *ycdW* replaced with J23108 (Anderson promoter) and BBa_0034 (synthetic RBS)	This study
GP3-J23100-*Y*	GP3 with the promoter and RBS preceding the gene *ycdW* replaced with J23100 (Anderson promoter) and BBa_0034 (synthetic RBS)	This study
GP3-J23119-*Y*	GP3 with the promoter and RBS preceding the gene *ycdW* replaced with J23119 (Anderson promoter) and BBa_0034 (synthetic RBS)	This study
GP3-J23119-*YAK*	GP3 with the promoter and RBS preceding the gene *ycdW,* and *aceA-aceK* replaced with J23119 (Anderson promoter) and BBa_0034 (synthetic RBS)	This study
GP0-EGP	GP0 with its *aceBAK* operon replaced with the TetR gene and *ycdW-aceA-aceK* operon preceded by a pTet promoter from pGLY-2	This study
GP0-EGP-EC	GP0-EGP carrying pETDuet-1 and pCDFDuet-1	This study
GP0-EGP-DHP	GP0-EGP carrying pDHP-1 and pDHP-2	This study

Plasmids

pETDuet-1	ColE1 (pBR322) *ori*, *lacI*, T7*lac*, Amp^R	Novagen
pCDFDuet-1	CloDF13 *ori*, *lacI*, T7*lac*, $Strep^R$	Novagen
pCOLADuet-1	ColA *ori*, *lacI*, T7*lac*, Kan^R	Novagen
pHHD01K	p15 *ori*, *tetR*, Ptet, Kan^R	This study
pGLY-1	pCOLADuet-1 harboring *ycdW* and *aceA-aceK* from *E. coli* MG1655	This study
pGLY-2	pHHD01K harboring the genes *ycdW, aceA and aceK* from *E. coli* MG1655 in an artificial operon similar in structure to the *aceBAK* operon	This study
pCOLA/aceA-aceK	pCOLADuet-1 carrying the *aceA-aceK* operon in MCSI	This study
pDHP-1	pETDuet-1 harboring *bktB* and *phaB* from *C. necator* named pET/bktB/phaB in Martin *et al*, 2013	Chapter 2
pDHP-2	pCDFDuet-1 harboring *pct* from *M. elsdenii*, and *tes*B from *E. coli* MG1655 named pCDF/pct/tesB in Martin *et al*, 2013	Chapter 2
pDHP2a	pCDFDuet-1 harboring *pct* from *M. elsdenii*, and *an artificial operon of the genes acs and tes*B from *E. coli* MG1655	This study

Table 4-2 | List of DNA oligonucleotide primers used in the cloning of genes and for qPCR reactions
Primer names correspond to the name of the gene or vector backbone that the primer amplifies, whether the primer is the forward primer (FP) or reverse primer (RP) of that gene or vector, and the restriction site incorporated into the primer sequence (in case of a primer used to generate a fragment for cloning). For primers used to amplify the *acs* and *tesB* genes from *E. coli* for the construction of the *acs-tesB* operon, sequences indicated in bold correspond to parts of the complementary overlapping regions for SOEing PCR.

Primer	Sequence 5'→3'
ycdW-FP-NdeI	TAAAAACATATGGATATCATCTTTTATCACCCAACG
ycdW-RP-XhoI	TAAAAACTCGAGTTAGTAGCCGCGTGCG
aceAK-FP-NcoI	TAAAAACCATGGGCATGGAGCATCTGCAC
aceAK-RP-EcoRI	TAAAAAGAATTCTCAAAAAAGCATCTCCCCATAC
pETDuet-ΔT7-FP-XmaI	GAAAAAACCCGGGGGCAGATCTCAATTGGATATCGG
ycdW-FP-EcoRI	AAAAAAGAATTCCAACGCTTTTCGGGAGTC
ycdW-RP	CATGTGCAGATGCTCCATAGTTATGTGGTGGTTTAGTAGCCG CGTGCGC
aceA-aceK-FP	ACCACCACATAACTATGGAGCATC
aceA-aceK-RP-BamHI	AAAAAAGGATCCTCAAAAAAGCATCTCCCCATAC
pKVS45-FP-AatII	AAAAAAGACGTCCATCGCAGTACTGTTGTAATTC
pKVS45-RP	AACAAAACAGTTTGTAGAAACGC
kanR-FP	GCCTTTTTGCGTTTCTACAAACTCTTTTGTTTATTTTTCTAAATA CTGCAGTGGGCTTACATGG
kanR-FP-AatII	AAAAAAGACGTCGTGTAGGCTGGAGCTGC
pBAD30-FP-XhoI	CTATCTCGAGGATAAGCTGTCAAACATGAGCAG
pBAD30-RP-AvrII	CTATCCTAGGTTTCTCCATACCCGTTTTTTTG
tetR-FP-XhoI	CTATCTCGAGTTAAGACCCACTTTCACATTTAAGTTG
tetR-FP-AvrII	CTATCCTAGGGTGCTCAGTATCTCTATCACTGATAGG
pETDuet-ΔT7-RP-XmaI	GAAAAAACCCGGGGATCTCGATCCTCTACGCCG
pCDFDuet-ΔT7-FP-XmaI	GAAAAAACCCGGGGGCAGATCTCAATTGGATATCGG
pCDFDuet-ΔT7-RP-XmaI	GAAAAAACCCGGGGAGTCGCATAAGGGAGAGCGTC
ycdW-qPCR-FP	CACATGTCGCCGCGATT
ycdW-qPCR-RP	GGCAATGGTGCGAGAAATGTA
aceA-qPCR-FP	ACCGGCGAGCGTACCA
aceA-qPCR-RP	CCAGGCCACGGCTGATC
NdeI-*acs*-FP	TAAAAACATATGAGCCAAATTCACAAACACAC
acs-RP	**TATATATCTCCTTCTTATTTACGATGGCATC**GCGATAG
tesB-FP	**GATGCCATCGTAAATAAGAAGGAGATATATA**ATGAGTCAGG CGATAAAAAATTTAC
PacI-*tesB*-RP	TAAAAAAATTAATTGTGATTACGCATCACCC

4.2.2. Culture conditions

Evaluation of glycolate, 3,4-DHBA and 3HBL synthesis by the various strains was performed in either 50 mL of Luria Bertani (LB) medium or M9 minimal salt medium (Sigma Aldrich) supplemented with varying amounts of glucose and appropriate antibiotics in 250 mL shake flasks. Strains GP0-1 and GP0-2 were grown in media supplemented with kanamycin sulfate (50 mg/L), while strains GP0-1-DHP, GP0-2-DHP, GP0-1EC, GP0-1-ΔT7 and GP1-2-DHP to GP4-2-DHP were cultured in media supplemented with ampicillin sulfate (50 mg/L), streptomycin sulfate (50 mg/L) and kanamycin sulfate (30 mg/L). For inoculation of the M9-glucose medium culture flasks, 5 mL seed cultures were grown overnight in LB (supplemented with appropriate antibiotics) at 37˚C and the centrifuged pellets were re-suspended in 1 ml of M9 minimal medium to minimize carryover of spent LB culture broth. These re-suspended cultures were used to inoculate 50 mL M9 minimal medium cultures supplemented with glucose to an initial OD_{600} of 0.1. The shake flask cultures were then incubated at 30°C on a rotary shaker at 250rpm. LB cultures were inoculated directly with 2% (vol./vol.) of an overnight LB seed culture. In both LB and M9 shake flask cultures, once the cells reached mid-exponential phase (when OD_{600} reached 0.8-1.0), pathway gene expression was induced by supplementing cultures with the appropriate inducers (250 ng/ml aTc and/or 100 μM or 1 mM IPTG). 1 mL of culture was withdrawn every 24 hours post-induction for up to 96 h to collect culture supernatants for HPLC analysis. Titers of various products reached a plateau by 72 h and there was essentially no difference in the titers between 72 h and 96 h; accordingly, only the peak titers observed at 72 h are reported. In general, experiments were performed in triplicates, and data are presented as the averages and standard deviations of the results.

4.2.3. Metabolite analysis

Various metabolites were analyzed on an Agilent 1200 series HPLC instrument equipped with an Aminex HPX-87H ion exchange column (Biorad Laboratories, Hercules, CA) with 5 mM sulfuric acid as the mobile phase and a refractive index detector (RID) as described in chapter 2. Standard curves were

constructed using respective commercially available standards. A commercial standard was not available for 2,3-DHBA and 3HBL and these were quantified using the method described in Chapter 2

4.2.4. SDS-PAGE gel analysis and preparation of protein lysates

To prepare protein lysates, the respective *E. coli* strains were cultured in 50 ml of M9 minimal medium supplemented with 1% (wt./vol.) glucose. The cultures were induced with IPTG (100μM or 1mM) in mid-exponential phase. Cell pellets prepared from 5 ml samples collected 6 hours post induction from each of the flasks were re-suspended in 1 mL of 10 mM Tris-HCl buffer (pH=8.0) containing 1 mg/mL lysozyme and were used to prepare crude lysates using cell disruption beads. Lysates were then clarified by centrifugation and separated electrophoretically into component proteins on 4-20% SDS-PAGE gels (BioRad Laboratories, Hercules, CA), loading about 15 μg of total protein into each well. Total protein levels in the crude lysates were measured using a modified Bradford assay (Zor and Seliger, 1996).

4.2.5. Quantification of mRNA transcript levels

The transcript levels for the mRNAs corresponding to *ycdW* and *aceA* were measured using a RT-qPCR assay. For this assay, the various strains were cultured in M9 minimal medium supplemented with 0.8% (wt./vol.) glucose and were induced with 1 mM IPTG in mid-exponential phase. mRNA was isolated from cell samples (~10^9 cells) collected 6 hours post induction, using the illustra RNAspin Mini Kit (GE Healthcare Bio-Sciences, Piscataway, NJ). cDNA was synthesized via reverse transcription from each of the mRNA samples, with 500 ng of total RNA in each case, using the QuantiTect Reverse Transcription Kit (Qiagen, Valencia, CA) with random hexameric primers. *ycdW* and *aceA* mRNA levels were measured by amplifying the corresponding mRNAs from the synthesized cDNA in a qPCR reaction using the Brilliant II Sybr Green High ROX QPCR Mix (Agilent Technologies, Santa Clara, CA) on an ABI 7300 Real Time PCR instrument (Applied Biosystems, Beverly, CA), using *ycdW*-qPCR-FP and *ycdW*-qPCR-RP for the *ycdW* mRNA and *aceA*-qPCR-FP and *aceA*-qPCR-RP for *aceA* mRNA, respectively (**Table 4-2**).

Transcript levels in each sample were measured in triplicate (three qPCR reactions each) with additional no-template and no-RT controls. Transcript levels for each of the mRNAs are reported relative to those for the same mRNA in strain GP0-1 (as determined using a standard curve), as averages of three flasks for each strain, each measured in triplicate.

4.3. Results

4.3.1. Comparing DHBA & 3HBL synthesis in MG1655 (DE3 *ΔendA ΔrecA*) and MG1655 (DE3)

The *E. coli* K-12 strain MG1655 (DE3) (strain GP0) was selected as the host strain for investigating direct synthesis of DHBA and 3HBL from glucose, owing to its amenability to chromosomal engineering via homologous recombination. We compared DHBA and 3HBL synthesis from exogenously supplied glycolate in this strain transformed with DHBA pathway plasmids (strain DHP0) with the previously described strain MG1655 (DE3 *ΔendA ΔrecA*) carrying the same plasmids (strain MG4, used for investigating the 3HA platform in Chapter 2) to establish a baseline for the product titers with this strain. It was observed that strain MG1655 (DE3) proved superior to MG1655 (DE3 *ΔendA ΔrecA*) in terms of 3HA synthesis, with 50% higher total DHBA + 3HBL, 34% higher 3HB titers (**Figure 4-3**) and an overall yield of 53% on the supplied glycolate. The reasons for these differences are not known.

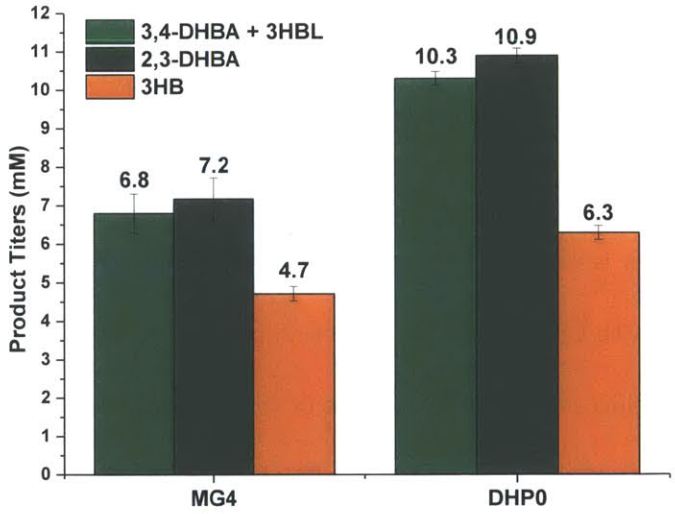

Strain	3,4-DHBA (mg/L)	3HBL (mg/L)	2,3-DHBA (mg/L)	([3,4-DHBA]+[3HBL]) / [3HB]	([3,4-DHBA]+[3HBL]) / [2,3-DHBA]
MG4 (MG1655 (DE3 *ΔendA ΔrecA*))	555 ± 52	221 ± 15	860 ± 65	2.58	0.95
DHP0 (MG1655 (DE3))	918 ± 12	271 ± 01	1309 ± 23	3.37	0.95

Figure 4-3 | DHBA / 3HBL synthesis by strains MG1655 (DE3 *ΔendA ΔrecA*) and MG1655 (DE3) Each of the strains were transformed with the DHBA pathway plasmids pDHP-1 and pDHP-2 and cultured in LB supplemented with 1% glucose and 40 mM glycolate. Product titer (in mM) 72 hours post induction are reported.

4.3.2. Investigating glycolate synthesis in *E. coli* with over-expression of pathway enzymes

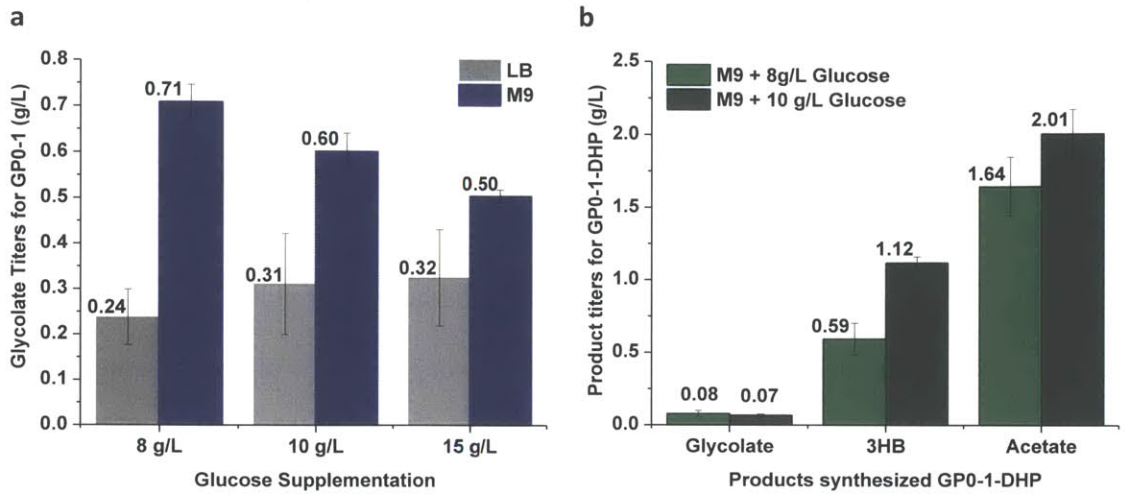

Figure 4-4 | Product synthesis by strains GP0-1 and GP0-1-DHP (a) Glycolate titers for GP0-1 cells cultured in LB or M9 supplemented with 8, 10 or 15g/L glucose **(b)** Titers for different products synthesized by strain GP0-1-DHP cultured in M9 minimal medium supplemented with 8 or 10 g/L glucose All cultures were induced with 1 mM IPTG and titers are reported 72 hours post induction. Data are presented as the mean ± s.d. (n=3).

Glycolate synthesis was then investigated in MG1655 (DE3) (strain GP0) transformed with pGLY-1 (strain GP0-1) that allows over-expression of the glycolate pathway enzymes YcdW, AceA and AceK from T7 promoters. Since part of the repression of the glyoxylate shunt during growth on glucose stems from transcriptional repression of expression of *aceA* and *aceK* from the *aceBAK* operon, over-expression of these genes is expected to relieve this repression and divert isocitrate flux towards glyoxylate. Experiments with GP0-1 were conducted in both LB and M9 minimal media supplemented with varying amounts of glucose with the objective of selecting appropriate culture conditions. GP0-1 was observed to synthesize about 0.7 to 0.8 g/L of glycolate in M9 minimal medium cultures supplemented with 0.8% glucose and induced with 1 mM IPTG (**Figure 4-4a**). These titers are 8 fold higher than the corresponding empty vector control, indicating that over-expression of glyoxylate shunt enzymes had indeed enabled glycolate synthesis. In comparison, GP0-1 cultures in the richer LB medium supplemented with glucose made considerably less glycolate with maximum titers of only 0.3

g/L, possibly due to repression of the glyoxylate shunt to a greater extent in the rich medium. Thus glucose supplemented M9 medium was selected for further studies.

4.3.3. Investigating integration of glycolate and 3,4-DHBA pathways

We sought to integrate the glycolate and 3,4-DHBA / 3HBL pathways in GP0-1 by co-transforming the 3,4-DHBA / 3HBL pathway plasmids pDHP-1 and pDHP-2 to construct the strain GP0-1-DHP. No 3,4-DHBA or 3HBL synthesis was observed with GP0-1-DHP when cultured in M9 supplemented with various glucose (0.6 to 2%) and inducer concentrations (100 µM to 1 mM). The cultures were only observed to synthesize the pathway byproduct acetate and the side-product 3HB, formed due to the natural tendency of the pathway enzymes to condense two acetyl-CoA molecules (**Figure 4-1** and **Figure 4-4b**). Further, in comparison to GP0-1, GP0-1-DHP cultures produced less than 0.1 g/L of glycolate (**Figure 4-4b**) indicating that the presence of the additional two 3,4-DHBA / 3HBL pathway plasmids and expression of additional pathway enzymes had hampered glycolate synthesis in this strain.

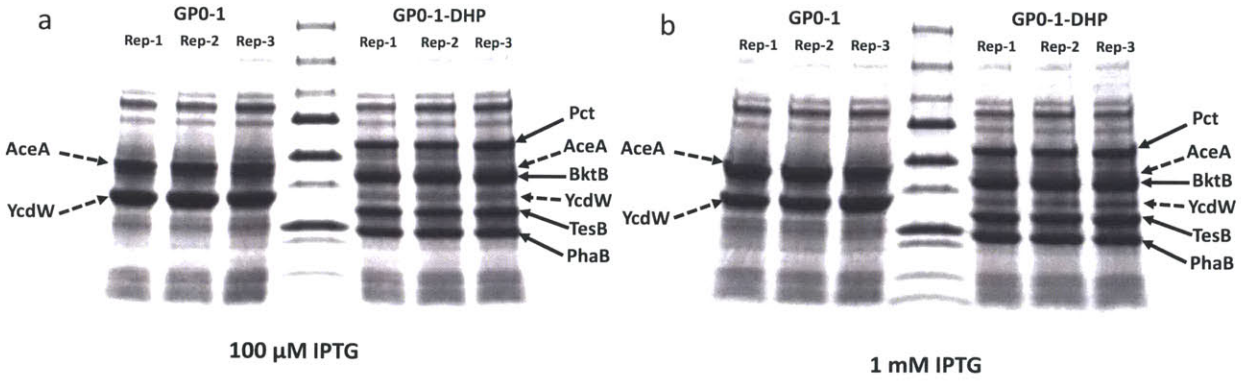

Figure 4-5 | Expression of pathway enzymes in recombinant strains GP0-1 and GP0-1-DHP. Protein lysates isolated from strains GP0-1 and GP0-1-DHP, grown in minimal medium supplemented with 1% glucose and induced with a) 100µM IPTG and b) 1 mM IPTG were loaded on a SDS-PAG gel for separation. For each gel , lanes 1-3 on the left show lysates from GP0-1 cultures (3 replicates) while 5-7 show lysates from GP0-1-DHP. Lane 4 was loaded with the unstained protein ladder. Similar results were observed for cultures induced with 500 µM IPTG.

To investigate this further, protein lysates were prepared from GP0-1 and GP0-1-DHP cultures for different levels of IPTG induction. Analysis on SDS-PAGE gels (**Figure 4-5**) revealed that while GP0-1

over-expressed the glycolate pathway enzymes AceA and YcdW, similar over-expression of these enzymes was not observed in strain GP0-1-DHP. Instead, GP0-1-DHP only over-expressed the 3,4-DHBA / 3HBL pathway enzymes Pct, BktB, PhaB and TesB. The negligible glycolate synthesis in GP0-1-DHP was thus attributed to insufficient expression of the glycolate pathway enzymes from pGLY-1 in the presence of the additional 3,4-DHBA / 3HBL pathway plasmids. It should be noted that a band corresponding to AceK over-expression is not observed, even in lysates isolated from strain GP0-1, possibly due to the combined effect of transcriptional and translational control mechanisms that result in a 1000 fold lower expression of AceK in comparison to AceA (Cortay et al., 1989; Cozzone, 1998; Kornberg, 1966). However, in wild type *E. coli*, AceK is known to be highly active and present in a large excess over that required for its regulatory function (Stueland et al., 1989) and this lack of over-expression does not seem to affect glycolate synthesis adversely in GP0-1.

Two possible phenomena may be hypothesized for this reduced expression of the glycolate pathway enzymes in the presence of additional pathway plasmids: a) plasmid instability or b) reduced T7 RNA polymerase (RNAP) availability. Restriction digests of plasmids isolated from the cultures 24 hours post induction indicated that all plasmids were retained as expected by the cells. Thus, additional experiments were directed towards investigating T7 RNAP availability.

4.3.4. Investigating reduced T7 RNAP availability

Integration of the pathways in GP0-1-DHP relies on the simultaneous over-expression of all seven pathway enzymes from their respective genes cloned downstream of T7*lac* promoters and ribosome binding sites in the three Duet vector derived plasmids pDHP-1, pDHP-2 and pGLY-1. All three pathway plasmids depend on T7 RNAP to initiate transcription of the pathway genes, which is synthesized in each of the strains from the chromosomally integrated DE3 prophage cassette upon induction with IPTG. While all of the T7 RNAP synthesized in the GP0-1 cells is exclusively available to

initiate expression of the glycolate pathway enzymes via transcription from multiple copies of pGLY-1, the same T7 RNAP in GP0-1-DHP is distributed between multiple copies of the three different plasmids (pDHP-1, pDHP-2 and pGLY-1), reducing the amount of T7 RNAP available to initiate transcription from each copy of the three different plasmids. We hypothesized that in GP0-1-DHP, this reduced T7 RNAP availability in the presence of the additional pDHP-1 and pDHP-2 plasmids was hampering the expression of the glycolate pathway enzymes from pGLY-1, preventing effective glycolate synthesis.

To test this hypothesis, glycolate synthesis and glycolate pathway enzyme transcript levels were compared in strains GP0-1, GP0-1-ΔT7, GP0-1-EC and GP0-1-DHP. Similar to T7 RNAP sequestration by pDHP-1 and pDHP-2 in GP0-1-DHP, the T7*lac* promoter sites in the empty plasmids are expected to sequester some of the available T7 RNAP from pGLY-1 in GP0-1-EC, though to a lesser extent due to lack of active sustained transcription, while also imposing a slightly decreased burden due to the inability to actually express any recombinant protein and a smaller size of the empty plasmid vectors. Indeed, GP0-1-EC is observed to have produced less glycolate than GP0-1 but more than GP0-1-DHP (**Figure 4-6a**). On the other hand, deletion of the T7 promoter sites in pETDuet-ΔT7 and pCDFDuet-ΔT7 is expected to alleviate the T7 RNAP sequestration problem. GP0-1- ΔT7 was observed to produce more glycolate than GP0-1-EC, though to a lesser extent than GP0-1, possibly due to the burden of maintaining the additional pETDuet-ΔT7 and pCDFDuet-ΔT7 plasmids (**Figure 4-6a**).

The transcript levels for *ycdW* and *aceA* mRNA in these different strains were measured and compared to determine if decreased expression of these enzymes in the presence of the additional pathway plasmids was indeed a result of decreased transcription (**Figure 4-6b** and **c**). The mRNA transcript levels for both *ycdW* and *aceA* in strains GP0-1-EC and GP0-1-DHP are several fold lower than the corresponding GP0-1 and GP0-1-ΔT7 transcript levels. In particular, for strain GP0-1-DHP, the *ycdW* transcript levels were 80 fold lower while the *aceA* transcript levels were 36 fold lower than those observed with GP0-1. Thus, the reduced transcript levels combined with an increased competition for

ribosomes for translation from the other mRNAs expressed from pDHP-1 and pDHP-2 result in poor expression of *ycdW* and *aceA* and negligible glycolate synthesis in GP0-1-DHP.

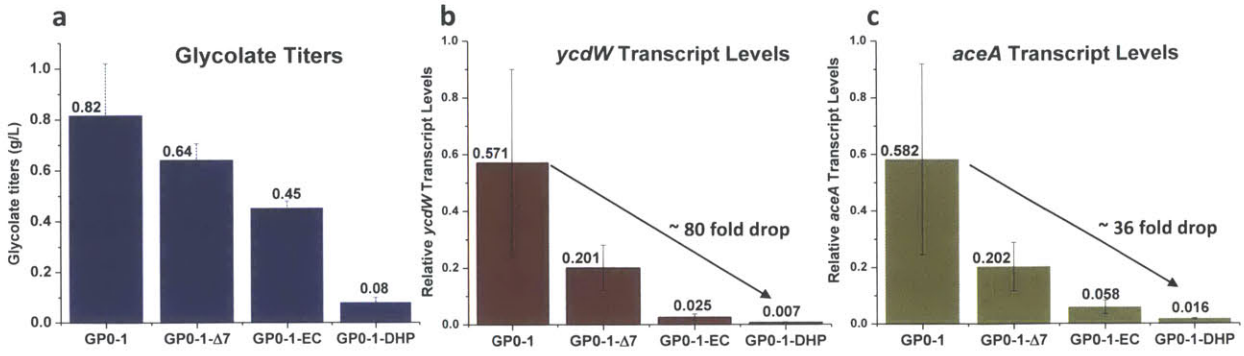

Figure 4-6 | Glycolate synthesis in engineered strains All strains were cultured in M9 supplemented with 0.8% glucose at 30 °C with 1 mM IPTG induction in triplicate. **(a)** Glycolate titers reported as mean ± s.d. (n=3). **(b)** *ycdW* mRNA transcript levels and **(c)** *aceA* mRNA transcript levels.

Strains: 1) GP0-1 = MG1655 (DE3) + pGLY-1, 2) GP0-1-ΔT7 = GP0-1 carrying pETDuet-ΔT7 and pCDFDuet-ΔT7, 3) GP0-1-EC = GP0-1 carrying pETDuet and pCDFDuet and 4) GP0-1-DHP = GP0-1 carrying pDHP-1 and pDHP-2

4.3.5. Alleviating T7 RNAP limitations through the use of an orthogonal expression system

To alleviate the T7RNAP limitation, we employed an orthogonal expression system that allows expression of the glycolate pathway enzymes independent of T7 RNAP. The glycolate pathway genes *ycdW*, *aceA* and *aceK* were cloned as an operon into pHHD01K downstream of an aTc inducible PTet promoter and ribosome binding site to construct pGLY-2. Strain GP0-2 carrying pGLY-2 cultured in minimal medium supplemented with 1% glucose upon induction with aTc resulted in glycolate synthesis superior to GP0-1 with titers up to 1455 ± 209 mg/L. The initial glucose concentration as well as the aTc concentration used for induction were observed to have a negligible effect on glycolate synthesis (**Figure 4-7a**) with GP0-2. Similar to GP0-1, strain GP0-2 was observed to synthesize glycolate to a much lesser extent in LB, with maximum titers of only about 0.5 g/L. Additionally, GP0-2-DHP carrying this new glycolate pathway plasmid pGLY-2 in addition to pDHP-1 and pDHP-2 cultured in M9-glucose medium synthesized up to 1280 ± 41 mg/L of glycolate. Protein lysates from GP0-2-DHP showed the expected

over-expression of the glycolate pathway enzymes in addition to the DHBA / 3HBL pathway enzymes (**Figure 4-7b**). Further, we observed direct synthesis of up to 699 ± 109 mg/L of 3,4-DHBA and 312 ± 12 mg/L of 3HBL from glucose as a sole carbon source in this integrated system alongside 317 ± 9 mg/L of 3HB and 633 ± 62 mg/L of 2,3-DHBA as side products (**Figure 4-9**).

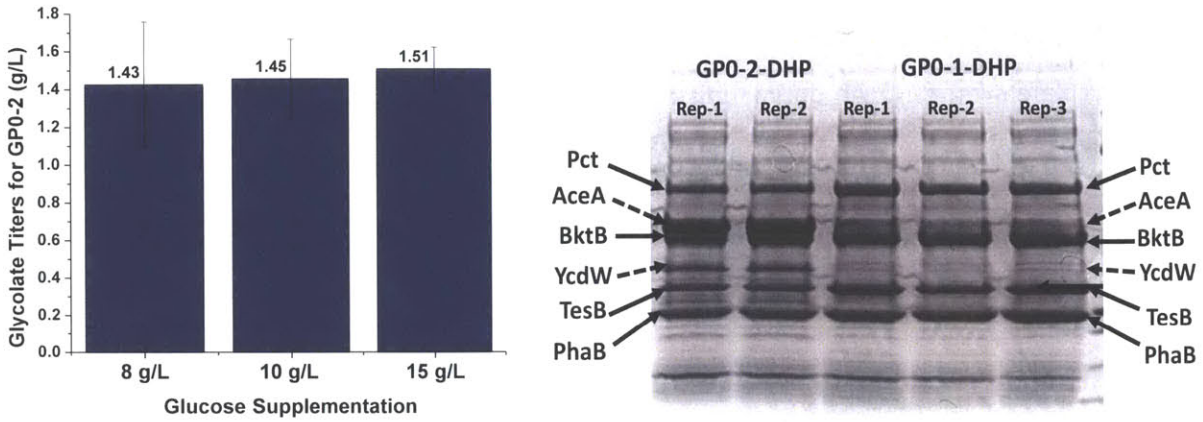

Figure 4-7 | Glycolate synthesis by GP0-2 and protein expression in GP0-2-DHP (a) Glycolate titers 72 hours post induction for GP0-2 cultured in M9 minimal medium supplemented different amounts of glucose and 250 ng/ml aTc. **(b)** Protein lysates from strains GP0-2-DHP and GP0-1-DHP, grown in glucose minimal medium were loaded on a SDS-PAG gel for separation. From the left, lanes 1-2 show lysates from GP0-2-DHP cultures (2 replicates) while 3-5 show lysates from GP0-1-DHP. While GP0-2-DHP shows over-expression of the glycolate pathway enzymes YcdW and AceA in addition to the DHBA / 3HBL pathway enzymes, GP0-1-DHP only shows over-expression of the DHBA / 3HBL pathway enzymes, with only faint bands corresponding to AceA and YcdW.

4.3.6. Carbon utilization and distribution between pathway products – Effect of inducer levels and glucose supplementation

The use of two orthogonal expression systems also allowed us to exercise independent control over the expression of the glycolate and DHBA / 3HBL synthesis pathway enzymes by varying the induction levels for each of the expression systems, resulting in variations in the total DHBA + 3HBL titers as well as the net glycolate synthesis levels and the relative carbon flux towards glycolate synthesis vs. the 3-hydroxyacid pathway products (**Figure 4-8a** and **b**). Variation in the aTc induction levels was observed to have less influence as compared to the variation in the IPTG levels at a given aTc inducer concentration. For a given aTc inducer concentration, increasing the level of IPTG from 50 to 100 μM is expected to increase the expression levels for the downstream pathway enzymes and results in an

increase in the titers of the total hydroxyacid products (DHBA+3HBL+3HB) from the downstream DHBA / 3HBL pathway. Interestingly, this increase in the downstream pathway products was accompanied by an increase in the net glycolate synthesized, indicating that consumption of glycolate along the pathway promotes more glycolate synthesis along the upstream pathway. However, further increasing the IPTG induction level to 200 µM imposed a metabolic stress resulting in reduced hydroxyacid product as well as net glycolate synthesis. An optimal distribution of carbon (acetyl-CoA) between the two pathways was observed at about 100 µM IPTG induction, with the highest total DHBA + 3HBL titers (about 10.5 mM) observed at 250 ng/ml aTc and 100 µM IPTG inducer concentrations.

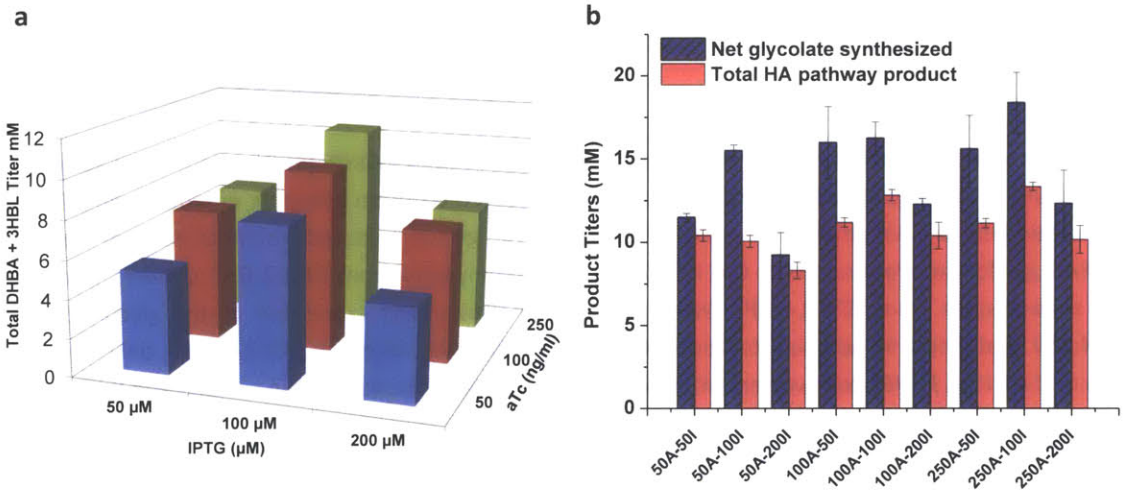

Figure 4-8 | Effect of varying inducer levels on DHBA synthesis. (a) Total DHBA (both isomers)+ 3HBL titers in mM for GP0-2-DHP cultured in M9 supplemented with 1% glucose for different induction levels. **(b)** Total hydroxyacid (HA) product titers are the sum of the titers for the two DHBA isomers, 3HBL and 3HB. Net glycolate synthesized is calculated as the sum of the glycolate titers at the end of 72 hours and the glycolate that ends up as DHBA + 3HBL (based on the t=72 h titers for the two DHBA isomers and 3HBL). The x-axis in the plot denotes different inducer combinations (e.g.:50A-50I denotes induction with 50 ng/ml aTc (A) and 50 µM IPTG (I) and so on).

We also investigated the effect of varying the supplied glucose substrate concentration on the product profile. The titers for 3,4-DHBA and 3HBL were observed to double with an increase in the glucose supplementation from 8 g/L to 10 g/L (**Figure 4-9a**), with a negligible influence of a further increase to 15 g/L. The glucose fed to the cultures is utilized for the synthesis of pathway products

(glycolate, 3,4-DHBA, 2,3-DHBA and 3HBL), the competing side product 3HB, by-product acetate and biomass and maintenance functions. The distribution of the supplied glucose between these products over the course of the fermentation determines the overall pathway yield and understanding this carbon distribution is important from the point of view of improving yield and productivity.

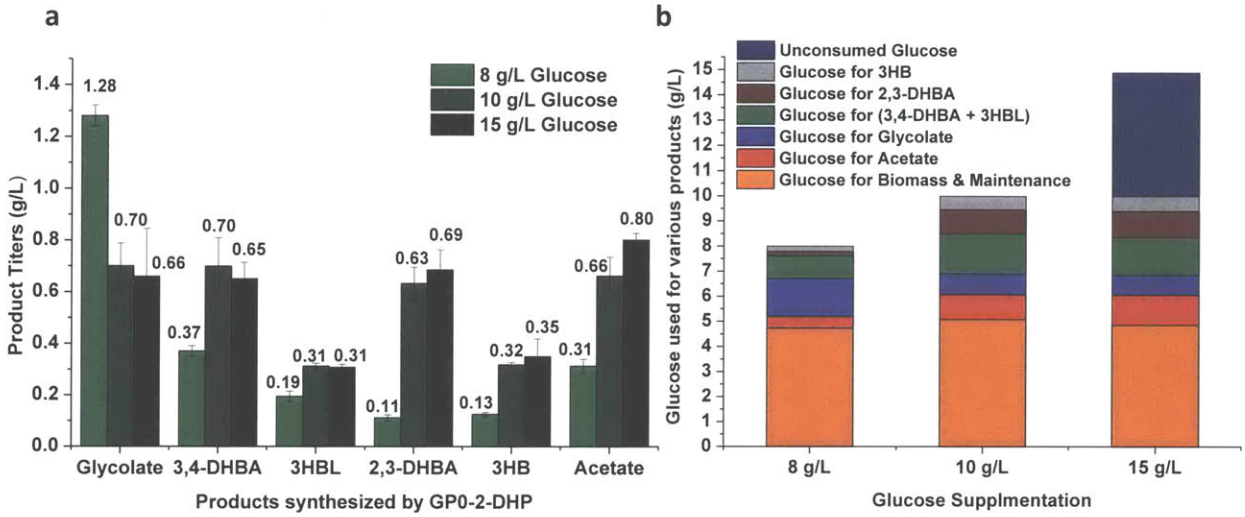

Figure 4-9 | Product profiles and distribution of carbon in the synthesis of glycolate, DHBA and 3HBL with GP0-2-DHP. GP0-2-DHP was cultured in M9 minimal medium supplemented with varying amounts of glucose (8, 10 and 15 g/L), induced with aTc (250 ng/ml) and IPTG (100μM). **(a)** Product titers **(b)** Glucose utilized for different products in g/L. All flask cultures were run in triplicate with product titers reported as mean ±s.d.(n=3).

As observed from (**Figure 4-9b**), for different starting glucose concentrations, the cells utilized roughly 5 g/L of the supplied glucose for building biomass (biocatalyst) and for maintenance functions and the balance was available for conversion to products. Thus in case of 8 g/L of supplied glucose, a large fraction of the remaining 3 g/L glucose was observed to be converted to glycolate with only a small amount converted to the final products of interest (DHBA and 3HBL). This is indicative of the fact that the cells exhaust glucose before the synthesized glycolate may be converted substantially along the downstream pathway to DHBA and 3HBL and highlights the sequential nature of synthesis of products in this fermentation. Indeed, when the supplied glucose concentration was increased to 10 g/L, the biocatalyst not only synthesized glycolate, but also converted it into DHBA and 3HBL using the additional available glucose, resulting in a two-fold increase in the titers for DHBA and 3HBL and corresponding

decrease in titers for glycolate. Further increasing the supply glucose concentration to 15 g/L however did not result in higher titers with about 5 g/L of glucose left unconsumed, indicating limitations in terms of conversion to products that remain to be investigated. We discuss some of these limitations in the next chapter.

While the overall titers for 3,4-DHBA and 3HBL obtained by such direct synthesis from glucose are slightly lower (by about 20%) than those obtained with exogenous glycolate feeding (**Section 4.3.1**), they represent about 24.2% of the maximum theoretical pathway yield (**Table 4-3**). If we include the 2,3-DHBA synthesized along the pathway in the yield calculation, the total DHBA + 3HBL yield on glucose amounts to 43.3% of the theoretical maximum, indicating that a little less than half of the carbon processed along the DHBA / 3HBL pathway ends up as the inevitable 2,3-DHBA isomer. Interestingly, direct synthesis from glucose resulted in a slightly higher selectivity ratio of 3,4-DHBA + 3HBL to the 2,3-DHBA isomer as well as a higher total DHBA + 3HBL to 3HB ratio in comparison to exogenous glycolate feeding (**Figure 4-3**), possibly due to a difference in the relative intracellular levels of glycolyl-CoA and acetyl-CoA.

Table 4-3 | Yield and selectivity for direct synthesis of DHBA / 3HBL from glucose

Supplied Glucose	Molar Yield (3,4-DHBA + 3HBL) on Glucose*	% of Theoretical Pathway Yield	$\frac{[DHBA]+[3HBL]}{[3HB]}$	$\frac{[3,4\text{-}DHBA]+[3HBL]}{[2,3\text{-}DHBA]+[3HB]}$	$\frac{[3,4\text{-}DHBA]+[3HBL]}{[2,3\text{-}DHBA]}$
8 g/L	0.112	17.0	4.93 ± 0.32	2.35 ± 0.23	5.41 ± 0.68
10 g/L	0.160	24.2	4.63 ± 0.26	1.07 ± 0.09	1.69 ± 0.18
15 g/L	0.152	23.0	4.26 ± 0.41	0.93 ± 0.07	1.48 ± 0.09

* Molar yield is calculated as ratio of moles of 3,4-DHBA + 3HBL synthesized to moles of glucose consumed and does not include 2,3-DHBA. The total molar pathway yield values including 2,3-DHBA are 0.148, 0.285 and 0.274 respectively for 8, 10 and 15 g/L of supplied glucose and amount to 22.4%, 43.2% and 41.5% of the theoretical maximum yield.

4.3.7. Glycolate, DHBA and 3HBL synthesis in engineered strains

We investigated glycolate, DHBA and 3HBL synthesis in various glycolate producing strains engineered to eliminate different endogenous glycolate and glyoxylate consumption pathways. Of the different strains tested, strains GP3 and GP4 showed improved glycolate synthesis in M9-glucose cultures in comparison to the parent strain GP0 (20-30% higher glycolate titers) at the shake flask scale (**Figure 4-10a**). These strains were then compared with GP0 for DHBA and 3HBL synthesis. Strain GP4-2-DHP showed improved DHBA and 3HBL synthesis as compared to GP0, in particular in M9 cultures supplemented with 15 g/L of glucose, with the average total DHBA + 3HBL titers roughly 20% higher (though the differences may not be statistically significant), possibly due to reduced glycolate consumption along competing pathways and better utilization of supplied glucose (**Figure 4-10b**). These preliminary observations warrant a more detailed study of strain GP4, in particular at the bioreactor scale.

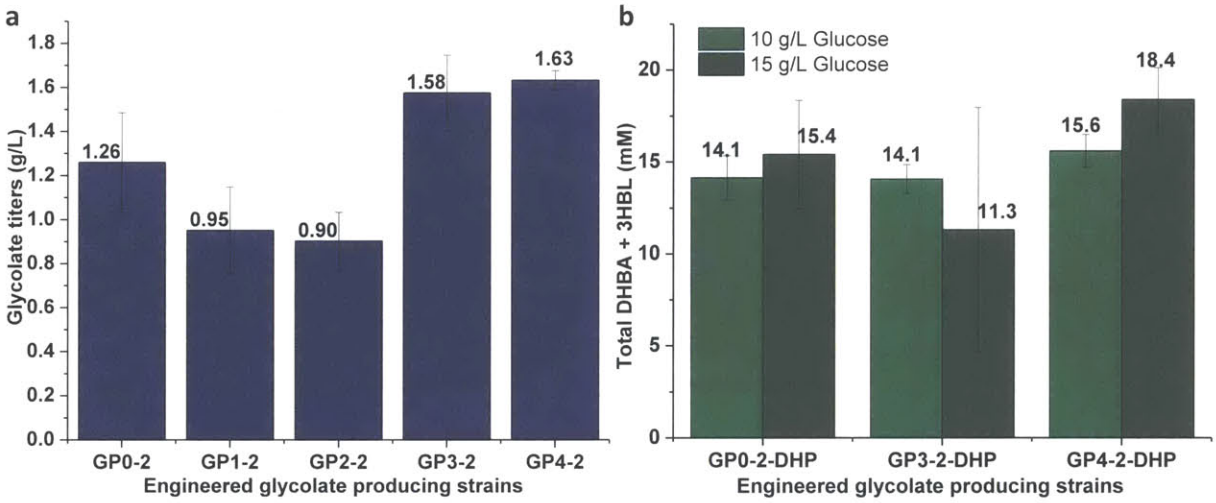

Figure 4-10 | Comparing Glycolate, DHBA and 3HBL synthesis in engineered strains

We also worked in collaboration with the Reed Group at the University of Wisconsin-Madison (personal communication, Prof. Jennifer Reed) to identify additional knockouts expected to boost yield and productivity using metabolic flux balance models and the OptORF algorithm (Kim and Reed, 2010). The various knockouts recommended by the Reed group are listed in **Appendix A4** with the more

promising candidates listed in **Table 4-4**. The maximum theoretical yield for an engineered strain predicted by this algorithm was 33.1% of the theoretical maximum yield of about 1 mole DHBA / mole of glucose (assuming acetate recycling) i.e. 0.33 mole DHBA / mole of glucose. In comparison, as noted in **Table 4-3,** our close to wild type parent strain GP0 affords an almost comparable yield of 0.28 moles of total DHBA + 3HBL / mole glucose, without any specific knockouts or other engineering efforts.

Table 4-4 | Knockouts identified using OptORF

Knockout								Growth (hr^{-1})	Yield (%)
gcl or glxK	*sucAB or sucC*	*nuoN*	*pta and eutD*	*glcC*	*lldP*	*aceB*		0.44	29.9
gcl or glxK	*sucAB or sucC*	*nuoN*	*pta and eutD*	*glcC*	*lldP*	*aceB*	*ptsH*	0.41	32.5
gcl or glxK	*sucAB or sucC*	*nuoN*	*pta and eutD*	*glcC*	*lldP*	*aceB*	*gdhA*	0.30	33.1

*Maximum theoretical yield is 11.8 mol / 10 mol glucose. Glucose uptake rate is 10 mmol/gDW/hr.

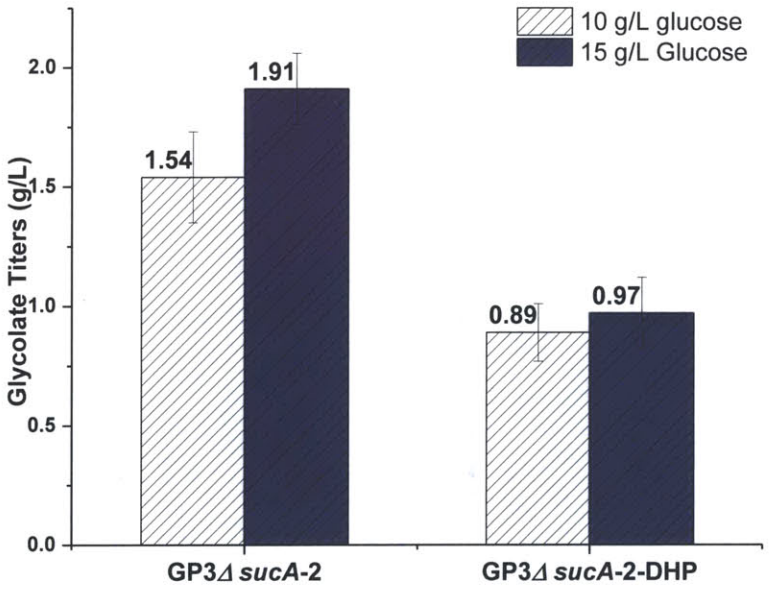

Figure 4-11 | Glycolate synthesis in GP3Δ*sucA*-2 *and* GP3Δ*sucA*-2-DHP

Thus, while we did not expect a drastic improvement in yield with the proposed knockouts, we were very much interested in experimentally testing the suggested knockouts to validate the approach. One of the knockouts that emerged out of this analysis was the *sucA* knockout, expected to interrupt the TCA cycle to re-direct isocitrate flux towards the glyoxylate shunt. *sucA* catalyzes the conversion of α-ketoglutarate to succinyl-CoA and features in the set of recommended knockouts for each of the

engineered strains listed in the **Table 4-4** above in addition to *gcl* and *aceB*. Since *gcl* and *aceB* had already been knocked out in GP3 (in addition to *iclR*), strain GP3 was selected as a host for introducing the *sucA* knockout.

GP3Δ*sucA*-2 cultured in M9-glucose medium showed glycolate synthesis titers up to 2 g/L (higher than GP3-2), however, the strain grew extremely slowly, attaining stationary phase 48+ hours post induction (in comparison to GP3-2 which hit stationary phase about 10-12 hours post induction). The slower growth rate was attributed to the interruption of the TCA cycle. Moreover, GP3Δ*sucA*-2-DHP carrying the DHBA / 3HBL pathway plasmids, showed negligible DHBA / 3HBL or 3HB synthesis, in spite of appreciable glycolate synthesis, suggesting potential protein expression limitations. Since all of the strains listed in **Table 4-4** included the *sucA* mutation, we abandoned further investigation of these.

4.3.8. Chromosomal expression of glycolate pathway enzymes

The maintenance of multiple copies of three different plasmids is expected to impose metabolic stress on the cell and a drain on the supplied carbon. Additionally, from a strain stability perspective, chromosomal expression of all pathway enzymes from chromosomally integrated gene copies is expected to be advantageous. The glycolate pathway enzymes are endogenous to *E. coli* and can be over-expressed directly from the chromosome to eliminate the glycolate pathway plasmid. Both constitutive and inducible promoters were investigated for over-expression of *ycdW*, *aceA* and *aceK* from the chromosome. For constitutive expression, initially, the promoters preceding the *ycdW* gene in strain GP3 were replaced with three different constitutive promoters from the Anderson promoter library (BBa_J23108, BBa_J23100 and BBa_J23119) (parts.igem.org) and the *aceA-aceK* genes were expressed from pCOLA/(aceA-aceK). Bba_B0034 was used a synthetic RBS.

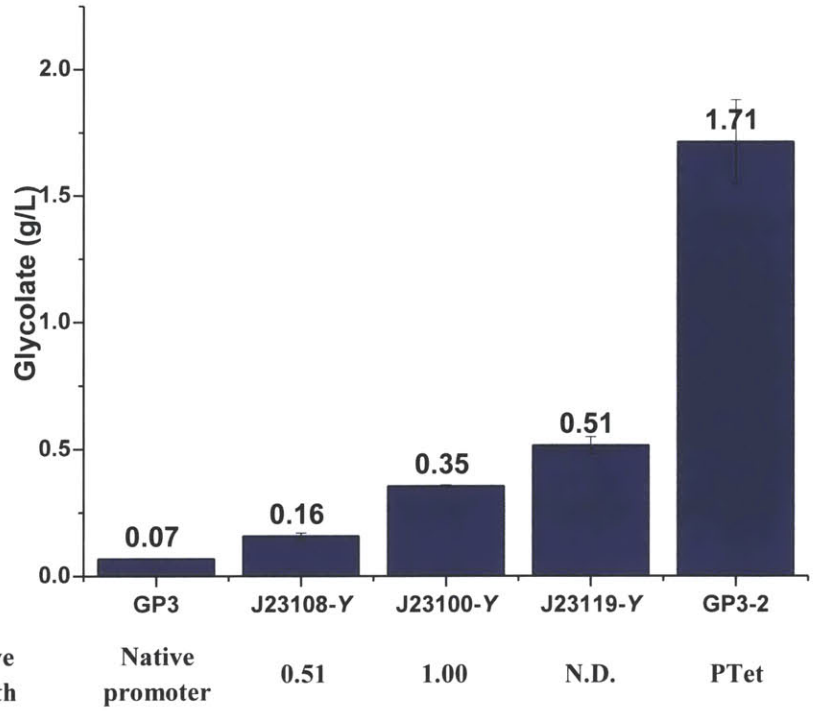

Figure 4-12 | Comparison of glycolate synthesis for *ycdW* promoter replacement strains. The native promoter preceding the *ycdW* gene in GP3 was replaced with promoters from the Anderson promoter library. R.S = relative promoter strength. The R.S. for the consensus sequence promoter J23119 is not defined, however, it is known that J23119 is the sternest in the Anderson library. The various promoter replacement strains carry pCOLADuet-*aceA-aceK* for expression of the AceA and AceK genes.

As observed from **Figure 4-12** the promoter replacement strains for *ycdW* (strains GP3-J23108-*Y*, GP3-J23100-*Y* and GP3-J23119-*Y*) allowed enhanced glycolate synthesis in comparison to the native promoter control (strain GP3), indicating that the promoters used to replace the native promoter allowed enhanced expression of the *ycdW* gene. Strain GP3-J23119-*Y* showed up to 0.5 g/L glycolate synthesis. This was however still 3 times lower than the titer obtained from plasmid based expression of the pathway enzymes (GP3-2), suggesting the need for stronger expression. The strain was nevertheless selected for subsequent promoter replacement studies for the genes *aceA-aceK*.

To allow chromosomal expression of the AceA and AceK enzymes, the native promoter preceding these genes in the natural operon in the above described strain (GP3-J23119-Y) was replaced with the consensus sequence promoter BBa_J23119 (strongest of the three) and the RBS Bba_0034.

Thus, the resulting strain (GP3-J23119-*YAK*) had promoters before both *ycdW* and *aceA-aceK* replaced with the constitutive promoter BBa_J23119 and the RBS Bba_0034 to allow enhanced chromosomal expression of these genes and was expected to synthesize glycolate endogenously. The strain however allowed synthesis of only up to 0.5 g/L of glycolate (three fold lower than those obtained with plasmid based expression) indicating that a promoter stronger than BBa_J23119 or expression from multiple gene copies may be necessary to effect expression comparable to plasmids. Moreover, the same strain carrying the DHBA / 3-HBL pathway plasmids (GP3-J23119-*YAK*-DHP) only showed synthesis of up to 0.5 g/L 3HB and negligible glycolate or DHBA / 3-HBL synthesis.

We also attempted inducible chromosomal expression from a single integrated copy of the *ycdW-aceA-aceK* artificial operon from a PTet promoter in strain GP0-EGP. The strain carrying empty DHBA / 3HBL plasmids (strain GP0-EGP-EC) showed better glycolate synthesis as compared to GP3-J23119-*YAK* (with titers up to 916 ± 196 mg/L), confirming the desired over-expression of the glycolate pathway enzymes. However, similar to GP3-J23119-*YAK*-DHP, the strain carrying the DHBA / 3HBL pathway plasmids (GP0-EGP-DHP) again only showed 3HB synthesis (398 ± 104 mg/L) with negligible glycolate synthesis and no DHBA / 3HBL synthesis. These results might suggest poor expression of the glycolate pathway enzymes due to saturation of the protein synthesis machinery by the over-expressed DHBA / 3-HBL pathway enzymes and a need for better chromosomal expression of the glycolate pathway genes, possibly by integrating multiple gene copies or using a stronger promoter-RBS combination.

4.3.9. Recycling of acetate to improve pathway yield

We attempted the expression of the endogenous acetyl-CoA synthetase gene (*acs*) from *E. coli* in strain DHP0 to recycle the acetate formed as a result of the activation of glycolate by Pct. DHBA and 3HBL synthesis from exogenously fed glycolate in LB was compared with and without Acs expression in strains DHP0+*acs* and DHP0 respectively. While the acetate titers with Acs expression were lower than those without (indicating some degree of acetate recycling), these did not translate to higher 3HB or DHBA / 3HBL titers (**Figure 4-13**). In fact, the expression of Acs seemed to hamper both the total DHBA + 3HBL and 3HB titers at the two induction levels tested, indicating a metabolic burden, either due to its expression or due to the consumption of ATP by Acs in the activation reaction. This suggests that the extent and timing of expression of Acs may need to be fine-tuned to successfully boost yields and titers using this approach.

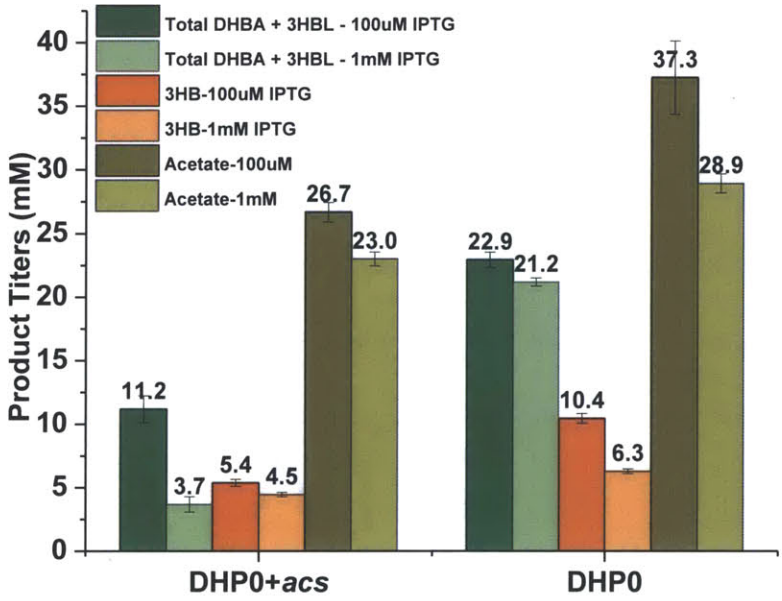

Figure 4-13 | DHBA and 3HBL synthesis with and without Acs expression Product titers, 72 hours post induction are reported for comparison at two different IPTG induction levels (100 μM and 1 mM).

4.4. Discussion

The direct synthesis of 3,4-DHBA and 3HBL from glucose as a sole carbon source via integration of the *de novo* constructed 3HA pathway with the endogenous glyoxylate shunt represents a promising opportunity for the stereospecific biosynthesis of these valuable chemicals from inexpensive simple sugars. This first demonstration of biosynthesis of up to 24.2% of this theoretical pathway maximum with a close to wild type *E. coli* strain at the shake flask scale while promising, warrants further improvement. We foresee enhancing pathway yield using two possible levers: a) improving pathway efficiency through the screening of alternative pathway enzymes that afford higher activity and selectivity and b) reducing loss of carbon towards excess biomass and unwanted products via better host and fermentation engineering.

The condensation reaction between glycolyl-CoA and acetyl-CoA is the first step that commits carbon flux towards 3,4-DHBA and 3HBL. BktB and other natural thiolases exhibit a natural activity towards synthesis of 3HB and 2,3-DHBA as inevitable major side products, with roughly 1 mole of 3HB + 2,3-DHBA synthesized per mole of 3,4-DHBA + 3-HBL (**Table 4-3**). Thus, screening or possibly engineering of a suitable thiolase enzyme with higher activity and selectivity towards the 3,4-DHBA precursor condensation product and reduced formation of 3HB or 2,3-DHBA as discussed in Chapter 3, can help enhance titers and yield by up to two fold. The observation that this selectivity ratio is also observed to improve slightly with endogenous glycolate synthesis in comparison to exogenous glycolate feeding, possibly due to differences in the relative intracellular levels of glycolyl-CoA and acetyl-CoA, indicates the potential to use specific glucose feeding and fermentation strategies to manipulate these pools to improve yield.

Part of the loss in theoretical pathway yield may be attributed to the generation of acetate as a by-product of the activation reaction of glycolate by Pct. Recycling this acetate to acetyl-CoA using Acs may allow us to boost the yield. Indeed, eliminating acetate as a by-product by incorporating this

recycle reaction in the theoretical pathway yield calculation increases Y^P to 1 mole / mole of glucose (**Appendix A3**). While recycling this acetate as acetyl-CoA comes at the expense of consumption of energy (in the form of ATP), the pathway produces an excess of energy rich reducing equivalents and this additional ATP consumption is in theory not expected to impose an unfavorable additional burden. However, our preliminary results suggest that over-expression of acetyl-CoA synthetase does in fact impose a burden, affecting product titers. Moving forward, a finer tuning of this over-expression may be required.

In this study, the use of two orthogonal expression systems to independently express the two sets of pathway enzymes was critical for the successful integration of the two pathways. The problem of hampered expression due to reduced transcript levels from multiple T7 promoters because of distribution of available T7 RNAP uncovered in the present study may similarly impede expression and limit synthesis of products in other pathways. The extent and gravity of this effect is expected to be highly context dependent and influenced by multiple factors including overall metabolic burden, efficiency of translation of generated transcripts, catalytic efficiency (activity) of individual enzymes with respective substrates and the required (optimal) level of over-expression for each enzyme. Indeed, in other pathways in our laboratory, we have effectively achieved simultaneous expression of multiple enzymes from up to four different Duet vectors with eight different T7 promoter sites (Tseng and Prather, 2012). Nevertheless, this highlights the need for well characterized orthogonal parts (such as promoters, RBSs etc.) and expression systems that can allow one to readily vary expression levels of multiple different pathway enzymes in the *de novo* construction of metabolic pathways.

The chromosomal modifications selected for the host engineering of our initial glycolate producing strains were chosen using a rational approach with the objective of eliminating pathways that impose a direct drain on glyoxylate and glycolate pools. While some of these resulted in improved glycolate synthesis, they did not similarly enhance 3,4-DHBA and 3HBL synthesis appreciably, indicating

that glycolate synthesis was no longer the limiting factor and mutations aimed at improving it would not necessarily translate into higher pathway yields. Indeed, such a rational approach cannot take into account effects on the global metabolic networks that influence pathway productivity and carbon distribution as evidenced by hampered glycolate synthesis in some of the knockout strains. Metabolic flux balance modeling algorithms such as MOMA (Segre et al., 2002) and OptORF (Kim and Reed, 2010) attempt to capture such global effects while identifying key pathway fluxes expected to influence pathway productivity and can be used to identify additional chromosomal modifications required to effect such changes. However, these too may not necessarily capture all of the intricate minutiae of metabolism and can lead to unexpected phenotypes as evidenced by an increase in glycolate yield at the cost of a substantially reduced growth rate with GP3*ΔsucA*.

In conclusion, we have been successful in meeting the thesis objective of establishing the first complete biosynthetic pathway for the direct synthesis of 3HBL from glucose as a sole feedstock in a close to wild type MG1655 (DE3) strain of *E. coli*, synthesizing up to 0.70 g/L of the free acid 3,4-DHBA and 0.31 g/L of 3HBL. In the process, we uncovered T7 RNA polymerase as a potential limitation that may impede expression of multiple pathway enzymes using multiple Duet vectors under metabolically stressful conditions. Distribution of pathway enzymes between orthogonal expression systems can serve to effectively alleviate this problem and afford reliable expression of multiple pathway enzymes. While the product titers are lower than those with exogenously fed glycolate, we have been successful in achieving up to 24.2% of the theoretical yield with potential for further enhancing pathway performance through the various approaches discussed here and in the next chapter. Finally, this preliminary demonstration of direct synthesis from glucose now opens avenues towards the synthesis of 3HBL as a value added biomass-derived biochemical from other simple sugars that are products of breakdown of biomass.

Chapter 5 Improving titers, yield and productivity for DHBA & 3HBL synthesis

5.1. Introduction

Having demonstrated direct synthesis of the two DHBA isomers and 3HBL from glucose at the shake flask scale with total yields up to 43% of the theoretical maximum, we were interested in improving the pathway performance metrics, namely, yield, titers and productivity. We foresee three approaches towards meeting this objective:

1) Improving pathway efficiency by screening / engineering enzymes that reduce by-product formation

2) Improving the characteristics of the biocatalyst through host engineering

3) Reducing by-product formation and loss of carbon by improving the fermentation process

The first two of these approaches and ongoing work with respect to them have already been discussed in previous chapters. The key to improving performance metrics by improving the fermentation process for microbial synthesis lies in understanding the fermentation and limiting factors or parameters that influence these metrics. We thus sought to study this fermentation at the bench-top bioreactor scale where various parameters may be controlled and studied in a systematic manner, with the objectives of 1) developing a bench-top fermentation process that would allow a meaningful evaluation of these key performance metrics and 2) understanding the influence of various parameters such as pH, aeration, glucose feeding strategy etc. on these metrics to develop strategies to improve their values. Such a fermentation process can then be used to evaluate the performance of various engineered strains.

5.2. Materials and Methods

5.2.1. Microbial strains and plasmids

The various glycolate, DHBA and 3HBL producing strains used in this study have been described in previous chapters and are listed again in **(Table 5-1).** *E. coli* DH10B (Invitrogen, Carlsbad, CA) and ElectroTen-Blue (Stratagene, La Jolla, CA) electrocompetent cells were again used for cloning and constructing various plasmids. For the construction of the plasmid pGlcA (plasmid pHHD01K/glcA), the glycolate symporter gene *glcA* was PCR amplified with flanking EcoRI and BamHI sites from MG1655 (DE3) gDNA template (using primers listed in **Table 5-2)** and cloned into the MCS of pHHD01K.

Table 5-1 | *E. coli* strains and plasmids

Name	Relevant Genotype	Reference
Strains		
DH10B	F⁻ *mcr*A Δ(*mrr-hsd*RMS-*mcr*BC) ϕ80*lacZ*ΔM15 Δ*lacX74 recA1 endA1 araD139*Δ(*ara, leu*)7697 *galU galK* λ⁻ *rpsL nupG*	Invitrogen
ElectroTen-Blue	Δ(*mcrA*)*183* Δ*(mcrCB-hsdSMR-mrr)173 endA1 supE44 thi-1 recA1 gyrA96 relA1 lac* Kan^r [F′ *proAB lacI*^{q}ZΔM15 Tn*10* (Tet^r)]	Stratagene
MG1655 (DE3)	F⁻ λ⁻ *ilvG- rfb-50 rph-1 with the DE3 prophage integrated*	Tseng 2010
GP0-2-DHP	MG1655 (DE3) transformed with pDHP-1, pDHP-2 and pGLY-2	
MG0	MG1655 (DE3 Δ*endA* Δ*recA*)	This study
MG4	MG0 transformed with pDHP-1 and pDHP-2	This study
MG4 + *glcA*	MG4 transformed with pGlcA	
Plasmids		
pETDuet-1	ColE1 (pBR322) *ori*, *lacI*, T7*lac*, Amp^R	Novagen
pCDFDuet-1	CloDF13 *ori*, *lacI*, T7*lac*, Strep^R	Novagen
pCOLADuet-1	ColA *ori*, *lacI*, T7*lac*, Kan^R	Novagen
pHHD01K	p15 *ori*, *tetR*, Ptet, Kan^R	Chapter 3
pGLY-2	pHHD01K harboring the genes *ycdW, aceA and aceK* from *E. coli* MG1655 in an artificial operon similar in structure to the *aceBAK* operon	Chapter 3
pGlcA	pHHD01K harboring the glycolate transporter genes *glcA*	This study
pDHP-1	pETDuet-1 harboring *bktB* and *phaB* from *C.necator* named pET/bktB/phaB in Chapter 2	Chapter 3
pDHP-2	pCDFDuet-1 harboring *pct* from *M. elsdenii*, and *tes*B from *E. coli* MG1655 named pCDF/pct/tesB in Chapter 2	Chapter 3

Table 5-2 | List of DNA oligonucleotide primers used in the cloning of genes

Primer names correspond to the name of the gene or vector backbone that the primer amplifies, whether the primer is the forward primer (FP) or reverse primer (RP) of that gene or vector, and the restriction site incorporated into the primer sequence (in case of a primer used to generate a fragment for cloning).

Primer	Sequence 5'→3'	Source
glcA-FP-EcoRI	TAAAAAGAATTCGCCTATATTTTACAGTTCAGTCCTCTTTTG	Sigma-Genosys
glcA-RP-BamHI	TAAAAAGGATCC TTACGAGACTAACATCCCGGTAAAC	Sigma-Genosys

5.2.2. Culture medium

In most of the experiments described in this chapter a 1X M9 salt medium (Sigma, Aldrich) containing 6.78 g/L $Na_2HPO_4 \cdot 7H_2O$, 3 g/L KH_2PO_4, 1 g/L NH_4Cl and 0.5 g/L NaCl, supplemented with 2 mM $MgSO_4$, 0.1 mM $CaCl_2$, glucose, trace elements and antibiotics was used as the culture medium. The trace element solution (100X) used contained 5 g/L EDTA, 0.83 g/L $FeCl_3 \cdot 6H_2O$, 84 mg/L $ZnCl_2$, 10 mg/L $CoCl_2 \cdot 6H_2O$, 13 mg/L $CuCl_2 \cdot 2H_2O$, 1.6 mg/L $MnCl_2 \cdot 2H_2O$ and 10 mg/L H_3BO_3 dissolved in water. This was added to a concentration of 1X to supplement the M9-glucose medium. Additionally, as described in section 5.3.1, a commercially available 100X trace mineral supplement from ATCC (MD-TMS, ATCC, Masnassas, VA) was also tested in addition to 0.2% casamino acids and 1 mg/L thiamine hydrochloride supplementation.

5.2.3. Bioreactor cultures

Fermentations at the bench-top bioreactor scale were performed using a Labfors 3 bioreactor (Infors; Bottmingen, Switzerland) with a maximum working volume of 2.3 L. A D140 OxyProbe dissolved oxygen sensor (Broadley-James; Irvine, CA) and an F-695 FermProbe pH electrode (Broadley-James) were used to monitor the dissolved oxygen and pH respectively. M9-glucose medium supplemented with trace elements or LB-glucose medium were used to grow the bioreactor cultures. M9-glucose cultures in the bioreactor were inoculated to an initial OD_{600} of 0.1 from cells obtained from a 50 mL

overnight LB seed culture. Initially a 5 mL LB seed culture was grown overnight from a colony picked from a LB agar plate and was used to inoculate a 50 mL LB culture in a 250 mL baffled flask (1% vol./vol. inoculum). The following day, this overnight culture was centrifuged to separate the cells from the spent LB broth and the cells were resuspended in M9 medium to serve as the inoculum for the reactor.

To set up the bioreactor, 1.5 L of M9 salt medium was autoclaved in the reactor. On the day of inoculation, the medium was supplemented with glucose, $CaCl_2$, $MgSO_4$, appropriate antibiotics (50 mg/L ampicillin sulfate, 50 mg/L streptomycin sulfate and 30 mg/L kanamycin sulfate) and trace elements. The reactor was inoculated to an initial OD_{600} of 0.1 using the previously described overnight seed culture. The dissolved oxygen setpoint was controlled at 35% of the saturation value using a cascade to agitation (250 rpm to 850 rpm), and air was provided at a constant flow rate of 1 vvm. pH was controlled at the desired setpoint using 4 M NaOH and 2 M H_3PO_4. Online data was logged using IRIS fermenter log and control software (Infors). Antifoam was manually added in 0.1 mL increments as needed. Samples were taken periodically to measure OD_{600} offline using a DU800 Spectrophotometer (Beckman Coulter, Brea, CA) and to collect culture supernatants for metabolite analysis.

5.2.4. Metabolite analysis using HPLC

Various fermentation products and metabolites were analyzed using HPLC analysis (see corresponding section in Chapter 2).

5.3. Results

5.3.1. Exploring the effect of media supplements on DHBA / 3HBL synthesis

As described in the previous chapter, M9 – glucose medium allows effective glycolate synthesis via the de-repression of the glyoxylate shunt and was selected as the medium of choice for the direct synthesis of DHBA and 3HBL from glucose at the shake flask scale. While M9 satisfies the nitrogen requirement and provides the cells with essential elements such as phosphorous, sulfur, magnesium and calcium, it does not explicitly provide trace elements essential for *E. coli* growth. While this trace element requirement at the shake flask scale is often satisfied by impurities present in water, flasks as well as M9 itself, it may become limiting for larger scale fermentation. We were thus interested in studying the effect of supplementing the M9 medium with trace element solutions. Two different trace mineral supplements (a commercially available ATCC supplement and a homemade supplement as described in the **Section 5.2.2.**) were tested in Medium 2 and Medium 3 respectively. Similarly, we also investigated the effect of supplementing the medium with casamino acids to create a semi-defined rich medium (Medium 4).

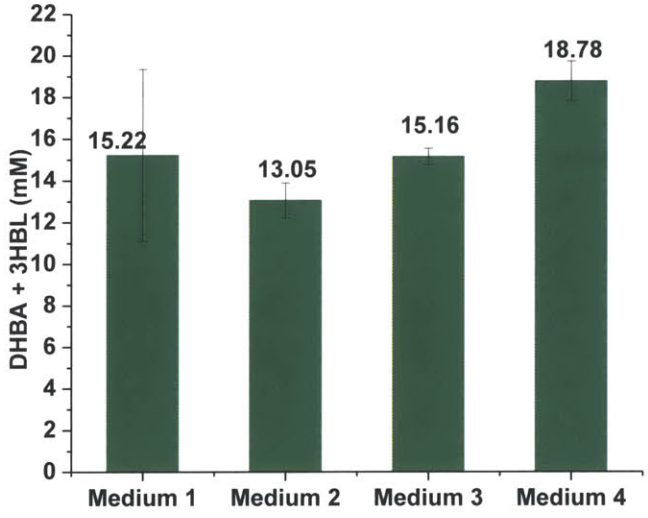

Figure 5-1 | Total DHBA + 3HBL titers in mM Medium 1 = 1X M9 + 1% glucose, Medium 2 = 1X M9 + 1% glucose + 1X ATCC trace mineral supplement, Medium 3 = 1X M9 + 1% glucose + 1X home-made trace mineral supplement and Medium 4 = 1X M9 + 1% glucose + 1X ATCC trace mineral suppl. + 0.2% casamino acids + 1mg/L thiamine hydrochloride.

As observed from **Figure 5-1**, the addition of trace elements to the medium reduced the variability in the product titers for DHBA + 3HBL synthesized by GP0-2-DHP. Addition of trace elements also promotes growth with Medium 2 and Medium 3 cultures growing to an average final OD_{600} of about 4.5, in comparison to a final OD_{600} of 3.5 obtained without trace element supplementation. Thus M9-glucose medium was supplemented with trace elements in subsequent experiments and in particular in experiments at the bioreactor scale. Interestingly, while GP0-2-DHP had showed negligible DHBA, 3HBL and glycolate synthesis in the rich LB medium, the same strain showed improved DHBA and 3HBL synthesis in the semi defined casamino acids supplemented M9-glucose medium (Medium 4) with 25% higher total DHBA + 3HBL titers (in comparison to Medium 3). This suggests that the addition of casamino acids helps relieve some of the metabolic stress associated with growth in M9 without causing the repression of the glyoxylate shunt observed in LB.

5.3.2. Studying the DHBA / 3HBL fermentation at the shake flask scale

We initially sought information about the DHBA / 3HBL fermentation from experiments at the shake flask scale. As observed from **Figure 5-2**, the DHBA / 3HBL fermentation from glucose at the shake flask scale is characterized by three distinct phases: 1) growth Phase, 2) product synthesis phase and 3) end phase.

1) Growth Phase: During the growth phase, the cells utilize glucose and nitrogen for growth. Growth is accompanied by the synthesis of 3HB and glycolate. The end of the growth phase (around 24 hours post inoculation) is marked by the first shift in metabolism. The cells have reached their final OD_{600} of 3.5 to 4 at this point, presumably due to the complete consumption of all the available nitrogen. 3HB synthesis is also observed to proceed during this phase. However, no DHBA synthesis is observed during the growth phase, in spite of the presence of glycolate.

2) Product synthesis phase: A few hours past the end of the growth phase and onset of stationary phase, DHBA synthesis begins. Glycolate synthesis continues during this phase until a second shift in metabolism around 36 hours, marking the end of the product synthesis phase. The exact reason for this second shift in metabolism is not immediately apparent, though it may be tied to the pH of the cultures as described later. 3HB synthesis may plateau or continue during this phase depending on the residual glucose concentration in the medium.

3) End Phase: The second shift in metabolism is marked by cessation of glycolate synthesis. Beyond this point, glycolate is essentially only consumed to support DHBA synthesis. DHBA synthesis continues until about 72 hours and is observed to plateau thereafter. The exact reason for the plateauing of DHBA synthesis beyond 72 hours is also not known. While in the case of 10 g/L of starting glucose concentration this cessation of DHBA synthesis coincides with the complete consumption of glucose, as described in the previous chapter, for 15 g/L of supplied glucose, up to 5 g/L of glucose remains unconsumed. Various reasons may be hypothesized for the cessation of product synthesis: 1) unfavorable pH or aeration conditions, 2) product inhibition and 3) biocatalyst death or degradation of enzymatic activity.

Additionally, these observations raise several interesting questions. What causes the initial lag in DHBA synthesis, in spite of the presence of glycolate, acetyl-CoA and pathway enzymes? Why aren't DHBA and 3HB synthesized concomitantly in the growth phase? Is 3HB synthesis favored over DHBA as a result of higher acetyl-CoA levels during the growth phase or is this because glycolate needs to build to a certain threshold before DHBA synthesis can commence? Is 3HB strictly a growth associated product? What causes the 2^{nd} shift in metabolism and cessation of glycolate synthesis? Is this simply a result of reduced fluxes through the TCA and glyoxylate shunt as a result of the onset of stationary phase or is it a

result of a metabolic change effected by some other factor? In the subsequent sections, we try to address these and other questions through various systematic experiments.

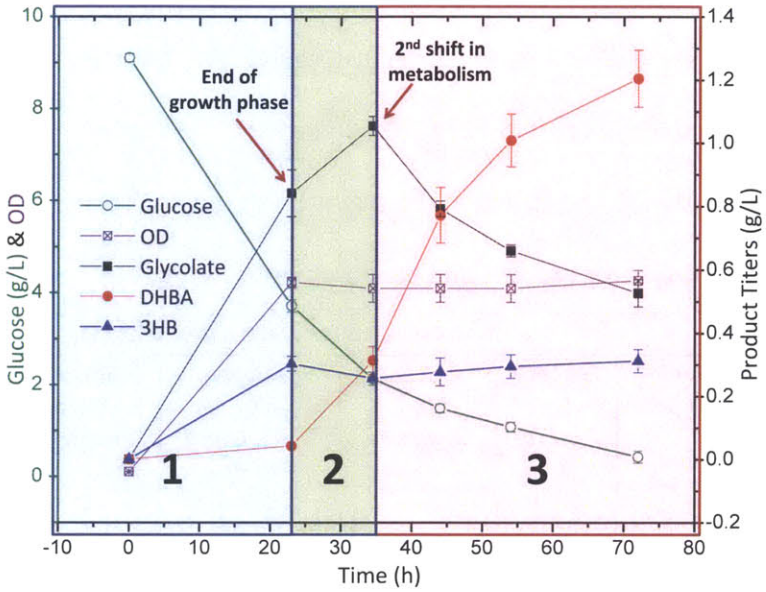

Figure 5-2 | DHBA / 3HBL synthesis time course data for substrate consumption and product formation GP0-2-DHP was cultured in 1X M9 minimal medium supplemented with 10 g/L glucose, induced with aTc (250 ng/ml) and IPTG (100 μM). All flask cultures were run in triplicate with product titers reported as mean ± s.d. (n=3)

5.3.3. Effect of varying the C/N ratio on DHBA / 3HBL synthesis

Given that DHBA and 3HBL are synthesized as non-growth associated products, while glycolate and 3HB synthesis seems to be largely tied to growth, we investigated the effect of varying the amount of biomass on product synthesis, titers and selectivity by varying the supplied C/N ratio using three different M9 salt medium concentrations (0.75 X, 1X and 1.5X M9 salt medium) and glucose supplementations (8 g/L, 10 g/L and 15 g/L) at the shake flask scale.

Table 5-3 | Glucose utilization for product and biomass synthesis

	Glucose used for various products in (g/L)*					
C/N	**Glucose for 3HB**	**Glucose for Acetate**	**Glucose for Glycolate**	**Glucose for (Total DHBA + 3-HBL)**	**Glucose for (Biomass + maintenance)**	**Unconsumed glucose**
0.75X M9 + 8 g/L Glucose	0.22	0.89	0.63	2.14	3.93	0.14
0.75X M9 + 10 g/L Glucose	0.52	1.22	0.45	2.42	3.92	1.42
0.75X M9 + 15 g/L Glucose	0.50	1.28	0.39	2.51	3.95	6.24
1X M9 + 8 g/L Glucose	0.22	0.47	1.52	1.07	4.73	0.00
1X M9 + 10 g/L Glucose	0.55	0.99	0.83	2.55	5.08	0.00
1X M9 + 15 g/L Glucose	0.61	1.20	0.78	2.55	4.87	4.88
1.5X M9 + 8 g/L Glucose	0.00	0.10	1.00	0.25	6.46	0.15
1.5X M9 + 10 g/L Glucose	0.08	0.54	1.43	0.37	7.30	0.16
1.5X M9 + 15 g/L Glucose	0.51	3.13	0.93	2.38	7.72	0.19

* The amount of glucose consumed for the synthesis of each of the products is estimated based on the corresponding final product titer, using the theoretical reaction for synthesis of each product as listed in the Appendix A3.

Table 5-4 | Yield and selectivity for direct synthesis of DHBA / 3HBL from glucose

C/N	Average OD_{600}	Total Molar Yield on Glucose ($Y_{P/S}$) **	% of Theoretical Maximum Pathway Yield	([DHBA]+[3HBL]) / [3HB]	([3,4-DHBA]+[3HBL]) / ([2,3-DHBA]+[3HB])	([3,4-DHBA]+[3HBL]) / ([2,3-DHBA])
0.75X M9 + 8 g/L Glucose	3.40 ± 0.06	0.274	41.5	9.75 ± 0.06	1.02 ± 0.02	1.25 ± 0.03
0.75X M9 + 10 g/L Glucose	3.20 ± 0.18	0.284	43.0	4.68 ± 0.34	0.89 ± 0.04	1.33 ± 0.06
0.75X M9 + 15 g/L Glucose	3.28 ± 0.09	0.294	44.5	5.10 ± 0.25	0.95 ± 0.03	1.40 ± 0.04
1X M9 + 8 g/L Glucose	4.71 ± 0.22	0.148	22.4	4.93 ± 0.32	2.35 ± 0.23	5.41 ± 0.68
1X M9 + 10 g/L Glucose	5.11 ± 0.27	0.286	43.3	4.63 ± 0.26	1.07 ± 0.09	1.69 ± 0.18
1X M9 + 15 g/L Glucose	4.50 ± 0.17	0.274	41.5	4.26 ± 0.41	0.93 ± 0.07	1.48 ± 0.09
1.5X M9 + 8 g/L Glucose	6.76 ± 0.08	0.032	4.8	-	-	-
1.5X M9 + 10 g/L Glucose	7.26 ± 0.42	0.038	5.8	-	-	-
1.5X M9 + 15 g/L Glucose	7.41 ± 0.22	0.162	24.6	4.26 ± 0.15	0.71 ± 0.02	0.71 ± 0.02

** Total Molar Yield, $Y_{P/S}$ is calculated as the ratio of moles of (2,3-DHBA + 3,4-DHBA + 3HBL) synthesized to moles of glucose consumed. % of Theoretical Maximum Pathway Yield is the ratio of $Y_{P/S}$ to the theoretical maximum pathway yield $(Y_{P/S})_{max}$ = 0.66 moles / mole of glucose, expressed as a percentage.

In each of the cases explored in this study, the supplied carbon was in an excess and growth was nitrogen limited as evidenced by the correlation between the final biomass density (measured as the corresponding OD_{600}) and concentration of M9 (nitrogen) used (**Table 5-4**). Depending on the amount of nitrogen supplied, a fixed amount of carbon was consumed to support biomass and maintenance with the balance excess utilized in part or full for product synthesis (**Table 5-3**). The peak glycolate titers observed during the course of the 100 hour fermentation increased with the amount of biomass, confirming that glycolate synthesis is largely growth associated (see **Appendix A5**). Interestingly, however, the overall DHBA + 3HBL titers as well as rate of product synthesis were more or less independent of the amount of biomass synthesized, but depended on the amount of excess glucose available in the medium. Thus, for 1.5X M9 cultures that required about 7 to 7.5 g/L glucose to support growth, negligible DHBA synthesis was observed in cultures supplemented with 8 and 10 g/L of glucose

(where this excess was less than 3 g/L), with the cells running out of glucose before the synthesized glycolate could be converted to DHBA / 3HBL. In each of the cultures where DHBA and 3HBL were synthesized, as observed previously, synthesis only commenced a few hours past the onset of the stationary phase, confirming these as non-growth associated products. In all cases, the biocatalyst showed a limited capacity to convert the excess supplied glucose into DHBA and 3HBL, with maximum total DHBA + 3HBL titers plateauing at about 13 mM – 15 mM and cessation of product synthesis after 72 hours, with the balance glucose remaining unconsumed. These results again corroborated our earlier observations and suggested that DHBA / 3HBL synthesis at the shake flask scale is not limited by the amount of biocatalyst present, but by other factors that need to be further investigated.

5.3.4. Investigating the effect of supplied glycolate concentration on DHBA / 3HBL synthesis

To investigate if the observed lag in DHBA synthesis was a consequence of a need to build glycolate titers to a certain minimum level in the culture medium, we investigated DHBA / 3HBL synthesis in strain MG4 cultured in LB and fed exogenously with different amounts of glycolate (between 5 mM and 40 mM). In GP0-2-DHP cultures, DHBA synthesis was observed to begin after the glycolate titers had built to a level of 0.9 g/L (about 12 mM) in the culture medium **Figure 5-2**. If this was indeed the minimum amount of glycolate essential for DHBA / 3HBL synthesis, we would expect negligible DHBA synthesis in MG4 cultures supplemented with 5 mM or 10 mM glycolate. However, cultures supplemented with both 5 and 10 mM glycolate were observed to readily synthesize DHBA within the first 24 hours (**Figure 5-3a**), indicating that the observed lag with GP0-2-DHP cultures was not correlated with the glycolate titers. The total DHBA + 3HBL titers at 24 hours (representative of the initial synthesis rate) and selectivity with respect to 3HB were both observed to increase almost linearly with an increase in the concentration of glycolate supplied, approaching saturation at higher glycolate concentrations (> 30 mM) (**Figure 5-3b**), presumably due to resulting higher intracellular glycolate and

glycolyl-CoA concentrations driving the reaction. This suggests that while there may not be a minimum glycolate concentration required for DHBA synthesis, higher glycolate titers in the medium are expected to drive up selectivity and productivity. Thus allowing glycolate to build to levels above 30 or 40 mM to achieve synthesis at close to saturation rates during direct synthesis from glucose may be an effective strategy to help boost productivity and selectivity.

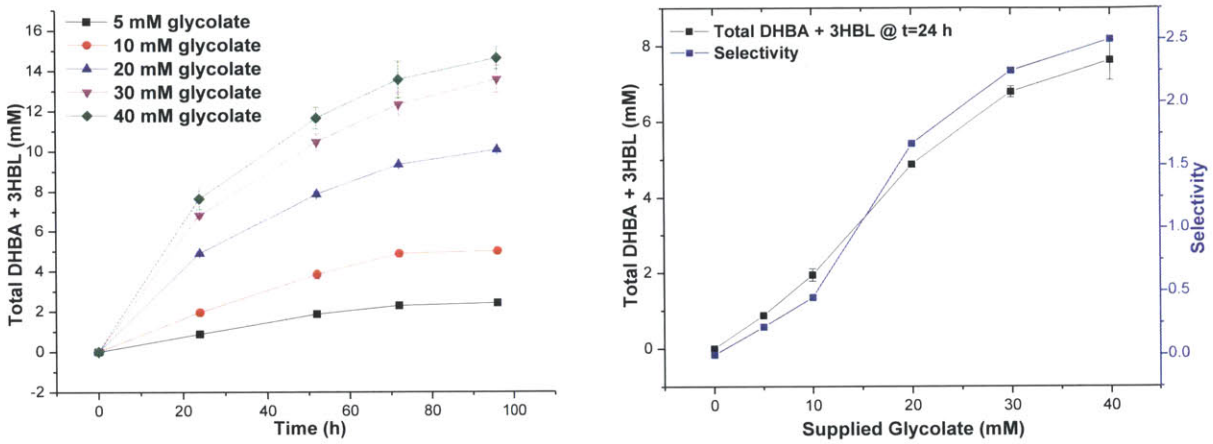

Figure 5-3 | DHBA / 3HBL synthesis at different glycolate feed concentrations Strain MG4 was cultured in LB medium supplemented with 10 g/L glucose and different amounts of glycolate, induced with IPTG (100 µM). (a) Time course data for Total DHBA + 3HBL titers for different amounts of supplied glycolate (b) Total DHBA + 3HBL titers at t=24 h and selectivity, calculated as the ratio of (Total DHBA + 3HBL) to 3HB, using final t=72 h titers for different amounts of supplied glycolate.

5.3.5. Effect of pH on the DHBA / 3HBL fermentation

To determine the effect of pH and pH control, the DHBA / 3HBL fermentation from glucose was studied at the bench-top bioreactor scale with strain GP0-2-DHP. At the shake flask scale, the pH of the culture medium is observed to progressively drop from about 7 to 5 over the course of a 72 hour fermentation (with a majority of the drop occurring within the first 35 hours). We hypothesized, that the progressive acidification of the medium may be detrimental to cellular health and may be the cause of biocatalyst death and cessation of product synthesis beyond 72 hours. Thus, DHBA / 3HBL synthesis was investigated at the bench-top bioreactor scale, maintaining the pH constant at 7 throughout the run. However, pH control severely hampered DHBA synthesis with final titers less than 0.15 g/L. Instead, during the growth phase, the cells actively synthesized 3HB and glycolate (**Figure 5-4**). At the

end of the growth phase the synthesis of 3HB slowed down and eventually plateaued, while glycolate synthesis continued until all the glucose in the medium was completely consumed. While the cells readily synthesized glycolate, with final titers around 2 g/L, this was however not converted to DHBA, indicating limitations in the processing of the synthesized glycolate along the downstream DHBA / 3HBL synthesis pathways. A control experiment designed to sample different aeration conditions at the shake flask scale allowed us to rule out the differences in aeration (between the bioreactor and shake flasks) as a potential cause of the hampered DHBA synthesis. Further, feeding the culture with glucose beyond the point of glucose exhaustion allowed its continued conversion to glycolate in the stationary phase, indicating that the cessation of glycolate synthesis previously observed at the shake flask scale was not a result of the onset of stationary phase, but rather that of a metabolic shift brought about by the progressive drop in pH. In other words, glycolate is not a growth associated product and its synthesis can proceed in both the growth and stationary phases.

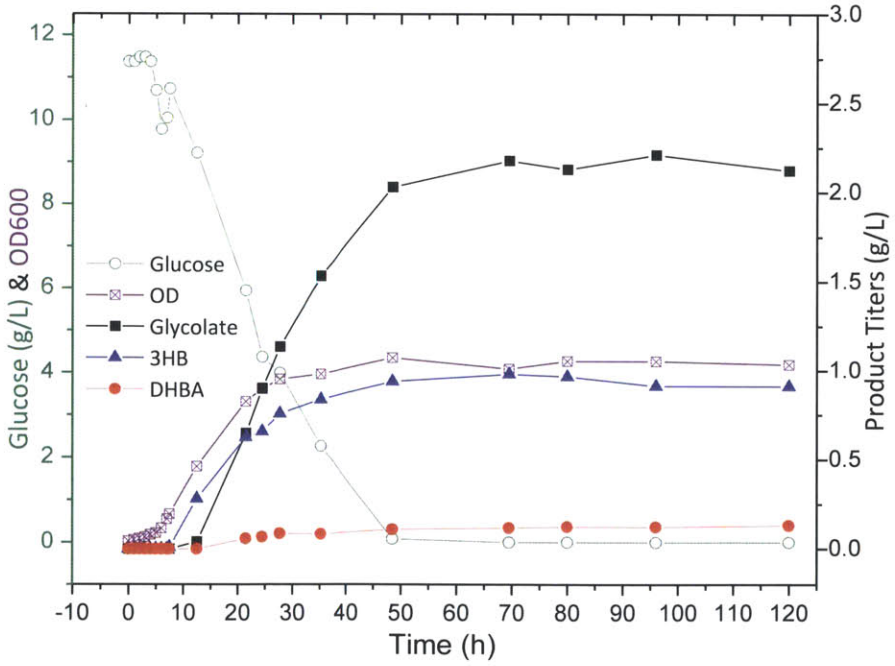

Figure 5-4 | DHBA / 3HBL synthesis at the bioreactor scale with pH control. DHBA / 3HBL synthesis was attempted in GP0-2-DHP at the bioreactor scale in M9 + 1% glucose, maintaining the pH constant at 7.

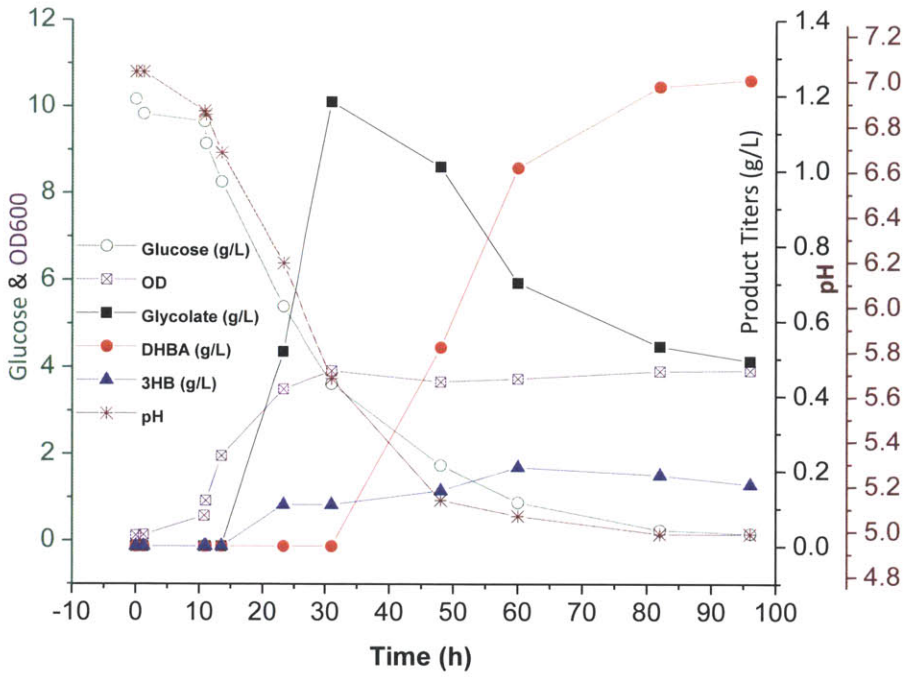

Figure 5-5 | DHBA/3HBL synthesis by in a bioreactor without pH controlled at 5.5 GP0-2-DHP cells were cultured in 1X M9 supplemented with 1% glucose. The pH of the culture was initially allowed to drop to 5.5 and thereafter held constant throughout the fermentation. DHBA synthesis (red curve) was observed to begin about 35 hours post inoculation.

On the other hand, if the pH of the culture medium in the bioreactor was allowed to progressively drop to 5 due to the accumulation of acids (similar to shake flasks), DHBA synthesis by GP0-2-DHP was restored with final titers comparable to those obtained at the shake flask scale (**Figure 5-5**). Additionally, just as at the shake flask scale, DHBA synthesis only commenced about 24 hours post inoculation. The lag in DHBA synthesis observed at both the shake flask and bioreactor scales, in addition to being correlated with the onset of stationary phase also seemed to be tied to the drop in the pH of the medium to about 5.5 and was in fact also observed in the case of DHBA / 3HBL synthesis from exogenously supplied glycolate (**Figure 5-6a** and **b**) in strain MG4.

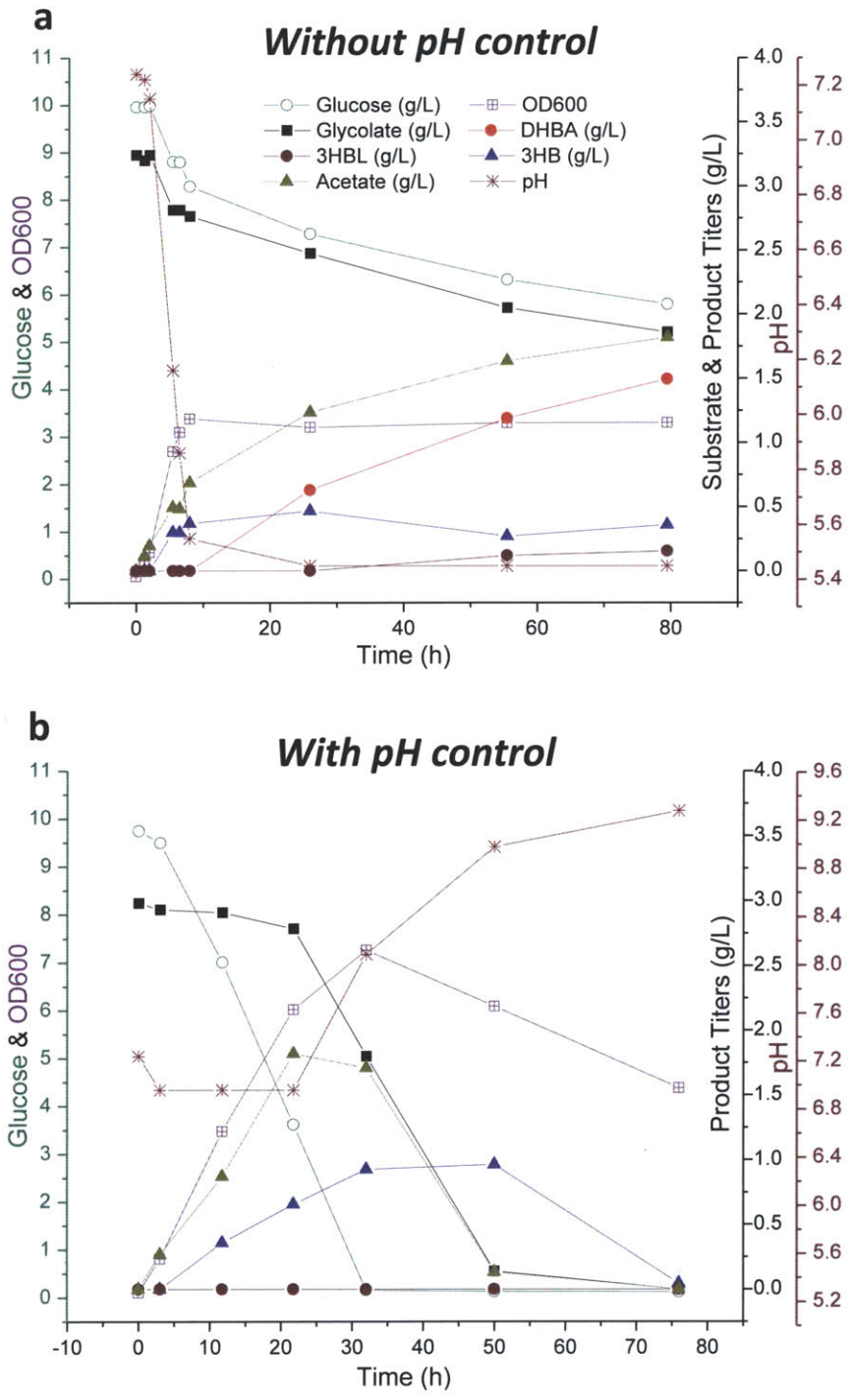

Figure 5-6 | DHBA/3HBL synthesis from exogenously supplied glycolate in LB in a bioreactor (a) without and (b) with pH control. MG4 cells carrying the DHBA / 3HBL pathway plasmids were grown in LB supplemented with 1% glucose and 40 mM glycolate. **Legend:** Total DHBA (closed red circles), 3HBL (closed brown circles), 3HB (closed blue triangles), glycolate (closed black squares), acetate (closed olive triangles), pH (brown asterisks) and glucose (green open squares).

As observed from **Figure 5-6b**, negligible DHBA synthesis was observed with strain MG4 cultured in LB supplemented with 40 mM glycolate, when the pH was maintained constant at 7. Interestingly, under constant pH conditions, glycolate uptake or consumption did not take place until glucose was completely consumed in the system, indicating the possibility of glycolate uptake limitations at pH=7 and the expression of glycolate transporters only in response to a need to utilize glycolate as a carbon source (under neutral pH conditions). On the other hand, without pH control, the pH of the culture medium rapidly dropped to 5 in about 8 hours. During this initial growth phase, cell growth was accompanied by 3HB synthesis. Once cell growth and 3HB synthesis had plateaued (around 8 hours) and the pH had fallen to around 5.5, DHBA synthesis began at the expense of glycolate uptake and consumption (**Figure 5-6a)**.

To determine if the magnitude of drop in pH influenced DHBA synthesis and product titers, we ran fermentations with GP0-2-DHP cultured in 1X M9 supplemented with glucose, initially allowing the pH to drop to a value of either 5.8 or 5.4, thereafter maintaining it constant. As observed from **Figure 5-7** , at the higher pH of 5.8, final DHBA titers as well as the initial rate of synthesis were roughly half of those observed at pH 5.4, indicating that a drop in pH to a value of 5.4 or lower favored DHBA and 3HBL synthesis. The pH 5.8 cultures continued to accumulate glycolate in the culture medium because of lesser consumption for DHBA synthesis. Interestingly, 3HB synthesis in these cultures also showed peculiarities. As observed from **Figure 5-7**, 3HB synthesis in these cultures continued beyond the growth phase and seemed to be correlated with the glucose titers as opposed to the growth itself. 3HB synthesis was observed to plateau when glucose levels fell to about 3 g/L.

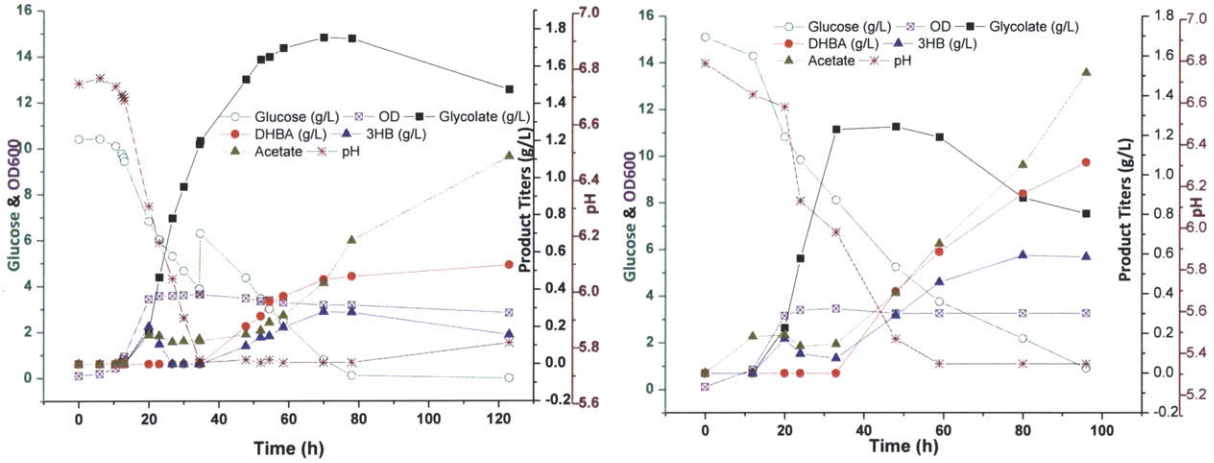

Figure 5-7 | DHBA/3HBL synthesis in GP0-2-DHP with pH controlled at 5.8 GP0-2-DHP cells were cultured in 1X M9 supplemented with 1% glucose. The pH of the culture was initially allowed to drop to 5.8 and thereafter held constant throughout the fermentation. DHBA synthesis (red curve) was observed to begin about 35 hours post inoculation.

In summary, these results suggest that, DHBA and 3HBL synthesis as non-growth associated products in the stationary phase either from endogenously synthesized or exogenously supplied glycolate requires a drop in the pH of the medium to a value of 5.5 or lower. Several mechanistic and metabolic phenomena may be hypothesized to explain the observed pH effect.

1. pH influences glycolate transport: Analogous to lactate transport, glycolate transport by symporters like *glcA* and *lldP* is known to be influenced by the extracellular pH and the pH gradient across the cell membrane with higher intracellular glycolate concentrations favored by lower extracellular pH and a larger pH gradient and proton motive force (PMF) across the cell membrane (Geros et al., 1996; Núñez et al., 2002). Such a boost in intracellular glycolate concentration may in turn favor its activation to glycolyl-CoA by Pct and the subsequent condensation reaction with acetyl-CoA catalyzed by BktB. This would be consistent with the observation of higher rate of product synthesis and lower glycolate titers in the external medium at lower pH of 5.4 in comparison to 5.8. The cessation of glycolate synthesis around 36 hours may also be correlated to product inhibition due to increased

intracellular glycolate levels with a drop in pH. Alternatively, it could also be hypothesized that pH influences transport by affecting the expression of specific glycolate symporters or transporters.

2. **pH influences a change in metabolism:** The drop in pH may also have a more complex influence on changing the metabolism and metabolite levels (such as acetyl-CoA) to allow DHBA synthesis. Indeed, in many of the bioreactor runs conducted, a drop in pH to 5.5 or lower was followed by a reduction in the oxygen utilization rate (OUR) and a corresponding increase in the pO_2, indicating a change in the metabolism of available glucose by the cells. It remains to be determined if this change in OUR is simply a consequence of the metabolic shift (and potential cell death) accompanying the pH drop or is in fact essential for DHBA synthesis. Indeed, in cultures where the pH is maintained constant, such a decrease in OUR is not observed.

3. **pH influences the activity of pathway enzymes**: While cells are capable of maintaining their intracellular pH via homeostasis, the capacity for this is limited and changes in the extracellular pH can influence variations in the intracellular pH that may affect the activity of the enzymes.

A detailed *in vitro* investigation of each of the pathway enzymes and the influence of pH and acetyl-CoA and glycolyl-CoA levels on their respective kinetics accompanied by a measurement of the changing intracellular levels of these metabolites *in vivo* through the course of a fermentation may help distinguish between these proposed hypotheses and develop an understanding of the observed pH effect.

In the meantime, in the absence of a clear mechanistic understanding, we can attempt to replicate the observed shifts in metabolism required for product synthesis while simultaneously overcoming any limitations imposed by the existing fermentation conditions. We discuss some of these approaches below. While none of them have resulted in spectacular successes in improving the product

titers and yields so far, the lessons learned are informative in guiding future approaches towards this objective.

5.3.6. Investigating a two-stage fermentation with pH shift

Given that a drop in pH to a value of 5.5 or lower was important to initiate DHBA synthesis, while neutral pH conditions were conducive for glycolate synthesis and cellular health, we were interested in exploring the possibility of a two stage fermentation process where glycolate is initially synthesized under neutral pH conditions to titers above 3 g/L (> 40 mM), followed by a drop in pH to 5.5 to initiate DHBA synthesis at close to maximum possible rates as described in section 5.3.4.

As a first pass at investigating the possibility of such a process, strain GP0-2-DHP was cultured in 1X M9 supplemented with 15 g/L of glucose and the pH was maintained constant at 7 for the first 30 hours to allow glycolate synthesis (**Figure 5-8**). During this period, glycolate was observed to accumulate to a concentration of about 0.7 g/L (about 9.2 mM). Following this, the pH was dropped to 5.5 by addition of 2 M phosphoric acid to initiate DHBA synthesis. The medium was also supplemented with 2.5 g/L glucose to replenish the consumed glucose. DHBA synthesis was observed to commence almost immediately after the pH shift. While the final DHBA titers obtained were roughly half of those observed in the case of DHBA / 3HBL synthesis without pH control (**Figure 5-5**), this may be a result of a premature shift in pH, resulting in insufficient glycolate synthesis before the initiation of DHBA synthesis (only about 9.2 mM in comparison to about 17 mM in the case of synthesis without pH control (**Figure 5-5**)). Indeed, these titers are comparable to those obtained with 10 mM of exogenously supplied glycolate with strain MG4. Similarly, the selectivity with respect to 3HB while much lower than that observed in GP0-2-DHP cultures without pH control, was comparable to that for 10 mM glycolate fed strain MG4 cultures. These preliminary findings are promising and portend well towards the success of the envisaged two stage fermentation.

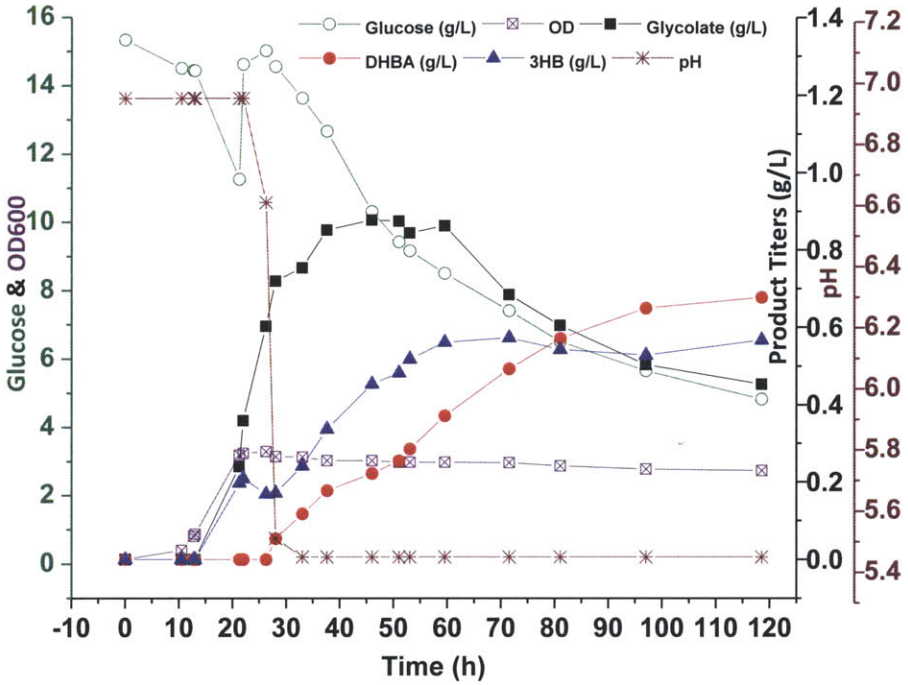

Figure 5-8 | Two stage fermentation with pH shift GP0-2-DHP cells were cultured in 1X M9 supplemented with 1% glucose. The pH of the culture was initially maintained at 7 for the first 30 hours to allow glycolate synthesis, followed by a drop in pH to 5.5 to initiate DHBA synthesis. DHBA synthesis (red curve) was observed to begin almost immediately after the pH shift.

5.3.7. Expressing the glycolate transporter GlcA to improve glycolate uptake

If the pH influenced the expression of glycolate transporters, the over-expression of glycolate transporters may help allow DHBA / 3HBL synthesis under neutral pH conditions and may boost productivity and product titers. We thus investigated over-expression of the glycolate symporter GlcA in strain MG4 + *glcA* at both the shake flask and bioreactor scales, to determine if this improved glycolate uptake and utilization. The total DHBA + 3HBL titers obtained with and without *glcA* expression (at three different expression levels) at various time points in the fermentation were observed to be comparable at the shake flask scale (final titers reported in **Table 5-5**), indicating that the over-expression of this symporter did not improve product synthesis.

Table 5-5 | Total DHBA + 3HBL titers with and without over-expression of *glcA*

Strain	aTc Inducer concentration	IPTG (μM)	Total DHBA + 3HBL Titers (mM)
MG4 + *glcA*	**50 ng/mL**	100	18.8 ± 0.5
MG4 + *glcA*	**100 ng/mL**	100	19.1 ± 0.5
MG4 + *glcA*	**250 ng/mL**	100	19.0 ± 0.3
MG4	**-**	100	19.4 ± 0.5

* MG4 + *glcA* and MG4 cells were cultured in LB supplemented with 1% glucose (wt./vol.) and 40 mM glycolate. Titers reported in the table above are for samples collected 72 hours post induction. *glcA* is expressed from an aTc inducible pTet promoter from the plasmid pGlcA in the strain MG4 + *glcA*.

Moreover, MG4 + *glcA* cultures at the bioreactor scale with pH controlled at 7 showed substrate and metabolite profiles similar to strain MG4 (**Figure 5-6b**) with negligible DHBA synthesis, indicating that simply over-expressing *glcA* was not enough to initiate DHBA synthesis under neutral pH conditions.

5.3.8. Investigating product inhibition by DHBA

To investigate product inhibition as a potential cause of cessation of product synthesis around 72 hours, DHBA/3HBL synthesis was investigated in strain MG4 cultured in media supplemented with DHBA.

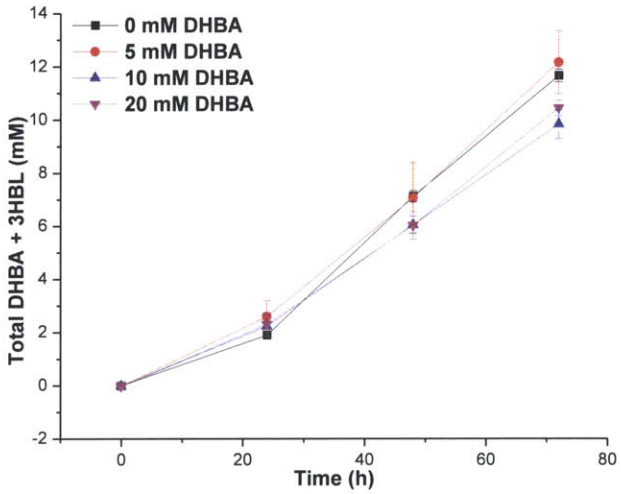

Figure 5-9 | Investigation product inhibition by DHBA MG4 cells were cultured in LB supplemented with 1% glucose, 40 mM glycolate and different amounts of neutralized DHBA.

As observed from **Figure 5-9**, negligible product inhibition by DHBA was observed, even with 20 mM DHBA (1.5 times the total DHBA + 3HBL titers typically observed at the end of a fermentation with

MG4). The inhibitory effect (if any) of other major products (such as acetate or 3HB) remains to be investigated.

5.4. Discussion

At the outset of this investigation, we were interested in understanding the DHBA / 3HBL fermentation to improve its performance beyond the value of 43% of the theoretical maximum achieved at the shake flask scale. While this study did not meet this goal, it helped answer several interesting questions about the synthesis of these products, while raising newer ones. The effect of various parameters, including pH, glycolate concentration, biomass concentration, expression of specific transporters and potential inhibitors was investigated in this study.

pH of the culture medium was identified as an important parameter influencing the synthesis of various products. While on the one hand, a drop in pH to 5.5 or lower is detrimental to glycolate synthesis and results in its cessation, on the other it is essential to initiate DHBA synthesis. The results thus far strongly suggest that a drop in pH may be influencing the transport of glycolate through symporters and the intracellular glycolate levels. This and the other proposed hypotheses now need to be investigated systematically with the experiments described in the earlier section. Additionally, in relation to this pH effect, it is important to note that the observation that DHBA and 3HBL are synthesized as non-growth associated products is somewhat confounded by the concomitant drop in pH. Indeed, it is difficult to say if cessation of growth is actually essential to initiate DHBA / 3HBL synthesis in addition to the pH drop or if a drop in pH by itself would suffice to initiate DHBA synthesis. While, one may propose addressing this question by studying DHBA synthesis in cells grown at pH 5.5, growth at this lower pH itself may confound these results. The proposed measurement of acetyl-CoA and glycolyl-CoA levels may help shed light on the changes in metabolism necessary to initiate DHBA synthesis.

It is particularly important to investigate the cause of cessation of DHBA and 3HBL synthesis that limits the overall product titers and yield. We have so far ruled out direct product inhibition by 3,4-

DHBA as a potential cause. Various other inhibitors present in the culture medium need to be investigated. If this is merely the result of biocatalyst death or protein degradation, regeneration of the catalyst by supplying small amounts of nitrogen to the culture may be a potential solution. However, in the absence of an understanding of the exact limiting factors, it seems like we would be limited to a fixed product synthesis phase following the pH drop. The proposed two stage process may allow one to make the most of this product synthesis phase by initially building biomass and glycolate to sufficiently high levels under neutral pH conditions, to allow DHBA synthesis at the maximum possible rate after the pH drop.

3HB is a major competing pathway side-product. The synthesis of 3HB in this study was observed to depend on the available glucose in the medium and was seen to plateau when the glucose levels fell to 3 g/L or lower. Additionally, as observed in Chapter 4, endogenous glycolate synthesis was observed to result in more selective synthesis of 3,4-DHBA and 3HBL in comparison to the 2,3-DHBA and 3HB isomers. The glyoxylate shunt itself is expected to be more active at lower levels of glucose. Thus investigating an optimal glucose feeding strategy to control the relative acetyl-CoA and glycolyl-CoA levels may be valuable in the light of these observations. Similarly, the level of aeration of the cultures is yet another parameter that warrants further investigation. Finally, as a better fermentation process evolves out of this understanding of the influence of various parameters, we envisage using it for an objective evaluation of various engineered host strains.

Chapter 6 Conclusions and Future Directions

6.1. Summary

Building new pathways for the microbial conversion of biomass into target value-added products is essential for transitioning from a petroleum and fossil reserves dependent chemical industry to a sustainable biobased one. In this thesis, we set out to explore one such versatile novel route towards the synthesis of 3-hydroxyalkanoic acids as target biomass derived chemicals, with a particular interest in the synthesis of 3,4-dihydroxybutyric acid (3,4-DHBA) and its lactone, 3-hydroxybutyrolactone (3HBL). Summarized below are the key findings from this investigation.

In Chapter 2, my collaborators and I demonstrated as a proof of concept, the synthesis of 5 new products (3,4-DHBA, 2,3-DHBA, 3HBL, 3H4MV and 3HH) using the 3-hydroxyalkanoic acid pathway. In particular, the pathway for the first time allowed the biosynthesis of up to 0.55 g/L of 3,4-DHBA, 0.22 g/L of 3HBL and 0.86 g/L 2,3-DHBA. While the product titers and yields for the novel products on respective substrates in this initial investigation were low (less than 50%), this demonstration validated our hypothesis about the biosynthetic capability and versatility of the enzymatic Claisen condensation and other pathway reactions and enzymes. The discovery of synthesis of 2,3-DHBA alongside 3,4-DHBA in particular highlighted the versatility of the carbon-carbon bond forming potential of the Claisen condensation, expanding the repertoire of product 3HAs accessible using the platform. Simultaneously, the need for screening alternative enzymes exhibiting better activity towards the synthesis of novel products was recognized, in particular to improve C6 as well as 3,4-DHBA and 3HBL synthesis.

In Chapter 3, I explored some alternative pathway enzymes, to improve the synthesis of 3HAs, and in particular C6 3HAs such as 3-hydroxyhexanoic acid. This led to characterization of the *R. rubrum* thiolase Rru_A0274 which was observed to exhibit activity and specificity similar to the *C. necator*

thiolase BktB. Similarly, FadAB, a thiolase I enzyme was also observed to allow synthesis of hydroxyacids such as 3HV (C5) and 3HH (C6), confirming that thiolase I enzymes are also capable of catalyzing the Claisen condensation reaction in the biosynthetic direction. While a number of other pathway enzymes were restrictive in their substrate range and observed to be inactive with the tested substrates, the activity (or inactivity) information garnered was valuable and is currently being used in conjunction with network maps for bioprospecting to guide future enzyme selection.

In Chapter 4, I addressed one of the main objectives of this thesis and established the first biosynthetic pathway for the synthesis of 3,4-DHBA and 3HBL from glucose as a sole carbon source by integrating the 3HA platform with the endogenous glyoxylate shunt in the close to wild type *E. coli* K-12 strain MG1655 (DE3). This integration posed a number of metabolic, regulatory and expression challenges and required overcoming the repression of the glyoxylate shunt using specific media and expression of pathway enzymes from two different orthogonal expression systems. T7 RNAP availability was identified as a potential limiting factor affecting expression from multiple Duet vectors in this study. Using this pathway, we demonstrated the synthesis of up to 0.7 g/L of 3,4-DHBA and 0.3 g/L of 3HBL. Simultaneously, synthesis of up to 0.7 g/L of the 2,3-DHBA isomer that can serve as a monomer for hyperbranched polymers was also observed. These titers collectively amounted to upto 43% of the maximum theoretical pathway yield for the two DHBA isomers and 3HBL and 24.2% of the theoretical maximum for 3,4-DHBA and 3HBL.

In Chapter 5, I studied the DHBA / 3HBL fermentation at the shake flask and bioreactor scales to identify limiting factors and improve product titers and yield. While glycolate and 3HB were observed to be synthesized both in the growth and stationary phases, DHBA and 3HBL synthesis was observed to occur in the stationary phase as non-growth associated products. While this initially suggested that the onset of stationary phase was essential for DHBA and 3HBL synthesis, further studies showed that their

synthesis was governed by pH. A drop in pH to a value of 5.5 or lower was essential for DHBA and 3HBL synthesis, however, this proved detrimental to endogenous glycolate synthesis. We believe that the pH influences the transport and / or partitioning of glycolate between the intracellular matrix and the external culture medium with higher intracellular glycolate levels at lower external pH. The opposing effect of pH on glycolate versus DHBA / 3HBL synthesis suggests the need for a two stage fermentation process where glycolate is initially synthesized under neutral pH conditions, followed by DHBA / 3HBL synthesis at pH of 5.5 (or lower). The possibility of synthesis of glycolate, DHBA and 3HBL as non-growth associated products is promising and helps us envisage a close to theoretical yield continuous conversion of supplied glucose to products, once a given amount of biomass (biocatalyst) is synthesized. So far however, even at the bioreactor scale, we have only been successful in achieving product titers and yields comparable to those obtained at the shake flask scale. Indeed, our results suggest the need to continue investigating limitations that prevent such high yield conversion of supplied carbon to products.

6.2. Recommendations and concluding remarks

Development of novel pathways is critical for biomass to biobased chemicals conversion technologies. The 3HA platform is one such novel route toward 3-hydroxyalkanoic acids as biomass derived value-added products. Our demonstration of the synthesis of 5 novel products using this platform highlights its versatility. However, the yields of novel products synthesized are low (1-50%) on the supplied substrates and require improvement before a realistic evaluation of this platform for commercial applications can be made. As described in Chapters 2 and 3, exploration of alternative pathway enzymes with better activity / selectivity is critical to overcome conversion limitations and improve yields. These yield considerations are particularly important for applications of this route for the synthesis of 3HAs as commodity chemicals (for example, monomers for commodity polymers).

We largely adopted a rational approach for enzyme selection and evaluated the activities of the enzymes on the supplied substrates using our 4 step combined *in vivo* assay. While this allowed us to gather valuable information about the activity / specificity of some enzymes, this approach suffers from the limitation that key limiting pathway enzymes cannot be identified. Moving forward, *in vitro* analysis of each of the enzymes with the different substrates of interest is essential to determine the limiting enzymes. The identification of such limiting enzymes can then allow us to systematically search for or engineer specific alternatives.

The thiolase enzyme catalyzes the key carbon-carbon bond forming reaction in the pathway. We hypothesize this to be one of the limiting pathway enzymes and identifying alternative thiolases or engineering desired activities would be of particular value. The collected activity / specificity information is currently being mapped onto thiolase network maps to identify thiolase clusters expected to exhibit desired activities (**Figure 6-1**). Thus, the clusters containing the *Z. ramigera* thiolase or Rru_1469 would be expected to contain thiolases that are specific to C4 3HA synthesis. On the other hand, we would expect the cluster containing Rru_A0274 to contain other thiolases capable of C5 and C6 synthesis. This approach towards classifying and identifying new enzymes has been previously used (Atkinson et al., 2009) and is being validated for selecting thiolases in the Prather Lab by experimentally characterizing thiolases from these clusters.

In addition to screening for naturally evolved thiolases, pursuing rational site-directed mutagenesis for protein engineering of thiolases to improve C6 synthesis as well as altering the specificity towards 3,4-DHBA vs. 2,3-DHBA synthesis also needs to be investigated. In particular, with respect to 3,4-DHBA and 2,3-DHBA synthesis, the thiolase BktB shows a roughly equal activity towards both isomers. Thus even in the best case scenario, if all of the exogenously supplied glycolate substrate or glucose supplied for endogenous glycolate synthesis were to be converted to product, half of the

supplied substrate would be converted into an undesired product. Similarly, all thiolases naturally synthesize 3HB as a competing side product. This selectivity ratio may be somewhat improved in favour of 3,4-DHBA and 3HBL through endogenous glycolate synthesis or in favour of 2,3-DHBA by employing PhaA as a thiolase. However, specific protein engineering efforts are essential to substantially reduce this side-product formation.

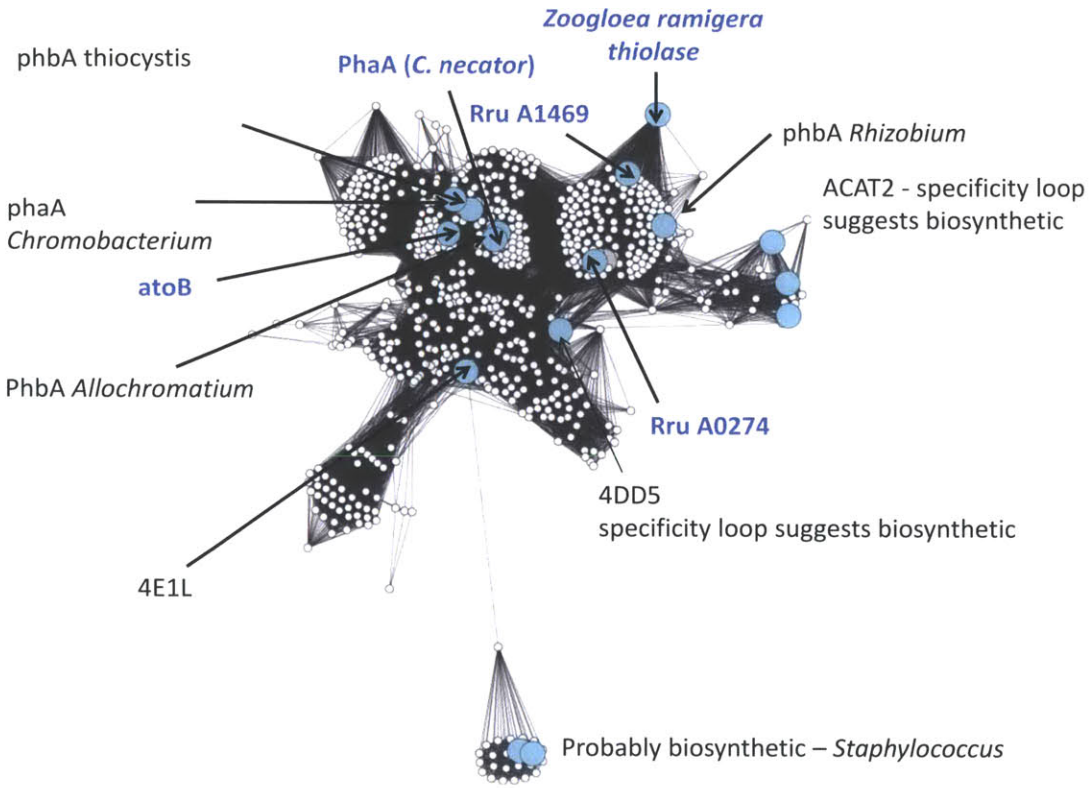

Figure 6-1 | Thiolase network map. Figure courtesy Dr. Michael Hicks, Prather Lab. Different thiolases were clustered together based on the degree of sequence similarity. The circles represent individual nodes composed of multiple proteins sharing a high degree of similarity with respect to each other. Shown in blue are thiolase clusters whose one or more members have been characterized as biosynthetic. Network map created using Pythoscape (Barber and Babbitt, 2012) and visualized using Cytoscape (Saito et al., 2012).

With respect to the synthesis of 3,4-DHBA and 3HBL from either exogenously supplied glycolate or from glucose as a sole carbon source, a major limitation is the incomplete conversion of the supplied substrate to products, limiting the total molar yields of the two DHBA isomers and 3HBL on glycolate or

glucose to 50% or less and total DHBA titers to less than 1.5 g/L. It is critical to investigate the causes of cessation of product synthesis beyond 72 hours of fermentation. While a pH of 5.5 or lower is essential to initiate DHBA synthesis, this may also be responsible for biocatalyst death and loss of activity. Different fermentation process strategies such as cycling the pH between neutral and 5.5 for short durations or a two-stage fermentation as proposed in Chapter 5 need to be further investigated. Moreover, pH may not be the only important factor affecting the titers and yield. A detailed design of experiments to determine the effect of other parameters such as aeration and glucose feeding strategy would be of value for the development of an optimal fermentation process. Similarly, while the various engineered host strains developed for DHBA/3HBL synthesis in our study showed negligible improvements in titers and yield at the shake flask scale, they may behave very differently in an optimized fermentation process and it would be of interest to evaluate these at the bench-top bioreactor scale.

Indeed, depending on the specific end application, improving the pathway performance and achieving product yields close to the theoretical maximum may be critical for the economic viability of the constructed pathway. For example, for DHBA/3HBL synthesis from glucose, the theoretical maximum pathway yield is 1 mole/mole of glucose (with acetate recycling), while the yield obtained currently at the shake flask or bioreactor scales is limited to about 0.3 mole/mole of glucose. Thus, depending on the yield, the expected glucose cost per kg of DHBA or 3HBL product ranges between $1 to 3 (assuming a wholesale cost of $0.5/kg for commercially available fermentation grade glucose). While this raw material cost may be tolerable for pharmaceutical or speciality polymer applications where the DHBA or 3HBL chiral building blocks may command prices as high as $450/kg, it is apparent that this will not be acceptable for bulk polymer applications, where the desired price of the DHBA monomer itself is of the order of a few dollars per kg. Additionally, downstream processing to separate the synthesized DHBA and 3HBL from the culture broth or to resolve the two DHBA isomers is expected

to add to the production cost, with costs ranging between 10-50% of total production cost for bulk fermentation products like lactic or malic acid to as high as 80-90% for PHAs (Hoek et al., 2003), depending upon the concentration in the culture broth. Thus increasing product titers significantly to the order of tens or hundreds of g/L may be essential to limit such separation costs. Further, the lack of redox neutrality of our engineered pathway limits the maximum pathway yield and when combined with high downstream processing costs, may preclude the use of this route for the synthesis of DHBA as a bulk or commodity chemical from glucose as a carbon source, motivating the use of cheaper carbon sources such as glycerol or lignocellulosic biomass.

Appendices

Appendix A1 | NMR analysis confirming 2,3-DHBA and 3,4-DHBA isomers

Appendix A2 | Computational Enzyme Design Scheme (courtesy Brian Bonk, Tidor Group, MIT)

Appendix A3 | DHBA / 3HBL synthesis from glucose –Reactions & Theoretical yield calculations

Appendix A4 | *E. coli* strain designs using Flux Balance Models for DHBA production in glucose under aerobic condition

Appendix A5 | Effect of varying the C / N ratio on DHBA / 3HBL synthesis

Appendix A1 | NMR analysis confirming 2,3-DHBA and 3,4-DHBA isomers

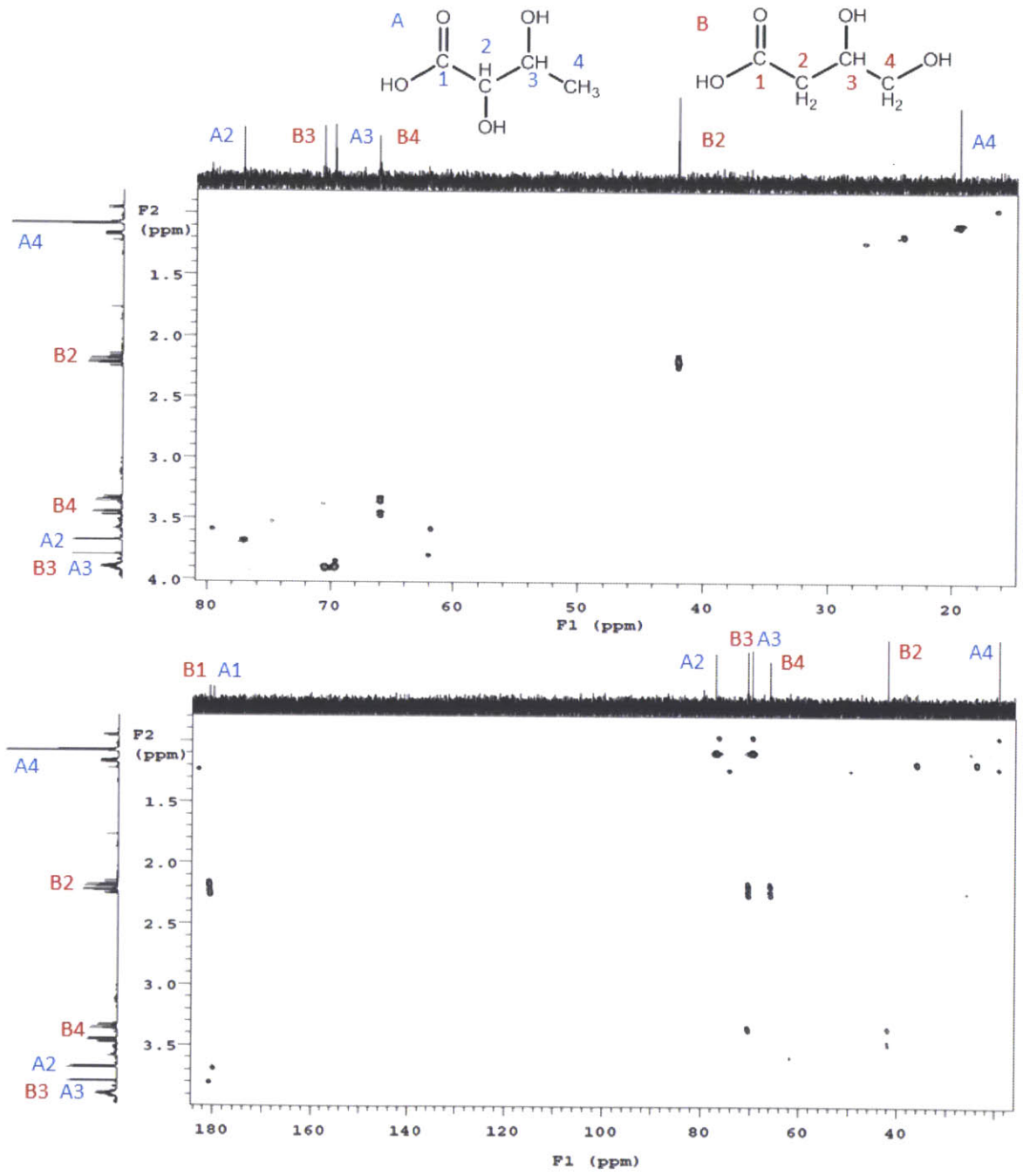

Identification of 2,3-DHBA and 3,4-DHBA via NMR. HSQC (top) and HMBC (bottom) NMR spectra of purified 2,3-DHBA and 3,4-DHBA. The ^{1}H and ^{13}C projections are from independent experiments with direct observation of ^{1}H and ^{13}C. ^{1}H and ^{13}C chemical shifts from either 2,3-DHBA (A-blue) or 3,4-DHBA (B-red) are labelled. NMR analysis and spectra, courtesy Dr. Christopher R. Reisch.

Appendix A2 | Computational Enzyme Design Scheme (courtesy Brian Bonk, Tidor Group, MIT)

The following is an excerpt of a personal communication from Brian Bonk describing the methodology used to identify thiolase mutations to preference formation of specific products.

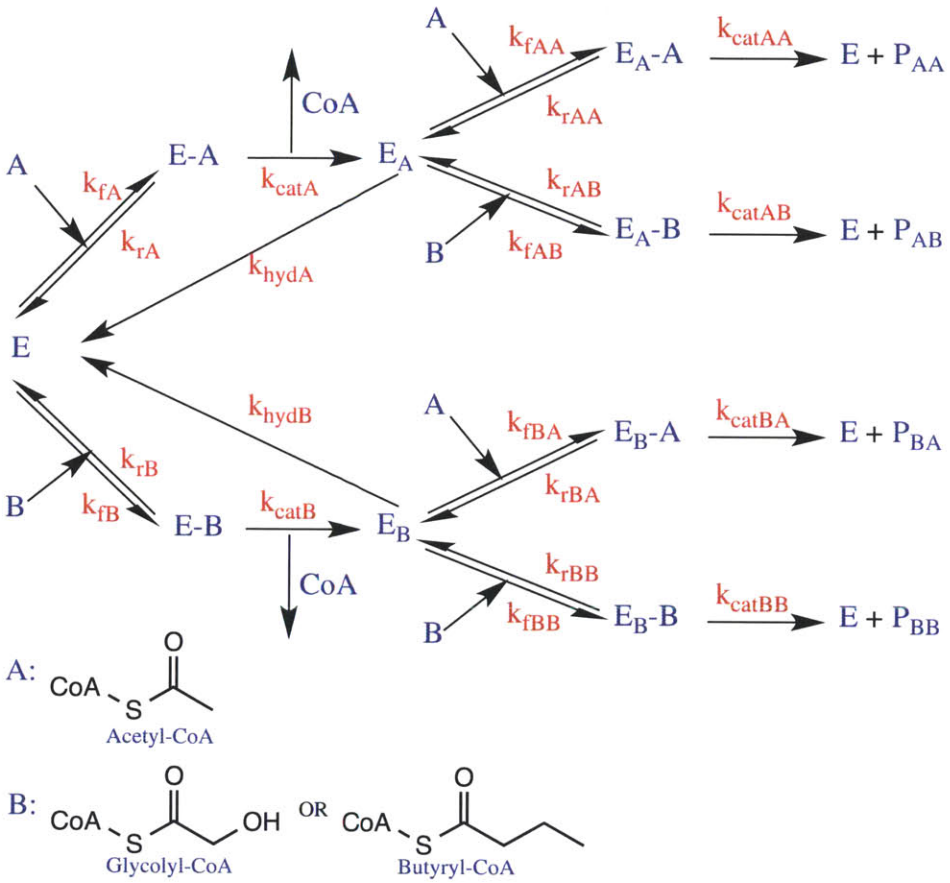

Using the nomenclature of the kinetic model pictured above, a computational design scheme was employed in order to identify thiolase mutations predicted to favor the formation of the P_{BA} product (resulting from the Type I Condensation) relative to the native P_{AA} product formed from the condensation of two acetyl-CoA molecules. To achieve this end, it was desired to identify mutants which minimized the quantity $\Delta\Delta G^{Mut\text{-}WT}{}_{B\text{-}A}$ (described below) at each of the two binding stages. Note that in the design scheme discussed below, B refers exclusively to butyryl-CoA.

An induced fit, rather than rigid binding model was used and thus the binding energy was be decomposed into two terms: a rigid docking energy of bringing the preformed receptor and ligand together, as well an induced fit term of bringing the receptor and ligand from their unbound forms in solution to their preformed docking structures. Thus the binding energies can be written as:

$$\Delta G^{Mut}_{Bind\ A} = \Delta G^{Mut}_{Dock\ A} + \Delta G^{Mut}_{Induced\ A}$$
$$\Delta G^{WT}_{Bind\ A} = \Delta G^{WT}_{Dock\ A} + \Delta G^{WT}_{Induced\ A}$$
$$\Delta G^{Mut}_{Bind\ B} = \Delta G^{Mut}_{Dock\ B} + \Delta G^{Mut}_{Induced\ B}$$
$$\Delta G^{WT}_{Bind\ B} = \Delta G^{WT}_{Dock\ B} + \Delta G^{WT}_{Induced\ B}$$

The rigid docking term can be represented as the difference between the bound complex energy, the preformed receptor and the preformed ligand:

$$\Delta G^{Mut}_{Dock\ A} = G^{Mut}_{Complex\ A} - G^{Mut}_{Receptor\ A,\ Pre} - G^{Mut}_{Ligand\ A,\ Pre}$$
$$\Delta G^{WT}_{Dock\ A} = G^{WT}_{Complex\ A} - G^{WT}_{Receptor\ A,\ Pre} - G^{WT}_{Ligand\ A,\ Pre}$$
$$\Delta G^{Mut}_{Dock\ B} = G^{Mut}_{Complex\ B} - G^{Mut}_{Receptor\ B.\ Pre} - G^{Mut}_{Ligand\ B,\ Pre}$$
$$\Delta G^{WT}_{Dock\ B} = G^{WT}_{Complex\ B} - G^{WT}_{Receptor\ B,\ Pre} - G^{WT}_{Ligand\ B,\ Pre}$$

The induced fit term consists of the sum of the energies of the receptor going from its unbound conformation in solution to its preformed conformation and the ligand going from its unbound conformation in solution to its preformed conformation:

$$\Delta G^{Mut}_{Induced\ A} = (G^{Mut}_{Receptor\ A,\ Pre} - G^{Mut}_{Receptor,\ Unbound}) + (G^{Mut}_{Ligand\ A,\ Pre} - G_{Ligand\ A,\ Unbound})$$
$$\Delta G^{WT}_{Induced\ A} = (G^{WT}_{Receptor\ A,\ Pre} - G^{WT}_{Receptor,\ Unbound}) + (G^{WT}_{Ligand\ A,\ Pre} - G_{Ligand\ A,\ Unbound})$$
$$\Delta G^{Mut}_{Induced\ B} = (G^{Mut}_{Receptor\ B,\ Pre} - G^{Mut}_{Receptor,\ Unbound}) + (G^{Mut}_{Ligand\ B,\ Pre} - G_{Ligand\ B,\ Unbound})$$
$$\Delta G^{WT}_{Induced\ B} = (G^{WT}_{Receptor\ B,\ Pre} - G^{WT}_{Receptor,\ Unbound}) + (G^{WT}_{Ligand\ B,\ Pre} - G_{Ligand\ B,\ Unbound})$$

It is possible that mutants that bind B more strongly than A compared to wild type may have a negative binding energy, but may be inherently less stable than the wild type structure. Thus, a folding energy was introduced into the objective function, and it is desired to find mutants whose folding energy is no more than 5 kcal / mol greater than the wild type folding energy. Folding energy will be modeled as the difference in energy between the preformed receptor and the sum of the individual isolated residues.

$$\Delta G^{Mut}_{Fold\ A} = G^{Mut}_{Receptor\ A,Pre} - G^{Mut}_{Receptor,\ Unfolded}$$
$$\Delta G^{WT}_{Fold\ A} = G^{WT}_{Receptor\ A,Pre} - G^{WT}_{Receptor,\ Unfolded}$$
$$\Delta G^{Mut}_{Fold\ B} = G^{Mut}_{Receptor\ B,Pre} - G^{Mut}_{Receptor,\ Unfolded}$$
$$\Delta G^{WT}_{Fold\ B} = G^{WT}_{Receptor\ B,Pre} - G^{WT}_{Receptor,\ Unfolded}$$

For both structures bound to ligand A and structures bound to ligand B, DEE / A* will be

performed using the folding + docking energy as the objective function, and resulting best list of mutants will be sorted by docking energy and filtered such that structures whose folding energy is more than 5 kcal / mol worse than wild type will be ignored. The folding + docking is used to simultaneously find conformations with both low folding and docking energy and consists of the following terms:

$$\Delta G^{Mut}_{Fold+Dock\ A} = G^{Mut}_{Complex\ A,Pre} - G^{Mut}_{Receptor,\ Unfolded} - G^{Mut}_{Ligand\ A,\ Pre}$$
$$\Delta G^{WT}_{Fold+Dock\ A} = G^{WT}_{Complex\ A,Pre} - G^{WT}_{Receptor,\ Unfolded} - G^{WT}_{Ligand\ A,\ Pre}$$
$$\Delta G^{Mut}_{Fold+Dock\ B} = G^{Mut}_{Complex\ B,Pre} - G^{Mut}_{Receptor,\ Unfolded} - G^{Mut}_{Ligand\ B,\ Pre}$$
$$\Delta G^{WT}_{Fold+Bind\ B} = G^{WT}_{Complex\ B,Pre} - G^{Mut}_{Receptor,\ Unfolded} - G^{WT}_{Ligand\ B,\ Pre}$$

Once the global minimum energy structures have been found for mutant and wild type structures in each of the above situations, the global minimum energies for each mutant relative to wild type will be computed:

$$\begin{aligned}\Delta\Delta G^{Mut-WT}_{Bind\ A} &= \Delta G^{Mut}_{Bind\ A} - \Delta G^{WT}_{Bind\ A} \\ &= G^{Mut}_{Complex\ A} - G^{Mut}_{Receptor,\ Unbound} - G^{WT}_{Complex\ A} + G^{WT}_{Receptor,\ Unbound} \\ \Delta\Delta G^{Mut-WT}_{Bind\ B} &= \Delta G^{Mut}_{Bind\ B} - \Delta G^{WT}_{Bind\ B} \\ &= G^{Mut}_{Complex\ B} - G^{Mut}_{Receptor,\ Unbound} - G^{WT}_{Complex\ B} + G^{WT}_{Receptor,\ Unbound}\end{aligned}$$

A similar procedure can be used to compute the difference in binding for ligand B versus ligand A for mutant relative to wild type:

$$\begin{aligned}\Delta\Delta\Delta G^{Mut-WT}_{Bind\ B-A} &= \Delta\Delta G^{Mut-WT}_{Bind\ B} - \Delta\Delta G^{Mut-WT}_{Bind\ A} \\ &= G^{Mut}_{Complex\ B} - G^{WT}_{Complex\ B} - G^{Mut}_{Complex\ A} + G^{WT}_{Complex\ A}\end{aligned}$$

Note that the unbound structure ground state is the same for ligand A and ligand B and that the ligand ground state also cancels out and that the rigid binding model can be considered using the same framework induced fit model can be considered.

Structure Preparation

Given the wealth of crystallographic data available for the Z. *ramigera* thiolase at each stage of its native catalytic cycle and the high degree of homology between the *Z. ramigera* and *R. eutropha* active sites, all design calculations were performed using Z. ramigera crystal structures[1,2]. The structures were prepared using CHARMM[3] with the CHARMM27 force field using the procedures outlined by Lippow et al[4].

The following structures were generated using this methodology (starting template pdb code in parentheses):

Acetyl-CoA bound with unacetylated Cysteine 89 (1m3z)[2]

Butyryl-CoA bound with unacetylated Cysteine 89 (1m3z)[2]

Acetyl-CoA bound with acetylated Cysteine 89 (1dm3)[1]

Acetyl-CoA bound with butyrylated Cysteine 89 (1dm3)[1]

Butyryl-CoA bound with acetylated Cysteine 89 (1dm3)[1]

Only the A and B subunits of the crystal structures were used in design calculations with the ligand only incorporated in subunit A.

Search Strategy

Mutants were evaluated using the hierarchical, design strategy based on the dead-end elimination and A* method of Lippow et al[4]. Folding and binding energies were computed for all mutants in the search space using and low energy structures were identified using a guaranteed rotameric search of side chain degrees of freedom in both the bound and unfolded states. For each mutant evaluated, all side chains within 5 Å of the mutant residue were included in the rotameric conformational search and allowed to relax. In the initial DEE / A* search a pairwise decomposable energy function was used to compute the changes in pairwise Coulombic, van der Waals and geometric strain energies upon folding and binding. The lowest energy structures from the initial DEE / A* based search were then re-evaluated using a Poisson-Boltzmann Surface Area implicit solvent model and the best mutations for each binding scenario (e.g. acetyl-CoA bound with Cys-89 acetylated, acetyl-CoA bound with Cys-89 butyrylated) were compared.

The base rotamer library used was the backbone independent rotamer Karplus and Dunbrack[5] with χ_1 and χ_2 each expanded by ± 10°. Acetyl-CoA, butyryl-CoA, acetylated cysteine and butyrylated cysteine each required a custom rotamer library which was generated by iteratively perturbing each dihedral angle of the residues or ligand of interest by 30°, computing potential energy surfaces for each pairwise combination of dihedral angles and then collecting rotamers that represented local minima on each of the potential energy surfaces. These rotamers were then expanded by ± 10° to generate 9 "fleximers" per rotamer.

Parameters not natively included in the CHARMM27 force field (such as butyrylated cysteine or butyryl-CoA) were adopted from either published acetyl-CoA parmaeters[6] and similar CHARMM27 parameters. Partial atomic charges for these residues were fit using the methods of Bayly, et al[7].

In the case of the acetyl-CoA and butyryl-CoA rotamer libraries, the pantothenic acid portion of the ligand was kept rigid with only the acyl group and the β-mercapto-ethylamine moeities allowed to rotamerize.

Initial Results

As a starting point, design calculations were performed using allowing only Leu-88 and Val-57 to mutate to either alanine or glycine, a search space of 9 sequences, including wild-type for 5 structures:

acetyl-CoA bound with Cys-89 acetylated (AcCoa_AcCys), acetyl-CoA bound with Cys-89 acetylated (AcCoa_AcCys), acetyl-CoA bound with Cys-89 butyrylated (AcCoa_ButCys), butyryl-CoA bound with Cys-89 acetylated (ButCoa_AcCys), acetyl-CoA bound with Cys-89 unacylated (AcCoa) and butyryl-CoA bound with Cys-89 unacylated (ButCoa). Energetic results for each mutant are shown in the figure below, where each colored line represents a different protein sequence and each circle represents a different in binding energy between the mutant and wild type for the binding scenario on the x-axis. A mutant that would be expected to produce more P_{BA} product relative to the P_{AA} product should have a low energy for 1) the structure of acetyl-CoA bound with Cys-89 butyrylated (AcCoa_ButCys) compared to acetyl-CoA bound with Cys-89 acetylated (AcCoa_AcCys) and butyryl-CoA bound with Cys-89 acetylated (ButCoA_AcCys) and also 2) butyryl-CoA bound with Cys-89 unacylated (ButCoA) compared to acetyl-CoA bound with Cys-89 unacylated (AcCoa). As shown in the figure below, the only mutant that satisfies this requirement is V57VL88G which was then experimentally screened.

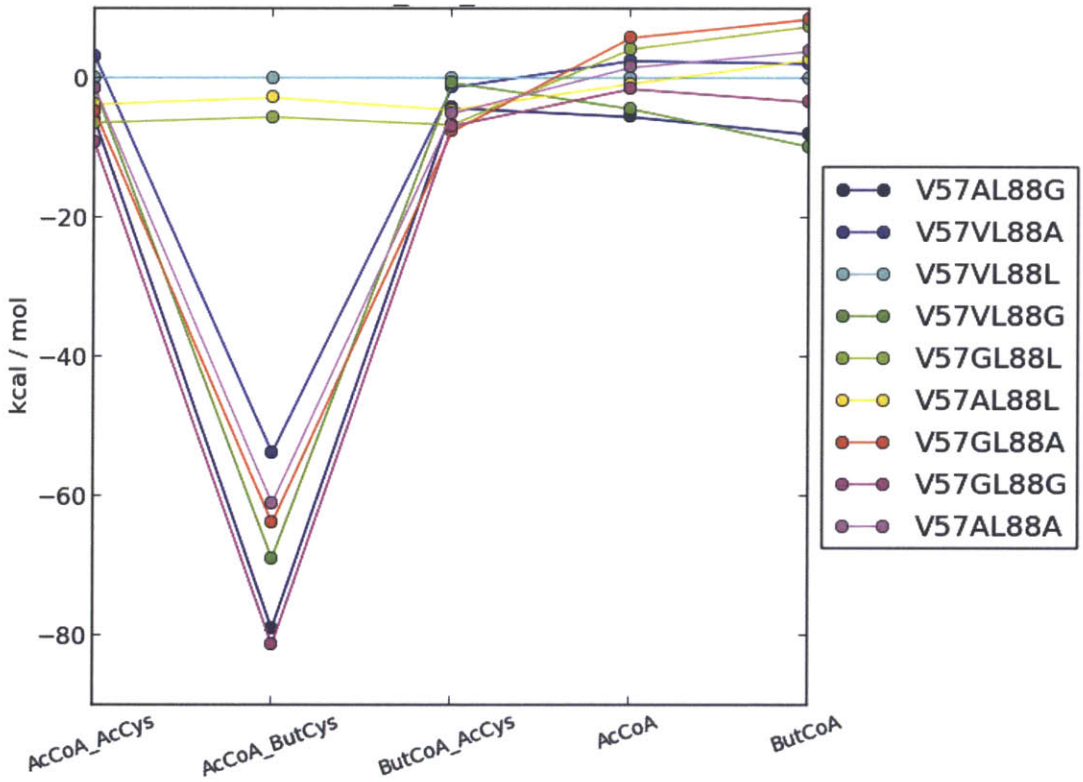

Results from a systematic screening of all single and double mutants in the *Z. ramigera* active site are currently being analyzed and screened.

References for Appendix A2

[1] Modis, Y., & Wierenga, R. K. (2000). Crystallographic analysis of the reaction pathway of Zoogloea ramigera biosynthetic thiolase. *Journal of molecular biology*, *297*(5), 1171–82.

[2] Kursula, P., Ojala J., Lambeir, A & Wierenga, R. (2002). The Catalytic Cycle of Biosynthetic Thiolase: A Conformational Journey of an Acetyl Group through Four Binding Modes and Two Oxyanion Holes. *Biochemistry*, 41 (52) 15543-15556

[3] Brooks, B. R., Brooks, C. L., Mackerell, A. D., Nilsson, L., Petrella, R. J., Roux, B., ... Karplus, M. (2009). CHARMM: the biomolecular simulation program. *Journal of computational chemistry*, *30*(10), 1545–614.

[4] Lippow, S. M., Wittrup, K. D., & Tidor, B. (2007). Computational design of antibody-affinity improvement beyond in vivo maturation. *Nature biotechnology*, *25*(10), 1171–6.

[5] Dunbrack, R. L., & Cohen, F. E. (1997). Bayesian statistical analysis of protein side- chain rotamer preferences. *Protein science : a publication of the Protein Society*, *6*(8), 1661–81.

[6] Aleksandrov, A., & Field, M. (2011). Efficient solvent boundary potential for hybrid potential simulations. *Physical chemistry chemical physics : PCCP*, *13*(22), 10503–9.

[7] Bayly, C. I., Cieplak, P., Cornell, W., & Kollman, P. A. (1993). A well-behaved electrostatic potential based method using charge restraints for deriving atomic charges: the RESP model. *The Journal of Physical Chemistry*, *97*(40), 10269–10280.

Appendix A3 | DHBA / 3HBL synthesis from glucose –Reactions & Theoretical yield calculations

Calculation of pathway independent theoretical maximum yield on glucose (Y^E)

The pathway independent maximum yield (Y^E), is a measure of the most efficient conversion of a given substrate into a product along a hypothetical (or real) route that is redox neutral and hence captures all the energy of the starting substrate into the product (Dugar and Stephanopoulos, 2011). For DHBA synthesis from glucose, the net reaction for this conversion is:

$$4 \text{ moles Glucose} \longrightarrow 3 \text{ moles 3,4-DHBA}$$

Thus, Y^E = **4/3 = 1.33 moles DHBA / mole of glucose**

Calculation of maximum theoretical pathway yield (Y^P)

Pathway Reactions (without acetate recycling)

Glycolate synthesis:

$$\tfrac{1}{2}\text{ Glucose} + \text{ADP} + P_i + 3NAD^+ + \text{FAD} \longrightarrow \text{Glycolate} + CO_2 + \text{ATP} + FADH_2 + 3\text{NADH} + \text{NADPH} + \text{CoASH} \longrightarrow + \text{NADP} + \text{CoASH}$$

DHBA / 3HBL synthesis:

$$\text{Glucose} + \text{Glycolate} + 2\text{ADP} + 2P_i + 4NAD^+ + \text{NADPH} \longrightarrow \text{3,4-DHBA} + 2CO_2 + \text{Acetate}^- + 2\text{ATP} + 2\text{CoASH} \longrightarrow + 4\text{NADH} + \text{NAPD} + 2\text{CoASH}$$

Net Reaction:

$$\tfrac{3}{2}\text{ Glucose} + 3\text{ADP} + 3P_i + 7NAD^+ + 2\text{NADPH} \longrightarrow \text{3,4-DHBA} + 3CO_2 + \text{Acetate} + 3\text{ATP} + \text{+FAD+ 3CoASH} \longrightarrow + 7\text{NADH} + 2\text{NAPD} + FADH_2 + 3\text{CoASH}$$

Theoretical pathway yield $Y^P_{w/o\text{-}acetate\text{-}recycling}$ = **0.67 moles 3,4-DHBA / mole of glucose**

The net reaction above shows that the pathway results in the synthesis of an excess of reducing equivalents which affect the overall yield. Separate reactions for regeneration of NADPH are not taken into account, assuming that the excess of NADH synthesized can supply some of the NADPH requirement through inter-conversion by transhydrogensases.

For every mole of 3,4-DHBA synthesized, a mole of acetate is formed as a by-product. The pathway above also shows an excess of reducing equivalents and ATP synthesis. Recylcing acetate into acetyl-CoA by activation with acetyl-CoA synthetase (Acs) using this excess of ATP can help improve the maximum theoretical pathway yield as below.

Pathway Reactions (with acetate recycling)

Net Reaction:

$$\text{Glucose} + \text{ADP} + P_i + 5\text{NAD}^+ + 2\text{NADPH} \longrightarrow 3,4\text{-DHBA} + 2CO_2 + \text{ATP} + 5\text{NADH} + 2\text{NAPD}$$

$$+\text{FAD} + 2\text{CoASH} \qquad\qquad +FADH_2 + 2\text{CoASH}$$

Theoretical pathway yield $Y^P_{\text{with-acetate-recycling}}$ **= 1.0 moles 3,4-DHBA / mole of glucose**

3HB synthesis reaction:

Net Reaction:

$$\text{Glucose} + 2\text{ADP} + 2P_i + 4\text{NAD}^+ + \text{NADPH} \longrightarrow 3\text{HB} + 2CO_2 + 2\text{ATP} + 4\text{NADH} + \text{NAPD}$$

$$+ 4\text{CoASH} \qquad\qquad + 4\text{CoASH}$$

2,3-DHBA synthesis reaction:

Net Reaction:

$$3/2\text{Glucose} + \text{ADP} + P_i + 5\text{NAD}^+ + 2\text{NADPH} \longrightarrow 2,3\text{-DHBA} + 2CO_2 + \text{ATP} + 5\text{NADH} + 2\text{NAPD}$$

$$+\text{FAD} + 2\text{CoASH} \qquad\qquad +FADH_2 + 2\text{CoASH}$$

Appendix A4 | *E. coli* strain designs for DHBA production in glucose aerobic condition using Flux Balance Models (*personal communication*, Prof. Jennifer Reed, University of Wisconsin-Madison)

Following are the recommendations for knockouts based on an analysis of metabolic fluxes using OptORF by Prof. Jennifer Reed's group.

Knockouts recommendations based on OptORF iMC1010v2

Knockout								Overexpress	Growth	MaxProd	MOMAprod
gcl	sucAB or sucC	nuoN	pta and eutD	glcC	lldP	aceB			0.44	3.53	1.43
gcl	sucAB or sucC	nuoN	pta and eutD	glcC	lldP	aceB	ptsH		0.41	3.83	0.64
gcl or glxK	sucAB or sucC	nuoN	pta and eutD	glcC	lldP	aceB	gdhA		0.396	3.9	1.83
gcl or glxK	sucAB or sucC	pnt and sthA	pgk	glcEF	lldP	aceB	pgi		0.237	4.97	0
gcl or glxK	gdhA	pnt and sthA	pgk	glcEF	lldP	aceB	pgi		0.207	5.34	0
gcl or glxK	sucAB or sucC	pnt and sthA	pgk	glcEF	lldP	aceB	pgi	mhpF	0.244	5.26	0
gcl or glxK	gdhA	pnt and sthA	pgk	glcEF	lldP	aceB	pgi	mhpF	0.212	5.48	0

Most promising candidates:

Knockout								Growth (hr^{-1})	Yield (%)
gcl or glxK	*sucAB or sucC*	*nuoN*	*pta and eutD*	*glcC*	*lldP*	*aceB*		0.44	29.9
gcl or glxK	*sucAB or sucC*	*nuoN*	*pta and eutD*	*glcC*	*lldP*	*aceB*	*ptsH*	0.41	32.5
gcl or glxK	*sucAB or sucC*	*nuoN*	*pta and eutD*	*glcC*	*lldP*	*aceB*	*gdhA*	0.30	33.1

*Maximum theoretical yield is 11.8 mol / 10 mol glucose. Glucose uptake rate is 10 mmol/gDW/hr.

gcl or glxK – glycolate and glyoxylate degradation.

sucAB or sucC – TCA cycle. To induce glyoxylate shunt.

nuoN – NDH-1. To limit the availability of NAD.

pta and eutD – pta-ack pathway. eutD is a predicted protein (possible not functional).

glcC – transcriptional activator for glcDEFGBA operon (or delete glcDEFGBA operon).

lldP – lactate transporter.

aceB – second enzyme of glyoxylate bypass (possibly repressed).

ptsH – PTS system. To decouple fluxes at pep-pyr nodes from glucose uptake.

gdhA – ATP-dependent glutamate synthase pathway from alpha-ketoglutarate.

There are a few other designs that involve methylglyoxal pathway by limiting glycolysis. These strains have higher product yield (42%~45%), but lower growth rates (0.2 ~ 0.24 hr^{-1}).

Appendix A5 | Effect of varying the C / N ratio on DHBA / 3HBL synthesis

Following are the plots showing substrate and product titers for strain GP0-2-DHP cultured in media with various M9 and glucose concentrations.

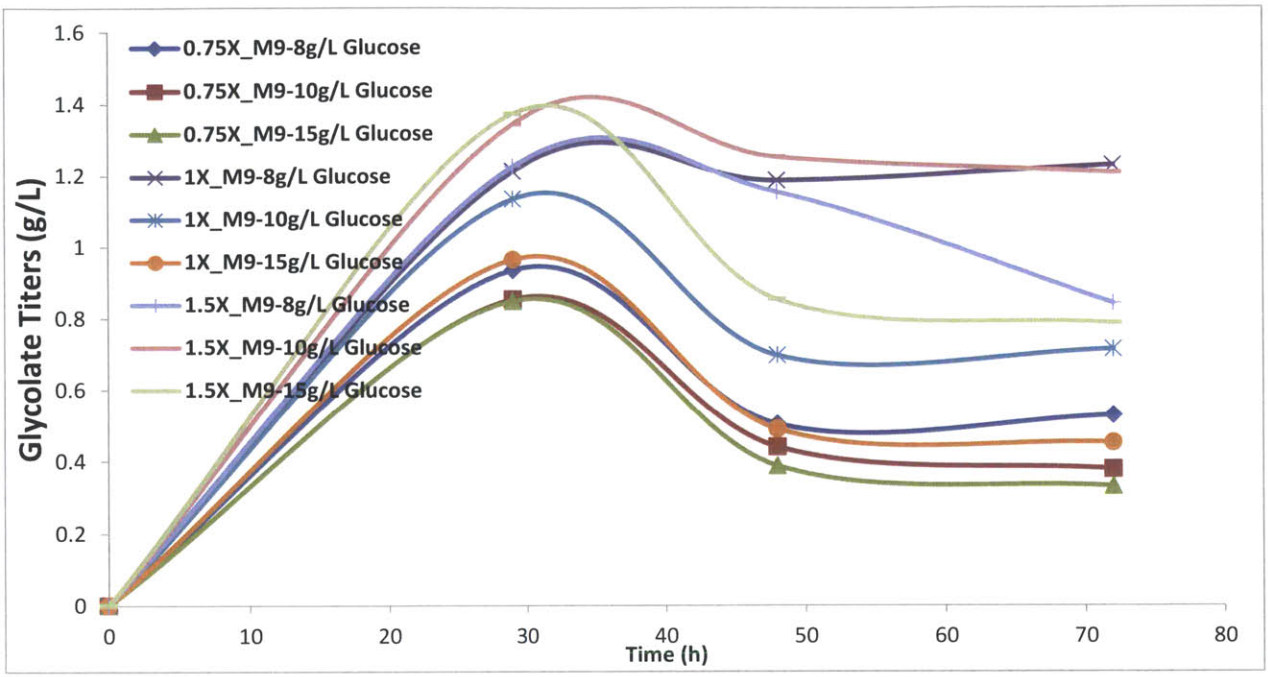

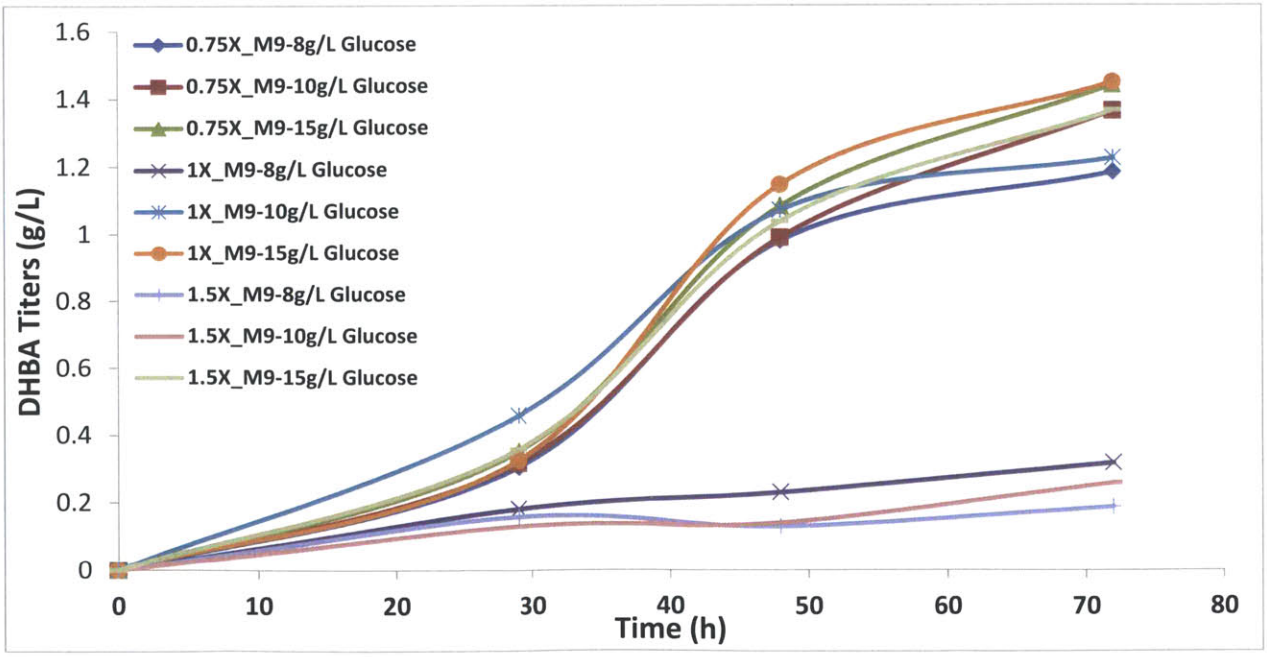

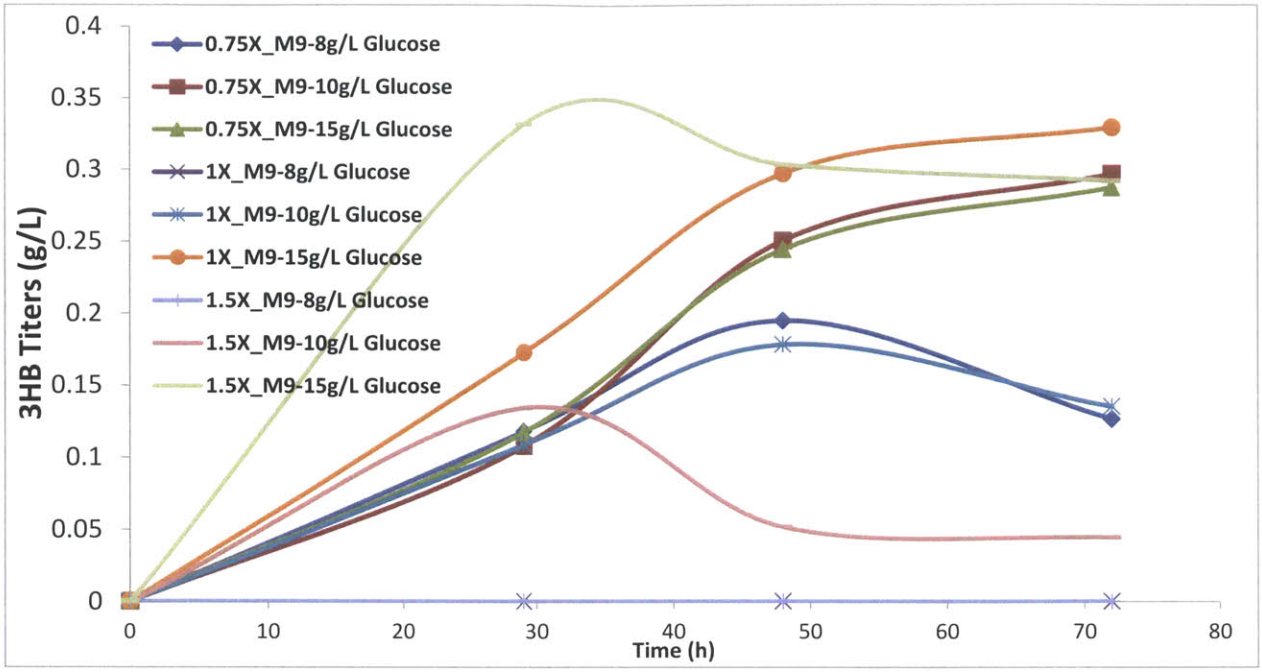
0.4
0.35
0.3
0.25
0.2
0.15
0.1
0.05
0
3HB Titers (g/L)
0.75X_M9-8g/L Glucose
0.75X_M9-10g/L Glucose
0.75X_M9-15g/L Glucose
1X_M9-8g/L Glucose
1X_M9-10g/L Glucose
1X_M9-15g/L Glucose
1.5X_M9-8g/L Glucose
1.5X_M9-10g/L Glucose
1.5X_M9-15g/L Glucose
0
10
20
30
40
50
60
70
80
Time (h)

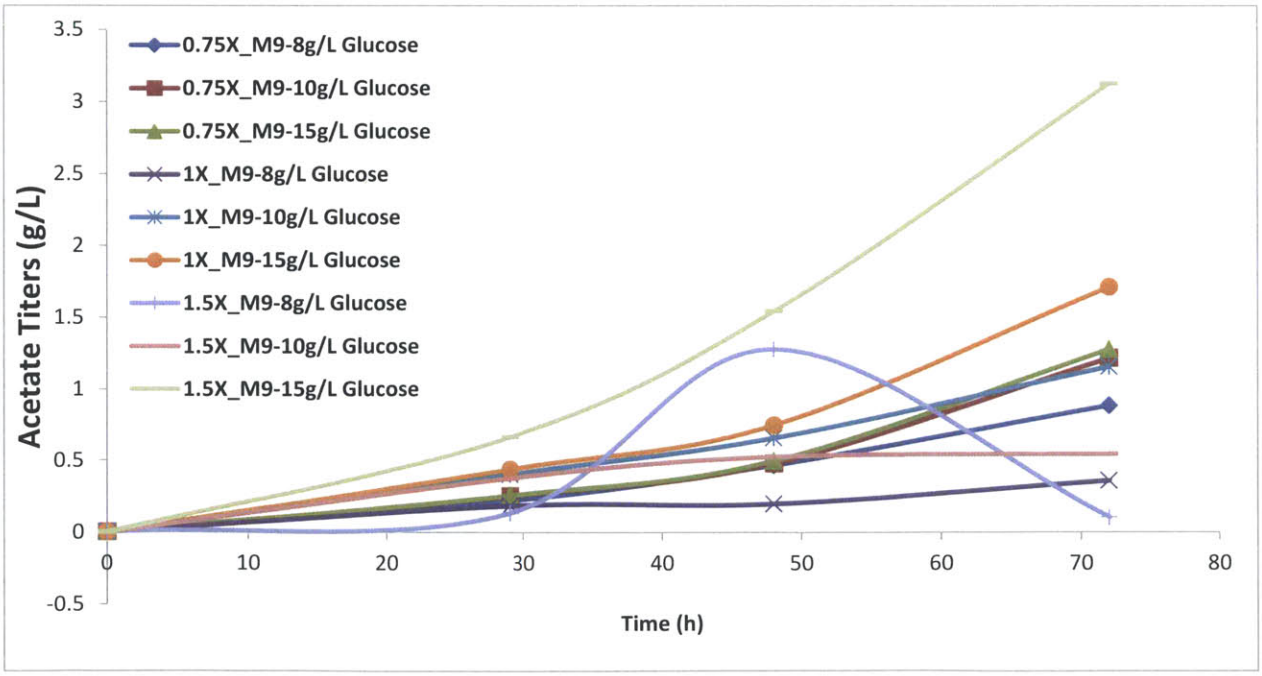
3.5
3
2.5
2
1.5
1
0.5
0
-0.5
Acetate Titers (g/L)
0.75X_M9-8g/L Glucose
0.75X_M9-10g/L Glucose
0.75X_M9-15g/L Glucose
1X_M9-8g/L Glucose
1X_M9-10g/L Glucose
1X_M9-15g/L Glucose
1.5X_M9-8g/L Glucose
1.5X_M9-10g/L Glucose
1.5X_M9-15g/L Glucose
0
10
20
30
40
50
60
70
80
Time (h)

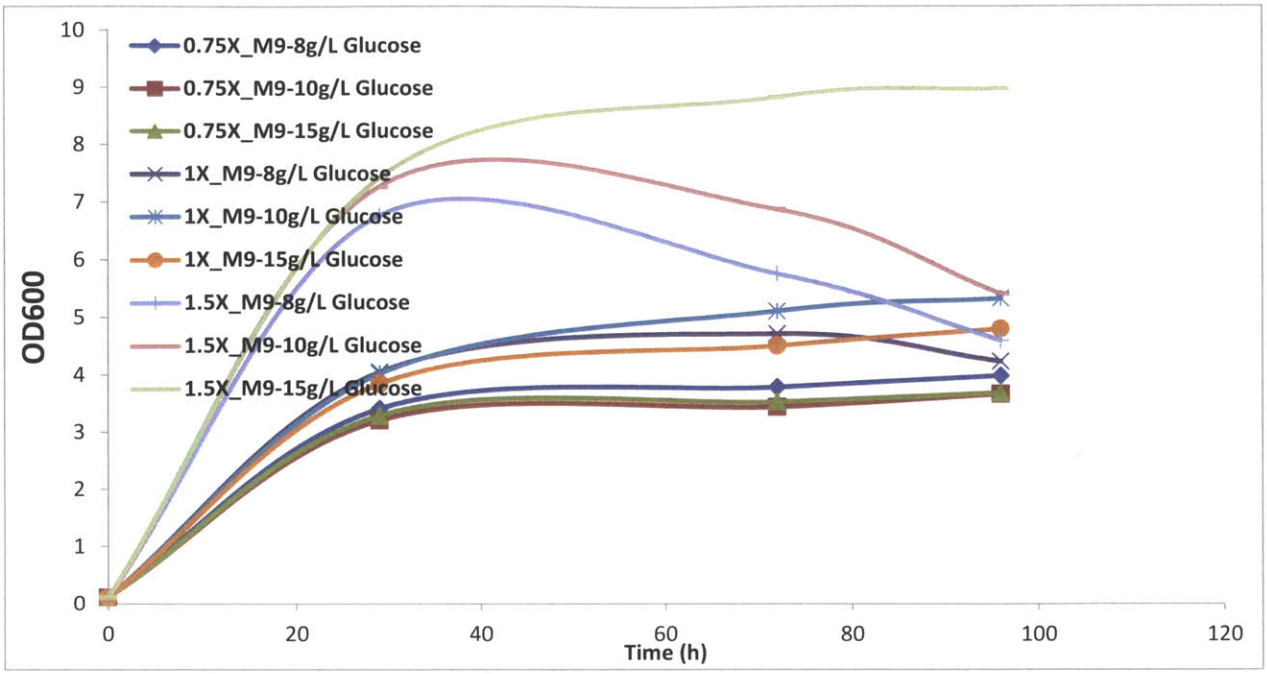
OD600
Time (h)
0.75X_M9-8g/L Glucose
0.75X_M9-10g/L Glucose
0.75X_M9-15g/L Glucose
1X_M9-8g/L Glucose
1X_M9-10g/L Glucose
1X_M9-15g/L Glucose
1.5X_M9-8g/L Glucose
1.5X_M9-10g/L Glucose
1.5X_M9-15g/L Glucose
0
1
2
3
4
5
6
7
8
9
10
0
20
40
60
80
100
120

References

Ajikumar, P. K., Xiao, W. H., Tyo, K. E. J., Wang, Y., Simeon, F., Leonard, E., Mucha, O., Phon, T. H., Pfeifer, B., Stephanopoulos, G., 2010. Isoprenoid Pathway Optimization for Taxol Precursor Overproduction in Escherichia coli. Science. 330, 70-74.

Anthony, J. R., Anthony, L. C., Nowroozi, F., Kwon, G., Newman, J. D., Keasling, J. D., 2009. Optimization of the mevalonate-based isoprenoid biosynthetic pathway in Escherichia coli for production of the anti-malarial drug precursor amorpha-4,11-diene. Metabolic Engineering. 11, 13-19.

Asadollahi, M. A., Maury, J., Schalk, M., Clark, A., Nielsen, J., 2010. Enhancement of Farnesyl Diphosphate Pool as Direct Precursor of Sesquiterpenes Through Metabolic Engineering of the Mevalonate Pathway in Saccharomyces cerevisiae. Biotechnology And Bioengineering. 106, 86-96.

Atkinson, H. J., Morris, J. H., Ferrin, T. E., Babbitt, P. C., 2009. Using Sequence Similarity Networks for Visualization of Relationships Across Diverse Protein Superfamilies. Plos One. 4.

Atsumi, S., Hanai, T., Liao, J. C., 2008. Non-fermentative pathways for synthesis of branched-chain higher alcohols as biofuels. Nature. 451, 86-U13.

Baba, T., Ara, T., Hasegawa, M., Takai, Y., Okumura, Y., Baba, M., Datsenko, K. A., Tomita, M., Wanner, B. L., Mori, H., 2006. Construction of Escherichia coli K-12 in-frame, single-gene knockout mutants: the Keio collection. Mol Syst Biol. 2.

Babtie, A., Tokuriki, N., Hollfelder, F., 2010. What makes an enzyme promiscuous? Current Opinion in Chemical Biology. 14, 200.

Barber, A. E., Babbitt, P. C., 2012. Pythoscape: a framework for generation of large protein similarity networks. Bioinformatics. 28, 2845-2846.

Baxevanis, A. D., Ouellette, B. F. F., 2005. Bioinformatics: a practical guide to the analysis of genes and protein. John Wiley and Sons, New Jersey.

Blankschien, M. D., Clomburg, J., Gonzalez, R., 2010. Metabolic engineering of Escherichia coli for the production of succinate from glycerol. Metabolic Engineering. 12, 409-419.

Bozell, J. J., Petersen, G. R., 2010. Technology development for the production of biobased products from biorefinery carbohydrates-the US Department of Energy's "Top 10" revisited. Green Chemistry. 12, 539-554.

Brandl, H., Knee, E. J., Fuller, R. C., Gross, R. A., Lenz, R. W., 1989. Ability of the photorophic bacterium Rhodospirillum rubrum to produce various poly(beta-hyrdroxyalkanoates) - potential sources for biodegradable polyesters. International Journal of Biological Macromolecules. 11, 49-55.

Byun, I. S., Kim, K. I., Bong, C. A., Process for the preparation of L-carnitine. In: Office, U. S. P., (Ed.). Samsung Fine Chemicals Company Ltd., KR, United States, 2002.

Carbonell, P., Faulon, J. L., 2010. Molecular signatures-based prediction of enzyme promiscuity. Bioinformatics. 26, 2012-2019.

Carey, F. A., 2000. Organic Chemistry. McGraw Hill, New York, NY.

Chang, M. C. Y., Keasling, J. D., 2006. Production of isoprenoid pharmaceuticals by engineered microbes. Nat Chem Biol. 2, 674.

Cortay, J. C., Bleicher, F., Duclos, B., Cenatiempo, Y., Gautier, C., Prato, J. L., Cozzone, A. J., 1989. Utilization of acetate in Escherichia coli - Structural organization and differential expression of the ace operon. Biochimie. 71, 1043-1049.

Cozzone, A. J., 1998. Regulation of acetate metabolism by protein phosphorylation in enteric bacteria. Annual Review Of Microbiology. 52, 127-164.

Debarbouille, M., Gardan, R., Arnaud, M., Rapoport, G., 1999. Role of BkdR, a transcriptional activator of the SigL-dependent isoleucine and valine degradation pathway in Bacillus subtilis. Journal Of Bacteriology. 181, 2059-2066.

Dhamankar, H., Prather, K. L. J., 2011. Microbial chemical factories: recent advances in pathway engineering for synthesis of value added chemicals. Current Opinion in Structural Biology. 21, 488-494.

Dugar, D., Stephanopoulos, G., 2011. Relative potential of biosynthetic pathways for biofuels and bio-based products. Nature Biotechnology. 29, 1074-1078.

Feigenbaum, J., Schulz, H., 1975. Thiolases of *Escherichia coli* - Purification and chain-length specificities. Journal Of Bacteriology. 122, 407-411.

Furrow, M. E., Schaus, S. E., Jacobsen, E. N., 1998. Practical access to highly enantioenriched C-3 building blocks via hydrolytic kinetic resolution. Journal Of Organic Chemistry. 63, 6776-6777.

Gao, H. J., Wu, Q. N., Chen, G. Q., 2002. Enhanced production of D-(-)-3-hydroxybutyric acid by recombinant Escherichia coli. Fems Microbiology Letters. 213, 59-65.

Geros, H., Cassio, F., Leao, C., 1996. Reconstitution of lactate proton symport activity in plasma membrane vesicles from the yeast Candida utilis. Yeast. 12, 1263-1272.

Gokarn, R. R., Selifonova, O. V., Jessen, H. J., Gort, S. J., Slemer, T., Buckel, W., 3-hydroxypropionicacid and other organic compounds. In: Office, U. S. P., (Ed.), United States Patent Application Publication. Cargill, Incorporated, Wayzata, MN, United States, 2011.

Guzman, L. M., Belin, D., Carson, M. J., Beckwith, J., 1995. Tight Regulation, Modulation, And High-Level Expression By Vectors Containing The Arabinose P-Bad Promoter. Journal Of Bacteriology. 177, 4121-4130.

Hansen, E. H., Moller, B. L., Kock, G. R., Bunner, C. M., Kristensen, C., Jensen, O. R., Okkels, F. T., Olsen, C. E., Motawia, M. S., Hansen, J., 2009. De Novo Biosynthesis of Vanillin in Fission Yeast (Schizosaccharomyces pombe) and Baker's Yeast (Saccharomyces cerevisiae). Applied And Environmental Microbiology. 75, 2765-2774.

Haywood, G. W., Anderson, A. J., Chu, L., Dawes, E. A., 1988. The role of NADH-linked and NADPH-linked acetoacetyl-CoA reductases in the poly-3-hydroxybutyrate synthesizing organism *Alcaligenes eutrophus*. Fems Microbiology Letters. 52, 259-264.

Heckman, K. L., Pease, L. R., 2007. Gene splicing and mutagenesis by PCR-driven overlap extension. Nat. Protocols. 2, 924.

Hermann, J. C., Ghanem, E., Li, Y., Raushel, F. M., Irwin, J. J., Shoichet, B. K., 2006. Predicting Substrates by Docking High-Energy Intermediates to Enzyme Structures. J. Am. Chem. Soc. 128, 15882.

Hoek, P. K., Aristidou, A., Hahn, H. H., Patist, A., Fermentation goes large-scale. CEP Magazine. AIChE, 2003, pp. 37-42.

Hollingsworth, R. I., 1999. Taming Carbohydrate Complexity: A Facile, High-Yield Route to Chiral 2,3-Dihydroxybutanoic Acids and 4-Hydroxytetrahydrofuran-2-ones with Very High Optical Purity from Pentose Sugars. The Journal of Organic Chemistry. 64, 7633-7634.

Horton, R. M., Hunt, H. D., Ho, S. N., Pullen, J. K., Pease, L. R., 1989. Engineering Hybrid Genes Without The Use Of Restriction Enzymes - Gene-Splicing By Overlap Extension. Gene. 77, 61-68.

Hwang, J. Y., Park, J., Seo, J. H., Cha, M., Cho, B. K., Kim, J., Kim, B. G., 2009. Simultaneous Synthesis of 2-Phenylethanol and L-Homophenylalanine Using Aromatic Transaminase With Yeast Ehrlich Pathway. Biotechnology And Bioengineering. 102, 1323-1329.

Kanehisa, M., Goto, S., Hattori, M., Aoki-Kinoshita, K. F., Itoh, M., Kawashima, S., Katayama, T., Araki, M., Hirakawa, M., 2006. From genomics to chemical genomics: new developments in KEGG. Nucleic Acids Research. 34, D354-D357.

Karp, P. D., Ouzounis, C. A., Moore-Kochlacs, C., Goldovsky, L., Kaipa, P., Ahren, D., Tsoka, S., Darzentas, N., Kunin, V., Lopez-Bigas, N., 2005. Expansion of the BioCyc collection of pathway/genome databases to 160 genomes. Nucleic Acids Research. 33, 6083-6089.

Khersonsky, O., Tawfik, D. S., 2010. Enzyme Promiscuity: A Mechanistic and Evolutionary Perspective. Annual Review Of Biochemistry, Vol 79. 79, 471-505.

Kim, E. E., Baker, C. T., Dwyer, M. D., Murcko, M. A., Rao, B. G., Tung, R. D., Navia, M. A., 1995. Crystal-Structure Of Hiv-1 Protease In Complex With Vx-478, A Potent And Orally Bioavailable Inhibitor Of The Enzyme. Journal Of The American Chemical Society. 117, 1181-1182.

Kim, J., Reed, J. L., 2010. OptORF: Optimal metabolic and regulatory perturbations for metabolic engineering of microbial strains. Bmc Systems Biology. 4.

Kornberg, H. L., 1966. Role and control of glyoxylate cyncle in Escherichia coli Biochemical Journal. 99, 1-12.

Kumar, P., Deshmukh, A. N., Upadhyay, R. K., Gurjar, M. K., 2005. A simple and practical approach to enantiomerically pure (S)-3-hydroxy-γ-butyrolactone: synthesis of (R)-4-cyano-3-hydroxybutyric acid ethyl ester. Tetrahedron: Asymmetry. 16, 2717-2721.

Kwak, B. S., 2003. Development of chiral pharmaceutical fine chemicals through technology fusion. Chimica Oggi-Chemistry Today. 21, 23-26.

Laporte, D. C., Koshland, D. E., 1982. A protein with kinase and phosphatase activities involved in regulation of tricarboxylic acid cycle. Nature. 300, 458-460.

Lee, E. G., Yoon, S. H., Das, A., Lee, S. H., Li, C., Kim, J. Y., Choi, M. S., Oh, D. K., Kim, S. W., 2009. Directing Vanillin Production From Ferulic Acid by Increased Acetyl-CoA Consumption in Recombinant Escherichia coli. Biotechnology And Bioengineering. 102, 200-208.

Lee, J. W., Kim, H. U., Choi, S., Yi, J., Lee, S. Y., 2011. Microbial production of building block chemicals and polymers. Current Opinion in Biotechnology. 22, 1-10.

Lee, S. H., Park, O. J., 2009. Uses and production of chiral 3-hydroxy-gamma-butyrolactones and structurally related chemicals. Applied Microbiology And Biotechnology. 84, 817-828.

Lee, S. H., Park, O. J., Uh, H. S., 2008a. A chemoenzymatic approach to the synthesis of enantiomerically pure (S)-3-hydroxy-gamma-butyrolactone. Applied Microbiology And Biotechnology. 79, 355-362.

Lee, S. Y., Park, J. H., Jang, S. H., Nielsen, L. K., Kim, J., Jung, K. S., 2008b. Fermentative butanol production by clostridia. Biotechnology And Bioengineering. 101, 209-228.

Lee, S. Y., Park, S. H., Lee, Y., Lee, S. H., 2001. Production of chiral and other valuable compounds from microbial polyesters. In: Dio, Y., Steinbuchel, A., Eds.), Biopolymers, Polyesters III. Wiley-VCH, Weinheim, pp. 375-387.

Leonard, E., Ajikumar, P. K., Thayer, K., Xiao, W. H., Mo, J. D., Tidor, B., Stephanopoulos, G., Prather, K. L. J., 2010. Combining metabolic and protein engineering of a terpenoid biosynthetic pathway for overproduction and selectivity control. Proceedings Of The National Academy Of Sciences Of The United States Of America. 107, 13654-13659.

Liu, Q., Ouyang, S. P., Chung, A., Wu, Q., Chen, G. Q., 2007. Microbial production of R-3-hydroxybutyric acid by recombinant E-coli harboring genes of phbA, phbB, and tesB. Applied Microbiology And Biotechnology. 76, 811-818.

Liu, S. J., Steinbuchel, A., 2000. Exploitation of butyrate kinase and phosphotransbutyrylase from Clostridium acetobutylicum for the in vitro biosynthesis of poly(hydroxyalkanoic acid). Applied Microbiology And Biotechnology. 53, 545-552.

Liu, X.-W., Wang, H.-H., Chen, J.-Y., Li, X.-T., Chen, G.-Q., 2009. Biosynthesis of poly(3-hydroxybutyrate-co-3-hydroxyvalerate) by recombinant Escherichia coli harboring propionyl-CoA synthase gene (prpE) or propionate permease gene (prpP). Biochemical Engineering Journal. 43, 72-77.

Martin, C. H., Development of metabolic pathways for the biosynthesis of hydroxyacids and lactones. Chemical Engineering, Vol. PhD. Massachusetts Institute of Technology, Cambridge, 2009.
Martin, C. H., Nielsen, D. R., Solomon, K. V., Prather, K. L. J., 2009. Synthetic Metabolism: Engineering Biology at the Protein and Pathway Scales. Chemistry & Biology. 16, 277.
Masamune, S., Palmer, M. A. J., Gamboni, R., Thompson, S., Davis, J. T., Williams, S. F., Peoples, O. P., Sinskey, A. J., Walsh, C. T., 1989. Bio-Claisen condensation catalyzed by thiolase from Zoogloea ramigera. Active site cysteine residues. J. Am. Chem. Soc. 111, 1879.
Moon, T. S., Dueber, J. E., Shiue, E., Prather, K. L. J., 2009. Use of modular, synthetic scaffolds for improved production of glucaric acid in engineered E. coli. Metabolic Engineering. 12, 298.
Moon, T. S., Dueber, J. E., Shiue, E., Prather, K. L. J., 2010. Use of modular, synthetic scaffolds for improved production of glucaric acid in engineered E. coli. Metabolic Engineering. 12, 298.
Naggert, J., Narasimhan, M. L., Deveaux, L., Cho, H. S., Randhawa, Z. I., Cronan, J. E., Green, B. N., Smith, S., 1991. Cloning, Sequencing, And Characterization Of Escherichia-Coli Thioesterase-Ii. Journal Of Biological Chemistry. 266, 11044-11050.
Nakagawa, A., Idogaki, H., Kato, K., Shinmyo, A., Suzuki, T., 2006. Improvement on production of (R)-4-Chloro-3-hydroxybutyrate and (S)-3-hydroxy-gamma-butyrolactone with recombinant Escherichia coli cells. Journal Of Bioscience And Bioengineering. 101, 97-103.
Nakamura, C. E., Whited, G. M., 2003. Metabolic engineering for the microbial production of 1,3-propanediol. Current Opinion in Biotechnology. 14, 454-459.
Nielsen, D. R., Leonard, E., Yoon, S. H., Tseng, H. C., Yuan, C., Prather, K. L. J., 2009. Engineering alternative butanol production platforms in heterologous bacteria. Metabolic Engineering. 11, 262-273.
Nimmo, G. A., Nimmo, H. G., 1984. The regulatory properties of isocitrate dehydrogenase kinase and isocitrate dehydrogenase phosphatase from Escherichia coli ML308 and the roles of these activities in the control of isocitrate dehydrogenase. European Journal of Biochemistry. 141, 409-414.
Niu, W., Molefe, M. N., Frost, J. W., 2003. Microbial synthesis of the energetic material precursor 1,2,4-butanetriol. Journal Of The American Chemical Society. 125, 12998-12999.
Núñez, M. a. F., Kwon, O., Wilson, T. H., Aguilar, J., Baldoma, L., Lin, E. C. C., 2002. Transport of l-Lactate, d-Lactate, and Glycolate by the LldP and GlcA Membrane Carriers of Escherichia coli. Biochemical and Biophysical Research Communications. 290, 824-829.
Park, Y. M., Chun, J. P., Rho, K. R., Yu, H. S., Hwang, I., Process for preparing optically pure (S)-3-hydroxy-γ-butyrolactone. In: Office, U. S. P., (Ed.), United States Patent Application Publication. Samsung Fine Chemicals Co., Ltd., United States, 2004.
Prather, K. L. J., Martin, C. H., 2008. De novo biosynthetic pathways: rational design of microbial chemical factories. Current Opinion in Biotechnology. 19, 468.
Punta, M., Coggill, P. C., Eberhardt, R. Y., Mistry, J., Tate, J., Boursnell, C., Pang, N., Forslund, K., Ceric, G., Clements, J., Heger, A., Holm, L., Sonnhammer, E. L. L., Eddy, S. R., Bateman, A., Finn, R. D., 2012. The Pfam protein families database. Nucleic Acids Research. 40, D290-D301.
Qian, Z. G., Xia, X. X., Lee, S. Y., 2009. Metabolic Engineering of Escherichia coli for the Production of Putrescine: A Four Carbon Diamine. Biotechnology And Bioengineering. 104, 651-662.
Qian, Z. G., Xia, X. X., Lee, S. Y., 2011. Metabolic Engineering of Escherichia coli for the Production of Cadaverine: A Five Carbon Diamine. Biotechnology And Bioengineering. 108, 93-103.
Raab, A. M., Gebhardt, G., Bolotina, N., Weuster-Botz, D., Lang, C., 2010. Metabolic engineering of Saccharomyces cerevisiae for the biotechnological production of succinic acid. Metabolic Engineering. 12, 518-525.

Rhie, H. G., Dennis, D., 1995. Role of FadR and AtoC (Con) mutations in Poly(3-hydroxybutyrate-co-3-hydroxyvalerate) synthesis in recombinant Pha(+) *Escherichia coli* Applied And Environmental Microbiology. 61, 2487-2492.

Rouhi, A. M., 2003. Custom Chemicals. Chemical & Engineering News Archive. 81, 55.

Saito, R., Smoot, M. E., Ono, K., Ruscheinski, J., Wang, P. L., Lotia, S., Pico, A. R., Bader, G. D., Ideker, T., 2012. A travel guide to Cytoscape plugins. Nature Methods. 9, 1069-1076.

Schomburg, I., Chang, A., Ebeling, C., Gremse, M., Heldt, C., Huhn, G., Schomburg, D., 2004. BRENDA, the enzyme database: updates and major new developments. Nucleic Acids Research. 32, D431-D433.

Schweiger, G., Buckel, W., 1984. On The Dehydration Of (R)-Lactate In The Fermentation Of Alanine To Propionate By Clostridium-Propionicum. Febs Letters. 171, 79-84.

Segre, D., Vitkup, D., Church, G. M., 2002. Analysis of optimality in natural and perturbed metabolic networks. Proceedings Of The National Academy Of Sciences Of The United States Of America. 99, 15112-15117.

Shin, H. I., Chang, J. H., Woo, Y. M., Yim, Y. S., A process for the synthesis of 3-hydroxy-γ-butyrolactone. In: Organization, W. I. P., (Ed.). LG Life Science Ltd., United States, 2005.

Slater, S., Houmiel, K. L., Tran, M., Mitsky, T. A., Taylor, N. B., Padgette, S. R., Gruys, K. J., 1998. Multiple beta-ketothiolases mediate poly(beta-hydroxyalkanoate) copolymer synthesis in Ralstonia eutropha. Journal Of Bacteriology. 180, 1979-1987.

Steinbuchel, A., Valentin, H. E., 1995. Diversity Of Bacterial Polyhydroxyalkanoic Acids. Fems Microbiology Letters. 128, 219-228.

Stueland, C. S., Ikeda, T. P., Laporte, D. C., 1989. Mutation of the predicted ATP binding-site inactivates both activities of isocitrate dehydrogenase kinase phosphatase Journal Of Biological Chemistry. 264, 13775-13779.

Suzuki, T., Idogaki, H., Kasai, N., 1999. Dual production of highly pure methyl (R)-4-chloro-3-hydroxybutyrate and (S)-3-hydroxy-gamma-butyrolactone with Enterobacter sp. Enzyme And Microbial Technology. 24, 13-20.

Taguchi, S., Yamadaa, M., Matsumoto, K., Tajima, K., Satoh, Y., Munekata, M., Ohno, K., Kohda, K., Shimamura, T., Kambe, H., Obata, S., 2008. A microbial factory for lactate-based polyesters using a lactate-polymerizing enzyme. Proceedings Of The National Academy Of Sciences Of The United States Of America. 105, 17323-17327.

Trantas, E., Panopoulos, N., Ververidis, F., 2009. Metabolic engineering of the complete pathway leading to heterologous biosynthesis of various flavonoids and stilbenoids in Saccharomyces cerevisiae. Metabolic Engineering. 11, 355-366.

Tseng, H.-C., Harwell, C., Martin, C., Prather, K., 2010a. Biosynthesis of chiral 3-hydroxyvalerate from single propionate-unrelated carbon sources in metabolically engineered E. coli. Microbial Cell Factories. 9, 96.

Tseng, H. C., Harwell, C. L., Martin, C. H., Prather, K. L. J., 2010b. Biosynthesis of chiral 3-hydroxyvalerate from single propionate-unrelated carbon sources in metabolically engineered E. coli. Microbial Cell Factories. 9.

Tseng, H. C., Martin, C. H., Nielsen, D. R., Prather, K. L., 2009a. Metabolic engineering of Escherichia coli for enhanced production of (R)- and (S)-3-hydroxybutyrate. Appl Environ Microbiol. 75, 3137 - 3145.

Tseng, H. C., Martin, C. H., Nielsen, D. R., Prather, K. L. J., 2009b. Metabolic Engineering of Escherichia coli for Enhanced Production of (R)- and (S)-3-Hydroxybutyrate. Applied And Environmental Microbiology. 75, 3137-3145.

Tseng, H. C., Prather, K. L. J., 2012. Controlled biosynthesis of odd-chain fuels and chemicals via engineered modular metabolic pathways. Proceedings Of The National Academy Of Sciences Of The United States Of America. 109, 17925-17930.

Voit, B., 2005. Hyperbranched polymers - All problems solved after 15 years of research? Journal Of Polymer Science Part A-Polymer Chemistry. 43, 2679-2699.

Wade Jr, L. G., 2006. The Claisen Ester Condensation. Organic chemistry. Prentice-Hall., New Jersey, pp. 1067-1071.

Wang, G. J., Hollingsworth, R. I., 1999a. Direct conversion of (S)-3-hydroxy-gamma-butyrolactone to chiral three-carbon building blocks. Journal Of Organic Chemistry. 64, 1036-1038.

Wang, G. J., Hollingsworth, R. I., 1999b. Synthetic routes to L-carnitine and L-gamma-amino-beta-hydroxybutyric acid from (S)-3-hydroxybutyrolactone by functional group priority switching. Tetrahedron-Asymmetry. 10, 1895-1901.

Werpy, T., Peterson, G., 2004. Top value added chemicals from biomass, Vol 1: results of screening for potential candidates from sugars and synthesis gas.

Xia, X. X., Qian, Z. G., Ki, C. S., Park, Y. H., Kaplan, D. L., Lee, S. Y., 2010. Native-sized recombinant spider silk protein produced in metabolically engineered Escherichia coli results in a strong fiber. Proceedings Of The National Academy Of Sciences Of The United States Of America. 107, 14059-14063.

Yang, H., Goyal, N., Ella-Menye, J. R., Williams, K., Wang, G. J., 2012. Synthesis of Chiral Five-, Six-, and Seven-Membered Heterocycles from (S)-3-Hydroxy-gamma-butyrolactone. Synthesis-Stuttgart. 44, 561-568.

Yim, H., Haselbeck, R., Niu, W., Pujol-Baxley, C., Burgard, A., Boldt, J., Khandurina, J., Trawick, J. D., Osterhout, R. E., Stephen, R., Estadilla, J., Teisan, S., Schreyer, H. B., Andrae, S., Yang, T. H., Lee, S. Y., Burk, M. J., Van Dien, S., 2011. Metabolic engineering of Escherichia coli for direct production of 1,4-butanediol. Nat. Chem. Biol. 7, 445-452.

Zor, T., Seliger, Z., 1996. Linearization of the bradford protein assay increases its sensitivity: Theoretical and experimental studies. Analytical Biochemistry. 236, 302-308.